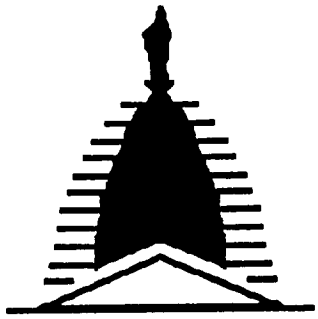

UNIVERSITY of
NOTRE DAME

NASA/USRA UNIVERSITY ADVANCED DESIGN PROGRAM 1989-1990

UNIVERSITY SPONSOR
BOEING COMMERCIAL AIRPLANE COMPANY

FINAL DESIGN PROPOSAL

THE SCREEM-J4D

A Proposal in Response to a Low Reynolds Number
Station Keeping Mission

May 1990

Department of Aerospace and Mechanical Engineering
University of Notre Dame
Notre Dame, IN 46556

FINAL DESIGN PROPOSAL

Presented By

AEROSPACE ENGINEERS
FOR THE
TWENTY-FIRST CENTURY

07 May 1990

University of Notre Dame
Department of Aerospace and Mechanical Engineering

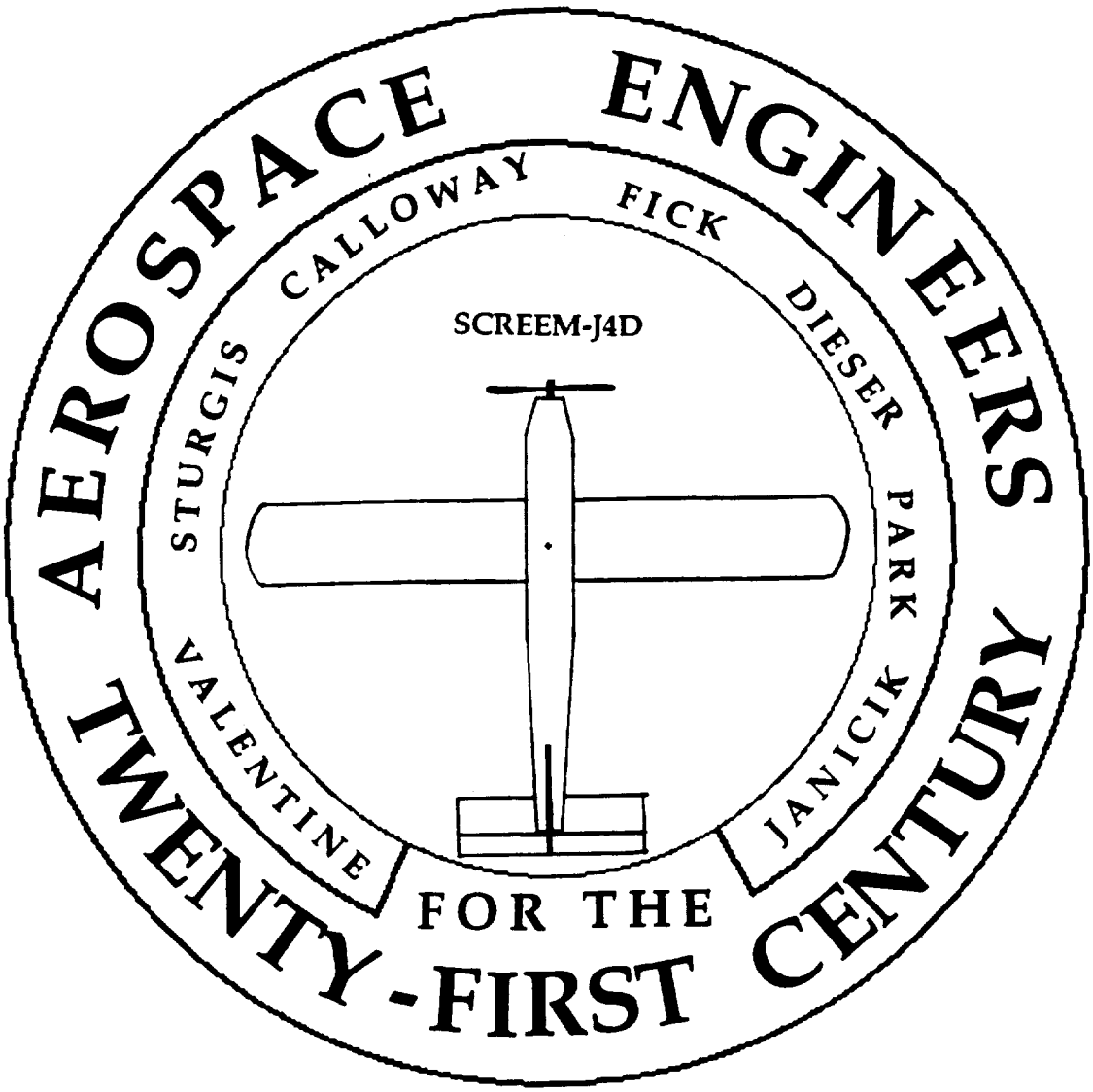

AEROSPACE ENGINEERS FOR THE TWENTY-FIRST CENTURY

Eric Fick	**Project Manager**
Michael Park	**Structures**
Ed Dieser	**Stability & Control**
Jeff Janicik	**Stability & Control**
Steve Valentine	**Aerodynamics**
Rob Calloway	**Propulsion**
Chris Sturgis	**Propulsion**

TABLE OF CONTENTS

EXECUTIVE SUMMARY

The Screem-J4D is a remotely piloted airplane that has been designed to fly at a chord Reynold's number of 100,000 while performing figure-8 maneuvers in a restricted area. It has a high aspect ratio main wing with a conventional empennage giving it a "sailplane" appearance. A specifications table and three-view drawing accompany this summary.

The flight plan calls for ascent to cruise altitude at 20 ft and then perform three figure-8 turns around pylons. These pylons will be separated by fifty yards and stationed inside a sports facility. Once completed, the pilot is to make use of any remaining power by loitering before landing the plane.

The propulsion system of the J4D consists of a propeller-electric motor combination with the prop mounted at the front of the fuselage. The Tornado 10 inch diameter, 6 inch pitch, two-bladed propeller is powered by an Astro 05 electric engine with 7 AA Nickel-Cadmium batteries. The system is capable of 50 watts of power and has throttling capabilities. Of the propellers with available data, the 10-6 was best fitted for the take-off distance and maximum current draw constraints. The 05 engine was chosen for being most lightweight while still supplying adequate power.

In order to provide sufficient lift for low speed travel, the J4D has an aspect ratio of 11.72 with an 8.2 inch mean chord. The wing consists of a spar and rib construction with Micafilm skin. Its low-mount and dihedral in combination with the vertical tail were prescribed to allow for excellent maneuverability. A major problem, however, is that due to the nature of a low-speed mission, there is little margin for error between the cruise and stall velocities. As far as center of gravity travel is concerned, a square fuselage will internally contain the servos, engine, and so that the CG of the airplane is kept at about 33% of the chord.

A combination of directional and longitudinal control will enable the J4D to perform the figure-8 maneuvers. However, in order to avoid the

construction and servo weight of ailerons, the rudder was designed to be over one-half the size of the vertical tail to insure that the proper roll motion could be attained.

After a semester of hard work and discussion, the members of Group D feel that this proposal is a well-established answer to the station keeping mission. We are confident in the success of our design and believe that the Screem-J4D is worthy of continued support.

Aerospace Engineers for the Twenty-First Century

SCREEM-J4D

Span = 96 inches
Chord = 8.2 inches
Length = 37 inches
Weight = 3.0 pounds
Dihedral = 10°
Control: Rudder and Elevator
Engine: Astro 05
Propeller: Tornado 10-6

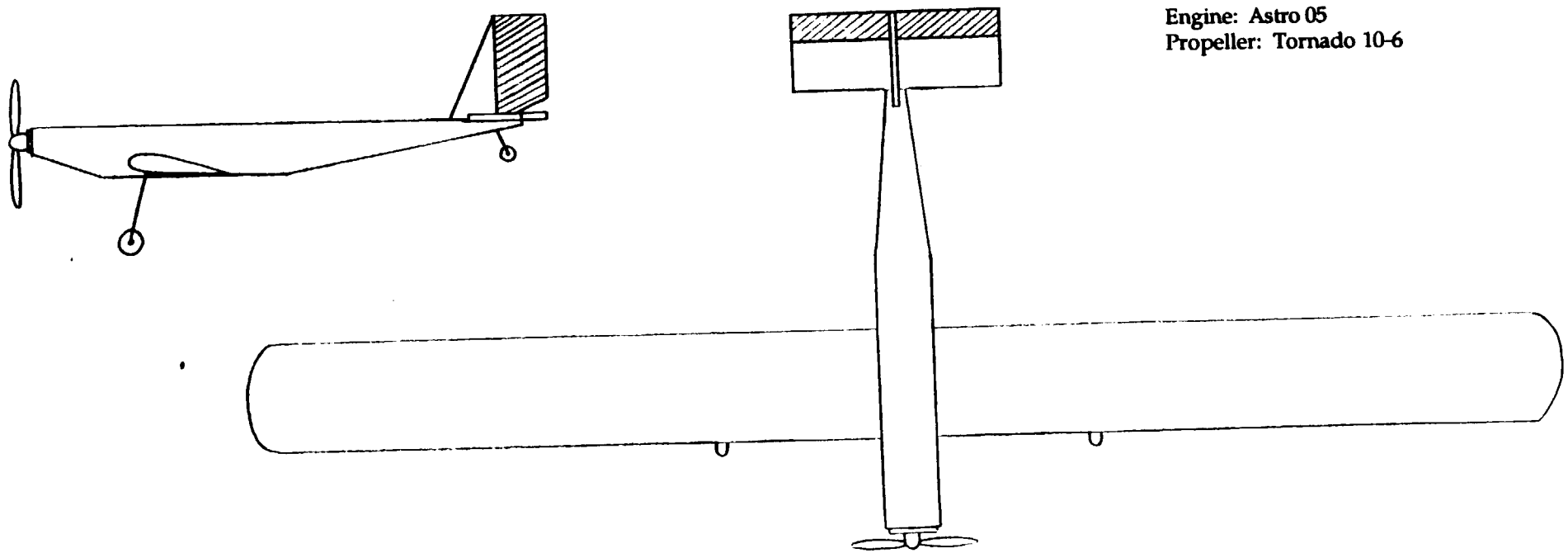

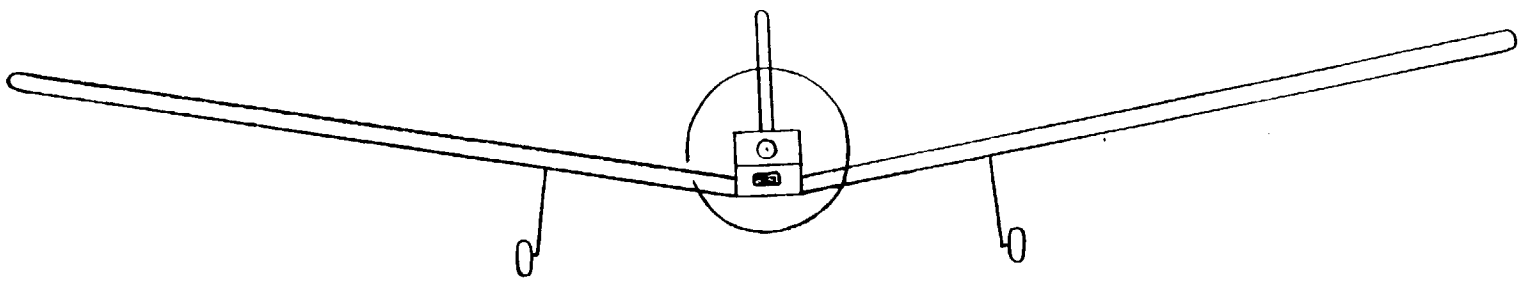

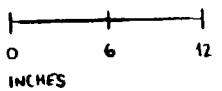

SCREEM - J4D SPECIFICATIONS

PERFORMANCE

Endurance	3.9 min @ 23 ft/s
Range	5500 ft @ 23 ft/s
Stall Velocity	18.9 ft/s
Maximum Velocity	58.6 ft/s
Maximum Rate of Climb	6.3 ft/s
Maximum Power Available	50 Watts
Maximum Bank Angle	30 degrees
Maximum Roll Rate	28.8 degrees/s
Minimum Turning Radius	28.6 ft
Minimum Glide Angle	- 4.1 degrees
Minimum Takeoff Distance	42 ft
Maximum C_l	1.3
Maximum Angle of Attack	14.5 degrees

CONFIGURATION

Wing Span	96 in (8 ft)
RPV Length	37 in (3.1 ft)
Weight	3 lbs (48 oz)
Wing	
Airfoil Section	NACA 4415
Angle of Incidence	3.5 degrees
Aspect Ratio	11.72
Chord	8.2 in
Dihedral	10 degrees
Taper Ratio	1.0
Fuselage	
Cross section	4 in X 4 in
Payload Volume	25.17 cu in
Empennage Airfoil Sections	Flat Plate
Horizontal Tail Area	.63 sq ft
Elevator Area	.21 sq ft
Vertical Tail Area	.38 sq ft
Rudder Area	.21 sq ft
Motor	Astro 05
Battery Pack	7 AA Nickel-Cadmium
Propeller	Tornado 10-6

INTRODUCTION

Upon receiving the request for proposals on January 18, 1990, in regards to a low Reynold's number station keeping flight vehicle, Design Group D began their design phase in pursuit of such a vehicle. Each member presented his ideas in regards to the mission requirements and goals which facilitated the group in their formal presentation of the Design Requirements and Objectives. The individuals also presented various conceptual designs from which the group as a whole chose one and then discussed modifications. Each member then concentrated his efforts on a particular aspect of the design phase. The group chose to divide responsibilities such that members assumed roles in the technical areas of aerodynamics, stability and control, propulsion, and structures. Each conducted extensive trade studies which shaped the design of the aircraft. The group presented the status of their design proposal in a comprehensive Preliminary Design Review on March 28, 1990.

Upon receiving approval for their design, the group began the manufacturing and formal documentation phases. The manufacturing began April 17, 1990, and progressed rather rapidly due to the assigning of a chief engineer and the eagerness of the other members. The aircraft assembly was complete on April 29 and was rolled out for ground testing on May 1, 1990. The aircraft was first flown successfully on May 4, 1990. In regards to the documentation of the design, each member contributed his expertise and studies to this final written report. It is presented as an overview of this design process and as a guide for other design teams to follow.

The members of Aerospace Design Group D have chosen to change their name to one that is less generic and more suggesting of their direction. They are now referred to as Aerospace Engineers for the Twenty-First Century, which is abbreviated AETC. Likewise, they have designated their aircraft the SCREEM-J4D. This is an acronym derived from the first letter in each member's name: Steve, Chris, Rob, Eric, Ed, Mike, and Jeff. The "4D" stands for "For Diploma". It is often referred to as the J4D.

This document represents the Final Design Proposal as presented by the Aerospace Engineers for the Twenty-First Century in response to the request for proposals for a low Reynold's number aircraft. It progresses in sections with the first being a look at the preliminary concepts. The next five sections deal with the particular technical areas related to the design -- aerodynamics, stability and control, propulsion, weights analysis, and structures. Performance parameters are then considered followed by discussion related to the technology demonstrator. Discussion of the design ends with the conclusions section and a final word from the design team. The references and appendices represent good sources of information for future design teams.

SECTION I

PRELIMINARY CONCEPT DESIGN

A. Request for Proposals

The following Request for Proposals (RFP) provided the design requirements for a remotely-piloted vehicle (RPV) to be created by AETC.

UNIVERSITY OF NOTRE DAME
DEPARTMENT OF AEROSPACE AND MECHANICAL ENGINEERING

AE441: Aerospace Design: Request for Proposals
Spring 1990

FLIGHT AT VERY LOW REYNOLDS NUMBERS - A STATION KEEPING MISSION

OPPORTUNITY

Most conventional flight vehicles are designed to operate in a flight regime such that the Reynolds number based on mean wing chord are in excess of 10^6 and some currently approaching 10^8. Recently there has been interest expressed in vehicles which would operate at much lower Reynolds numbers, less than 10^5. Particular applications are low speed flight at very high altitudes, low altitude flight of very small aircraft and flight in other planets' atmospheres such as Mars. There are many unique problems associated with low speed flight which pose challenges to the aircraft designer and which must be addressed in order to understand how to exploit this low Reynolds number regime. Since many of the anticipated missions for this type of aircraft are unmanned, it is necessary to couple developments in unmanned aircraft development with our knowledge of low Reynolds number aerodynamics in order to develop an aircraft which can fly as slow as possible at sea level conditions. This study will help to better understand the problems associated with flight at these very low Reynolds numbers. Considering the potential applications, the aircraft must be very robust in its control and be highly durable.

OBJECTIVES

1. Develop a proposal for an aircraft and associated flight control system which must be able to:

a. Maintain level controlled flight and fly a closed course at flight speeds corresponding to Reynolds numbers less than 2×10^5 and as close to 1×10^5 as possible. The greatest measure of merit is associated with achieving the lowest mean chord Reynolds number possible and maximizing the loiter time on a closed course.

b. Be maneuverable and controllable so that it can fly a closed pattern and remain within a limited airspace.

c. Use a propulsion system which is non-airbreathing and does not emit any mass (i.e. rocket, etc.).

d. Be able to be remotely controlled by a pilot with minimal flying experience or an autonomous onboard control system.

e. Carry an instrument package payload which weighs 2.0 oz and is 2"x2"x2" in size.

2. Take full advantage of the latest technologies associated with lightweight, low cost radio controlled aircraft and unconventional propulsion systems.

3. All possible considerations must be taken to avoid damage to surroundings or personal injury in case of system malfunction.

4. Develop a flying prototype for the system defined above. The prototype must be capable of demonstrating flight worthiness of the basic vehicle and flight control system. The prototype will be required to fly a closed figure "8" course within a highly constrained envelope. A basic test program for the prototype must be developed and demonstrated with flight tests.

5. Evaluate the feasibility of the extension of the aircraft developed under this project to high altitude station keeping application for atmospheric sampling.

SYSTEM REQUIREMENTS AND CONSTRAINTS

The system designed shall satisfy the following.

a. All basic operation will be line-of-sight with a fixed ground based pilot, although automatic control or other systems can be considered.

b. The aircraft must be able to take-off from the ground and land on the ground.

c. The aircraft must be able to maximize the loiter time within a restricted altitude range on a figure "8" course with a spacing of 150 ft between two pylons which define the course.

d. Ground handling and system operation must be able to be accomplished by two people.

e. The complete aircraft must be able to be disassembled for transportation and storage and fit within a storage container no larger than 2'x2'x4'.

f. Safety considerations for systems operation are critical. A complete safety assessment for the system is required.

SPECIAL CONSIDERATIONS FOR THE TECHNOLOGY DEMONSTRATOR

a. The Technology Demonstrator will be a full sized prototype of the actual design.

b. The flight tests for the Technology Demonstrator will be conducted in the Loftus Center on a closed course similar to the one described above. The Demonstrator will be required to complete 3 laps on the course. The altitude must not exceed 25' at any point on the course.

c. Takeoff must be accomplished within the 150' takeoff region shown on the enclosed figure.

d. Loiter time will be based on the time needed to complete the 3 complete laps in the air.

e. The design team must make provisions for estimating altitude and flight speed during the tests. This information is to be monitored from ground based observers.

f. The propulsion system for the Technology Demonstrator must not contain any chemicals or any other substance which could prove harmful to the Loftus Center or the aircraft operators.

g. The radio control system and the instrumentation package must be removable and a complete system installation should be able to be accomplished in 30 min.

h. System control for the flight demonstrator will be a Futaba 6FG radio system with up to 4 S28 servos or a system of comparable weight and size.

i. All FAA and FCC regulations for operation of remotely piloted vehicles must be complied with.

B. Mission Evaluation

In order that the aircraft possess the ability to perform the basic mission, there are several additional constraints regarding the aircraft and its mission which need to be specified. In order to maintain a lightweight and relatively simple airframe, no ailerons will be used. All banking and turning will thus be accomplished by deflection of the rudder. Due to the possible complications of flying into and out of ground effect, it is desirable for the aircraft to be above the influence of ground effect before banking into the first turn. Therefore, the aircraft must enter and leave all turns at the design cruise altitude, losing or gaining as little altitude as possible. This may require elevator deflections and/or throttle setting adjustments. For safety, the aircraft will be flown at an altitude of 20 feet, which is 5 feet below the absolute ceiling of the test area. This gives the pilot a margin (although small) to make adjustments to save the plane in the event it would act unpredictedly.

Combining these two constraints, it is evident that upon take-off the aircraft should climb quickly to its cruise altitude of 20 feet and remain there for the duration of the mission. By somewhat arbitrarily selecting the take-off distance to be 75 feet (which is one-half of the available runway), it becomes necessary for the aircraft to climb at a flight path angle of 15 degrees to reach the cruise altitude of 20 feet over a horizontal distance of 75 feet.

As stated in the RFP, the flight envelope is very constrained, and as such the aircraft needs to be very maneuverable. With that in mind, AETC feels that the aircraft must have the capability to complete the turns using a 40 foot radius, leaving no less than 20 feet between the aircraft and any side boundary of the flight envelope during the duration of the mission. Since a large loiter time is the greatest figure of merit, flying the mission at the lowest possible velocity is a must. But everything is related, and since wing surface area (and thus weight) go up as velocity goes down, a compromise exists somewhere in between. It is our goal to find that compromise.

C. Design Requirements and Objectives

In order to insure that the minimum goals defined in the RFP as well as those specified in the above mission evaluation are satisfied, AETC has imposed some additional (or more stringent) constraints on its RPV. They are:

1. Maintain controllability while taxiing. Since the aircraft must be ground launched, it is necessary for it to be steered while still on the ground at speeds lower than those necessary for the lifting surfaces to provide this directional control. For this reason, the landing gear must be coupled with the avionics system to avoid the necessity of an additional servo to control the ground steering.
2. Achieve airborne flight after a takeoff run of no more than 75 feet. This constraint forces the aircraft to be off the ground and climbing with no less than half of the runway left. This means that should some problem occur immediately upon takeoff, there will still be sufficient runway left to put the aircraft back on the ground without running it into a wall. Additionally, this gives the aircraft a relatively long time to reach its cruise altitude of 20 feet; mandating a flight path angle of approximately 15 degrees.
3. Climb at no less than 6 feet per second. Based on a cruise velocity of 23 feet per second; if the aircraft takes off in 75 feet this rate of climb will allow the aircraft to climb to its cruise altitude of 20 feet by the end of the runway.
4. Maintain controllable flight at a chord Reynolds number of no more than 1×10^5. This is the lower limit of the Reynolds numbers targeted in the RFP. Setting the design point at this Reynolds number ensures that should small increases in velocity become necessary to avoid stall, the Reynolds number will not be pushed over the 2×10^5 upper limit.
5. Maintain altitude during turns of no less than 270 degrees on no more than a 40 foot radius at bank angles of up to 30 degrees. This constraint evolved from safety considerations for the operator of the aircraft and for the preservation of the aircraft itself. The figure "8" course mandates the turns of at least 270 degrees; without these turns the aircraft will surely find its way into a wall. The radius requirement ensures that the aircraft will possess the ability to turn well within the maximum allowable radius of 60 feet given by the geometry of the test flight area. Finally, the bank angle constraint ensures

that even at severe bank angles, the aircraft will be in no danger of dragging a wing on the ground due to lost altitude. Please note that in order to maximize the loiter time, the final test flight may not be flown at these target values, but the aircraft must possess the ability to fly there should the situation or need present itself.

6. Weigh no more than 3 pounds. This constraint evolved from comparisons with other remotely piloted vehicles of similar size or mission. The primary consideration here was that a lighter weight would allow for a lower velocity and subsequently higher loiter time.

These constraints provided the guidelines by which AETC's aircraft, the SCREEM-J4D, was designed and ultimately constructed. While not specifically directed at any one area or sub-system of the aircraft, these constraints had far-reaching implications in all aspects of the aircraft's design and construction. Table 1-1 is a summary of these constraints.

TABLE 1-1: Design Constraints for the SCREEM-J4D

1. Maintain controllability while taxiing.
2. Take-off in distance $\leq$ 75 ft.
3. Climb at $\geq$ 6 ft/s and fly at altitude = 20 ft.
4. Maintain contollable flight at a chord Reynolds number $\leq 1 \times 10^5$.
5. Maintain altitude during turns $\geq$ 270 degrees with turn radius < 40 ft at bank angles $\leq$ 30 degrees.
6. Weight $\leq$ 3 lbs.

D. Concept Selection Study

The selection of a concept became a laborious task for AETC once the Design Requirements and Objectives (DR&O) were completed. The constraints given by the RFP in addition to those in the DR&O had to be weighed very carefully in the process of selecting a final concept. The approach that AETC took was

considering three different concepts which were unrelated to each other but were proposed by at least one member of the group. This was reasonable due to the fact that each concept was considered in a more general form with relation to the constraints. A more detailed analysis followed once one of the three concepts was selected.

One of these concepts was a biplane configuration with a conventional empennage (Figure 1-1). The main advantage of the biplane was that it could provide extra lift which is vital to flying at low Re. Nonetheless, the disadvantages were too numerous. The complications in resolving the interference effects, the construction and connection of the two wings, and the additional weight with the added wing were the main disadvantages which prompted our decision to reject the biplane concept.

Another concept which AETC labored over for about a week was a canard configuration with a vertical tail (Figure 1-2). The canard was considered able to provide extra lift while maintaining maneuverability and not adding weight. However, after doing further research on low speed RPV flight, AETC discovered that the canard would have to be too large in order to have a significant contribution toward the total lift. As a result, the airplane would have just as much if not more wing surface area as a conventional airplane without the convenience of the classical stability equations. Thus, the canard concept was considered "pretty" but not the most efficient concept for the mission.

A third concept which AETC decided to chose for the mission was the "sailplane" type airplane with a conventional empennage. The most important factor in the selection of this concept was that the theories and equations which were such a big part of undergraduate aerospace study could be most readily applied to the conventional airplane. In addition, the learning process of the design and construction of this concept is useful in gaining a better understanding of the process involved with the 747's, DC-10's, etc., becoming a realistic part of the transportation industry.

Table 1-2 is a comparison matrix of the three concepts with regard to several critical factors found in the DR&O or assumed from low speed flight. A +1

Figure 1-1: Biplane Configuration

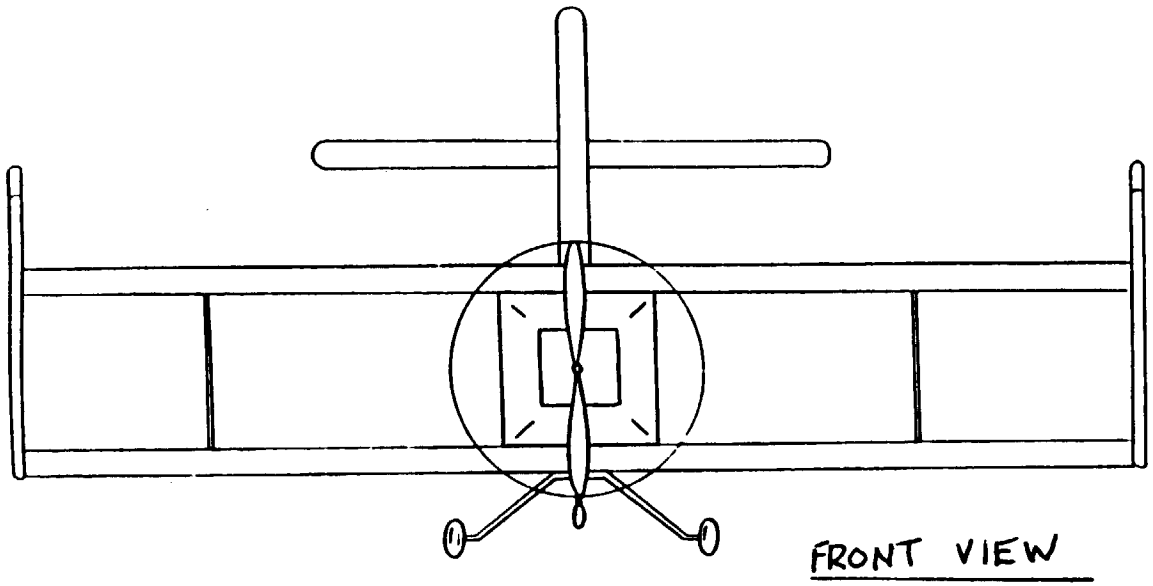

FRONT VIEW

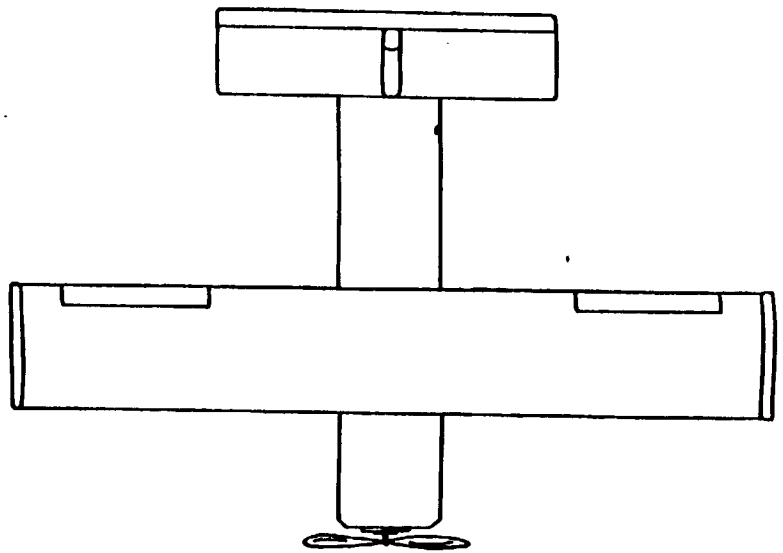

PLAN VIEW

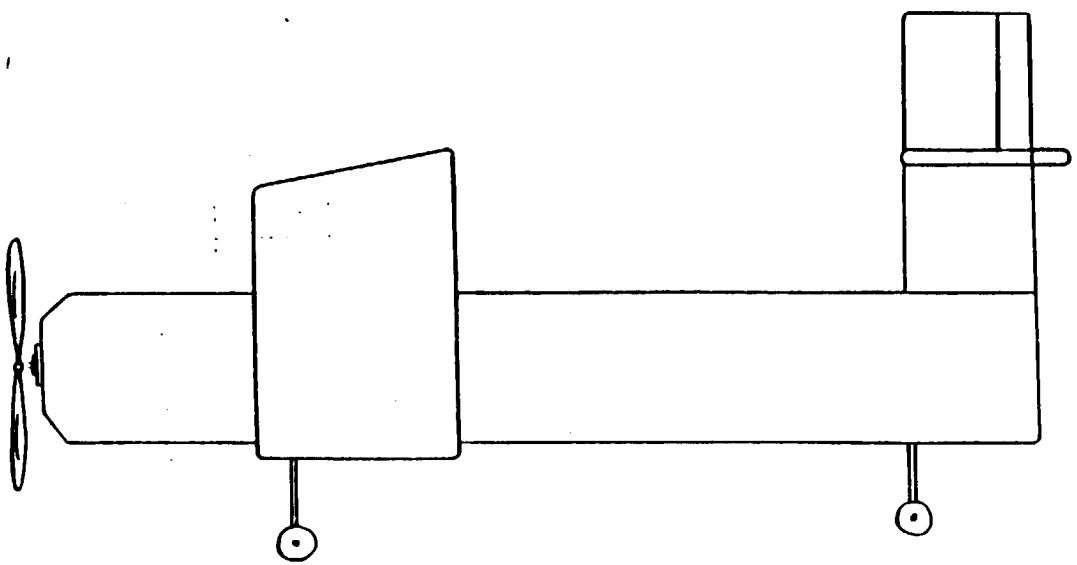

SIDE VIEW

Figure 1-2: Canard Configuration

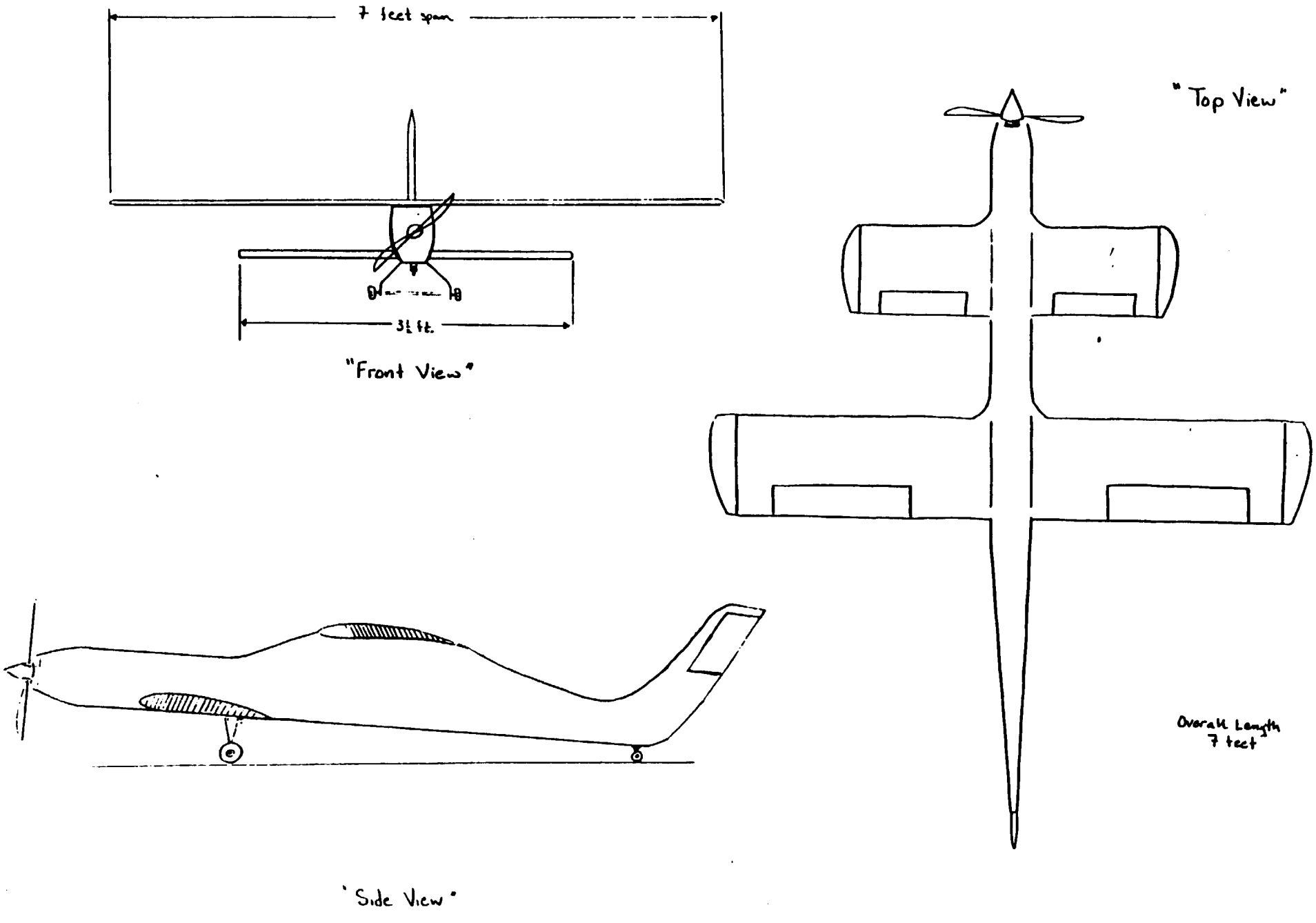

denotes that the design would benefit from the concept while a -1 denotes that it would be detrimental. This table enabled AETC to be more easily convinced that selecting a high aspect ratio conventional airplane as their concept would best suit the mission.

TABLE 1-2: Comparison Matrix for Concepts Considered

FACTOR	BI-PLANE	CANARD	CONVENTIONAL
Added Lift	+1	0	0
Ease of Construction	-1	+1	+1
Weight	-1	0	0
Use of Equations	-1	-1	+1
Maneuverability	-1	-1	-1
TOTAL	-3	-1	+1

The initial analysis for providing a little more detail to the concept was based on the Reynold's number constraint of 100,000 and the weight constraint of 3 pounds. Given that the Re is proportional to the mean chord length and the velocity and inversely proportional to the kinematic viscosity, it was seen that by selecting a target Re and varying the mean chord, a velocity which satisfied the constraint would be produced. Using this velocity and chord and estimating a target lift coefficient, the span necessary to produce the required lift was calculated. This process was aided by use of Computer Program A which is located in Appendix I. However, knowing that no piece of the aircraft can be longer that 4 feet required that the span be kept reasonably low in order to avoid having a wing with too many sections. Using this method with the lift coefficient of 0.9 and a weight of 3 pounds, it was found that the allowed velocity and required span for a chord of 5 inches was 40 ft/s and 4.2 feet, respectively; while for a 12 inch chord, the same quantities would be 16 ft/s and 11 ft.

Because the loiter time is dependent on velocity, the first case is not optimal, and because lightweight is of critical importance, the large wing area of the

second case, with its smaller velocity, is not optimal. Obviously, AETC's solution fell between these cases.

AETC made seveal other decisions about the conventional concept once it became obvious it was best suited for the mission. In addition to the high aspect ratio wings, AETC decided against tapering the wing because the chord at the tips would become too low and possibly introduce problems with extremely low Re flight. Additionally, an untapered wing is much easier to construct since the airfoil sections are all the same size. Ailerons were discarded as a possibility because the added weight of a servo and the construction required outweighed the advantages of better roll performance. Past RPV's and research proved that the same roll performance could be attained with just the elevator and rudder in the first place. Sweep is not advantageous for low speed flight since it reduces the effective velocity the wing sees. However, dihedral aids in roll control. Winglets were considered in the concept study in order to reduce induced drag. But when the high aspect ratio of the wing was considered, it was decided that the effect of winglets would be too small to justify the added weight and construction difficulties. A low-mount wing was selected to help destabilize the roll which would facilitate the figure-8 maneuvers.

The fuselage was selected to be a box configuration for ease of construction and containment of the propulsion system. The aft section of the fuselage was tapered to reduce weight and skin friction drag.

The empennage was designed to contain two control surfaces -- rudder and elevator. A relatively large rudder (55% of vertical tail area) was needed to produce the yaw required to attain the desired roll moment. The rudder, in conjunction with a large wing dihedral (10 degrees), enabled the aircraft to perform the figure-8 turns as desired. The elevator comprised 33% of the horizontal tail area, ensuring positive longitudinal stability and control. The center of gravity was placed behind the aerodynamic center so that the horizontal tail would produce lift rather than a downward force.

Lastly, the landing gear was comprised of three wheels -- one on either side of the fuselage mounted to the wing and one in the rear as a tail dragger. The

two on the wing were spaced well enough to prevent tipping during take-off. The tail dragger was connected to the rudder so that one servo could be used for turning control during ground roll and flight.

These characteristics of the basic concept may be seen in the three view drawing in the Executive Summary.

SECTION II

AERODYNAMIC CONFIGURATION

A. Airfoil Selection

At low Reynolds numbers, viscous effects become more significant with respect to inertial effects. The viscous region extends beyond the surface of the body both in the lateral and longitudinal direction. The wake retards the oncoming freestream, while interaction between the viscous and inviscid regions is strong and nonlinear. Therefore, small changes in the position (i.e., attack angle) of the body exposed to the flow will cause significant changes in the surface pressure distribution. Due to the effects of this viscous region, the flow is less capable of negotiating an increase in pressure. The adverse pressure gradient can grow large enough to affect a peculiar aerodynamic phenomenon--a separation "bubble," which is an enclosed region of stagnant air that develops on the upper surface(s).

The flow over a smooth airfoil at low Reynolds numbers is often laminar, unless means are employed to disturb the flow and thereby induce turbulence. (Disturbing the flow energizes the boundary layer, thereby increasing inertial effects and delaying separation). As the Reynolds number decreases in laminar (undisturbed) flow, a separation bubble develops on the upper surface and effectively increases the camber of the airfoil, thus providing additional lift. However, the separation bubble is extremely sensitive to disturbances (such as surface roughness and sound), and/or an increase in the angle of attack. If the separation bubble breaks down, the pressure drag will increase drastically. In addition, hysteresis is particularly significant in airfoil data taken at low Reynolds numbers and at high angles of attack. Therefore, the airfoil performance depends strongly on whether the angle of attack is increasing or decreasing. Thus, in selecting an airfoil, it is important to keep in mind the characteristics of that airfoil in the low Reynolds number regime, as well as the flight plan dictated by the mission requirements. In particular, selection criterion should include gradual stall, high stall angle and/or low stall speed, and lift performance which suits the flight plan and aircraft gross weight.

Measures of Merit: To select the airfoil intended for operation in a low Reynolds number regime, the following characteristics are necessary:

1. Favorable lift curve slope and high $C_{L_{max}}$

2. Gradual stall
3. High lift/drag ratio
4. Ease of fabrication

Design Constraints and Considerations: There are several fixed aerodynamic performance parameters which are influential in the design of the airfoil. The following were most critical to the J4D:

1. Cruise Reynolds number (based on mean wing chord), $Re_c=10^5$
2. Cruise velocity, $V_\infty = 23$ ft/s
3. Mean wing chord, c = 0.683 in.
4. Freestream density, $\rho=2.37 \times 10^{-3}$ slugs/ft^3

Besides these constraints, there are two are other important guidelines which were used during the design phase. The first was the capability of precise fabrication of the selected airfoil. For example, very thin airfoils, although popular for low Reynolds number operation, are difficult to construct precisely with the materials and tools which were available to AETC. In addition, thin airfoil sections are subjected to higher stresses in flight and under static conditions. The second important consideration was that stall characteristics must be amenable to the desired flight conditions. Given the requirements for lift performance, the maximum lift desired must be achievable without flying at a geometric angle of attack close to the stall angle (α_{stall}). Therefore, finite lift characteristics yielded by the airfoil parameters and the wing geometry must be acceptable for the mission requirements while restraining the wing size to reasonable limits to minimize the aircraft overall weight.

Assumptions: Because the airfoil data used in the selection process [Ref. 12] was taken at Reynolds numbers close to, but not exactly, the design operating Reynolds number for our vehicle (10^5), interpolation was necessary to determine the important parameters (zero-lift angle of attack, C_{lmax}, lift curve slope, α_{stall}, and maximum L/D). Figure 2-1 is an indication of the estimated data for Re= 10^5, for the NACA 4415. A linear variation with Reynolds number was assumed for determining this data. In addition, hysteresis effects were neglected since the intended flight plan is a steady state cruise at a constant α.

Figure 2-1

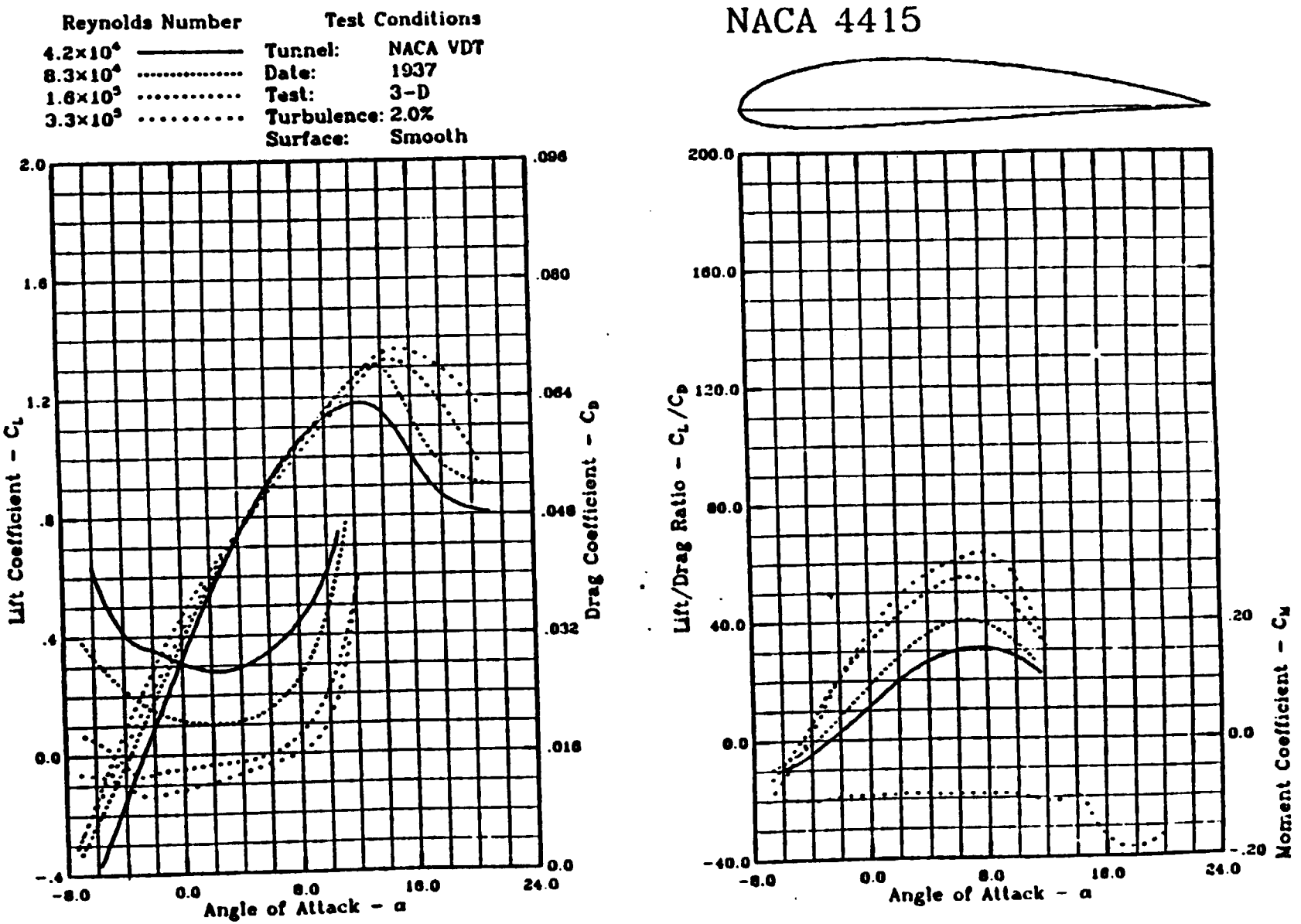
NACA 4415
Reynolds Number
4.2×10⁶
8.3×10⁶
1.6×10⁷
3.3×10⁷
Test Conditions
Tunnel: NACA VDT
Date: 1937
Test: 3-D
Turbulence: 2.0%
Surface: Smooth
Lift Coefficient - C_L
Drag Coefficient - C_D
Angle of Attack - α
Lift/Drag Ratio - C_L/C_D
Moment Coefficient - C_M

Selection Procedure: To avoid the separation difficulties associated with flight in the low Reynolds number regime, there are two primary design options: (1) provide means for energizing the boundary layer and thereby delaying separation, and (2) fly at geometric attack angles well below α_{stall}. There are, however, disadvantages associated with each of these options. Option (1) implies a substantial skin friction drag penalty, since the wall shear stress is greater for turbulent flow. If option (2) is selected, the risk of separation and stall are greater with an unexpected increase in α (gust, nose up). Because minimizing drag is an important objective in this design, and because the desired lift performance can be achieved at angles of attack well below α_{stall}, option (2) was employed on the SCREEM-J4D.

The research for airfoils at low Reynolds numbers was conducted with Reference 11, critically evaluating each airfoil based on the measures of merit above. A number of laminar flow airfoils were rejected with relatively sharp leading and trailing edges because of substantial fabrication difficulty and the concern with high stresses in these thin regions. In addition, the precision requirements of laminar flow airfoil construction are unrealistic given the time and resources available to AETC. Very slight disturbances, particularly at the leading edge, will produce undesirable effects if design option (2) is to be used. (Option (1) is not compatible with laminar flow airfoils, due to the associated skin friction drag penalty). Thus, although better lift characteristics are produced in the low Reynolds number regime by laminar flow airfoils, disturbance of the laminar flow is very difficult to avoid; therefore, a thicker airfoil profile is desirable.

After a thorough evaluation of the low speed airfoils found in Reference 12, two were selected for final analysis, the AH 79-100C and the NACA 4415 (see Figures 2-2 - 2-8). A finite wing lifting-line analysis was performed for each airfoil using the computer program listed as Item 2 in the Appendix. The computer analysis requires the infinite lift curve slope and the zero-lift angle of attack of each airfoil. These parameters, coupled with the wing planform geometry, provide enough information to obtain reasonable predictions of the lift and induced drag characteristics of the finite wing. It was found that although the AH 79-100C achieved a better performance rating for the desired

Figure 2-2: Airfoils Considered

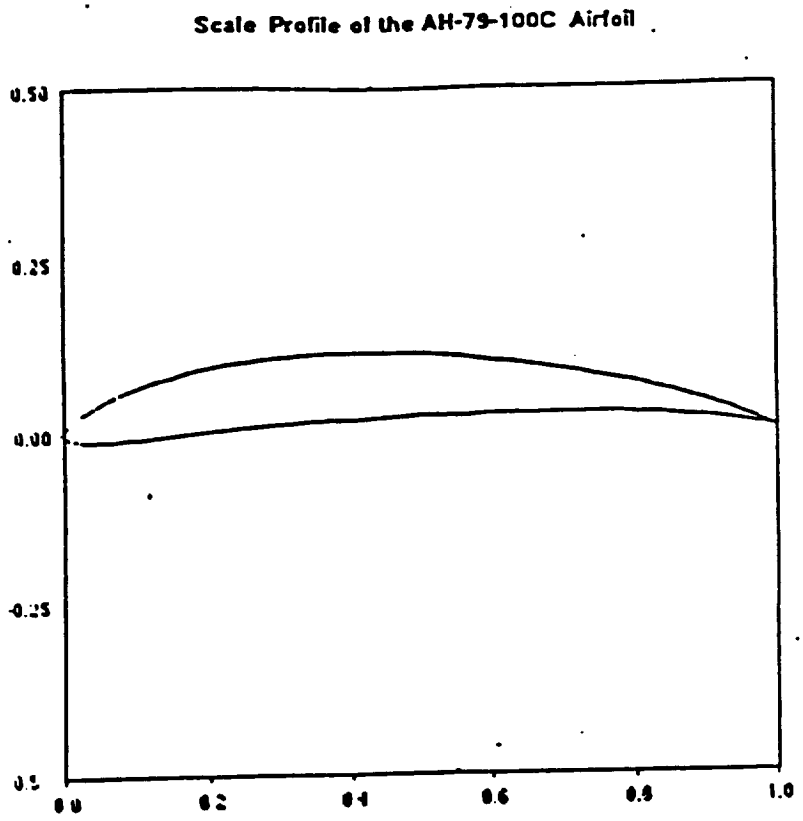

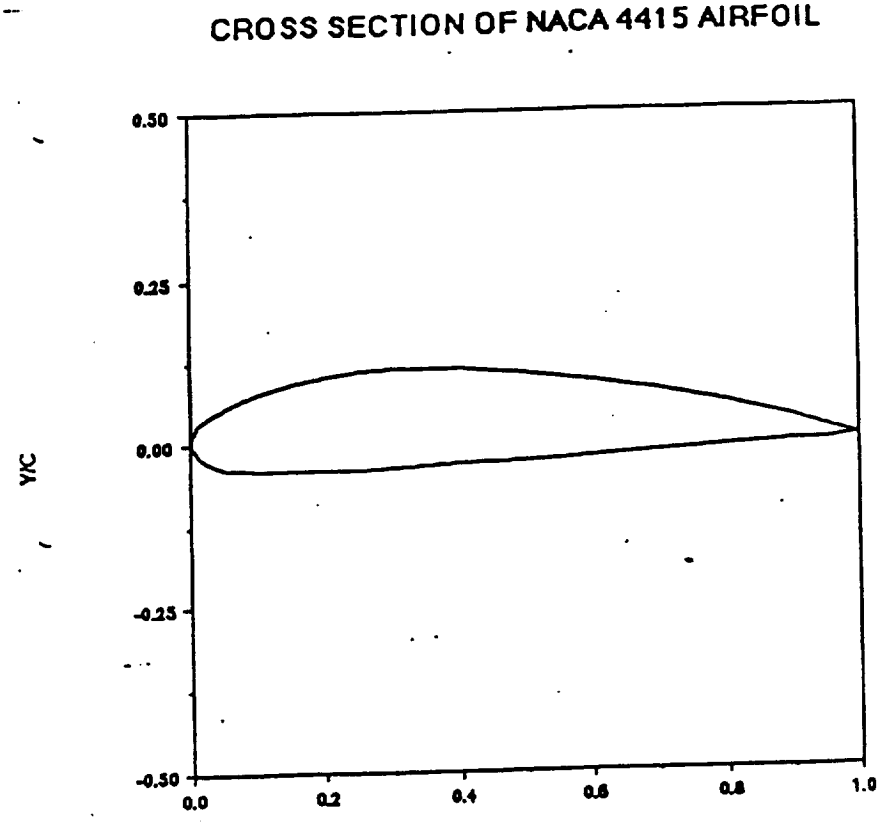

Figure 2-3. NACA 4415 Finite Lift Curve Slope

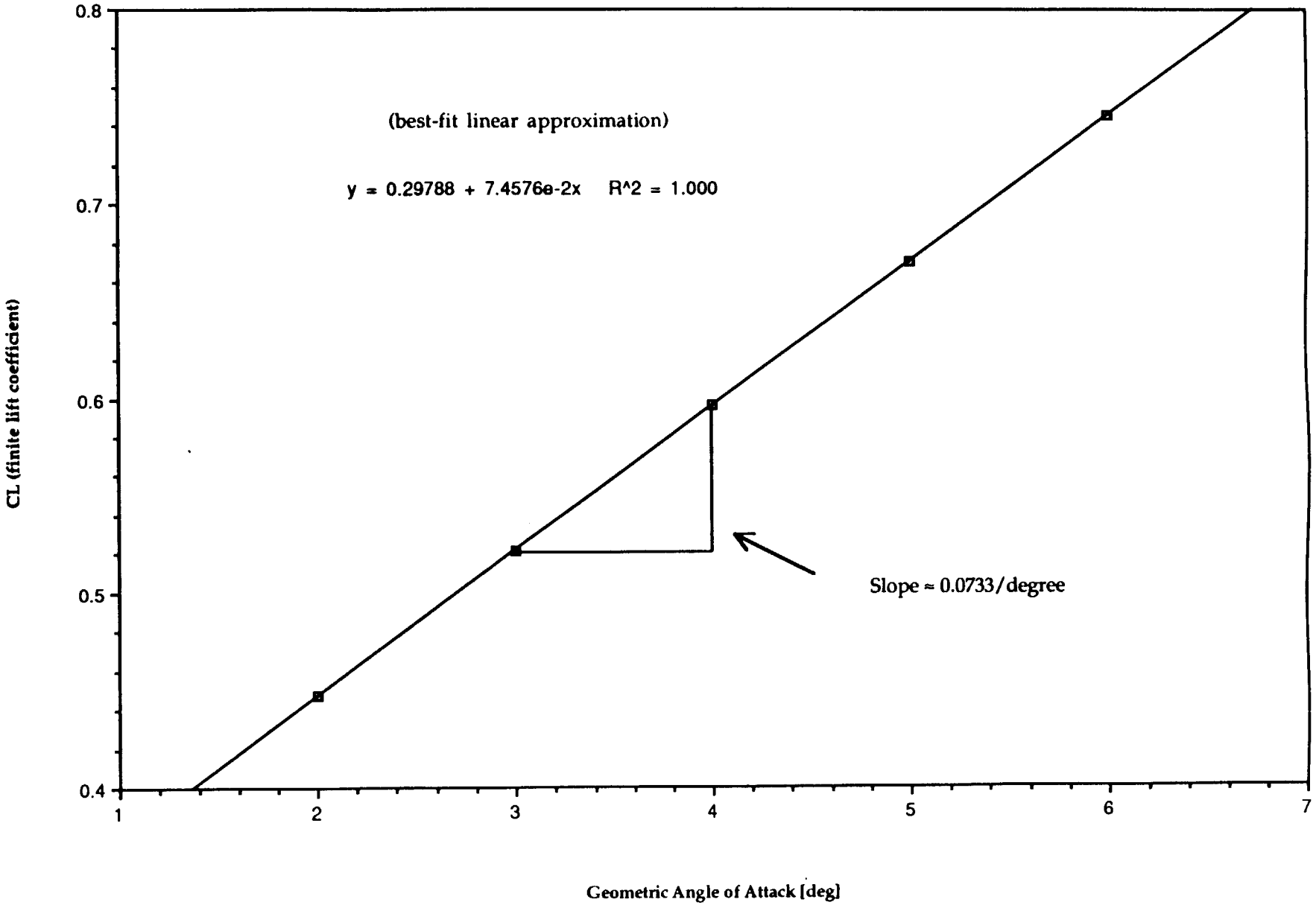

Figure 2-4. AH 79-100C Finite Wing Slope

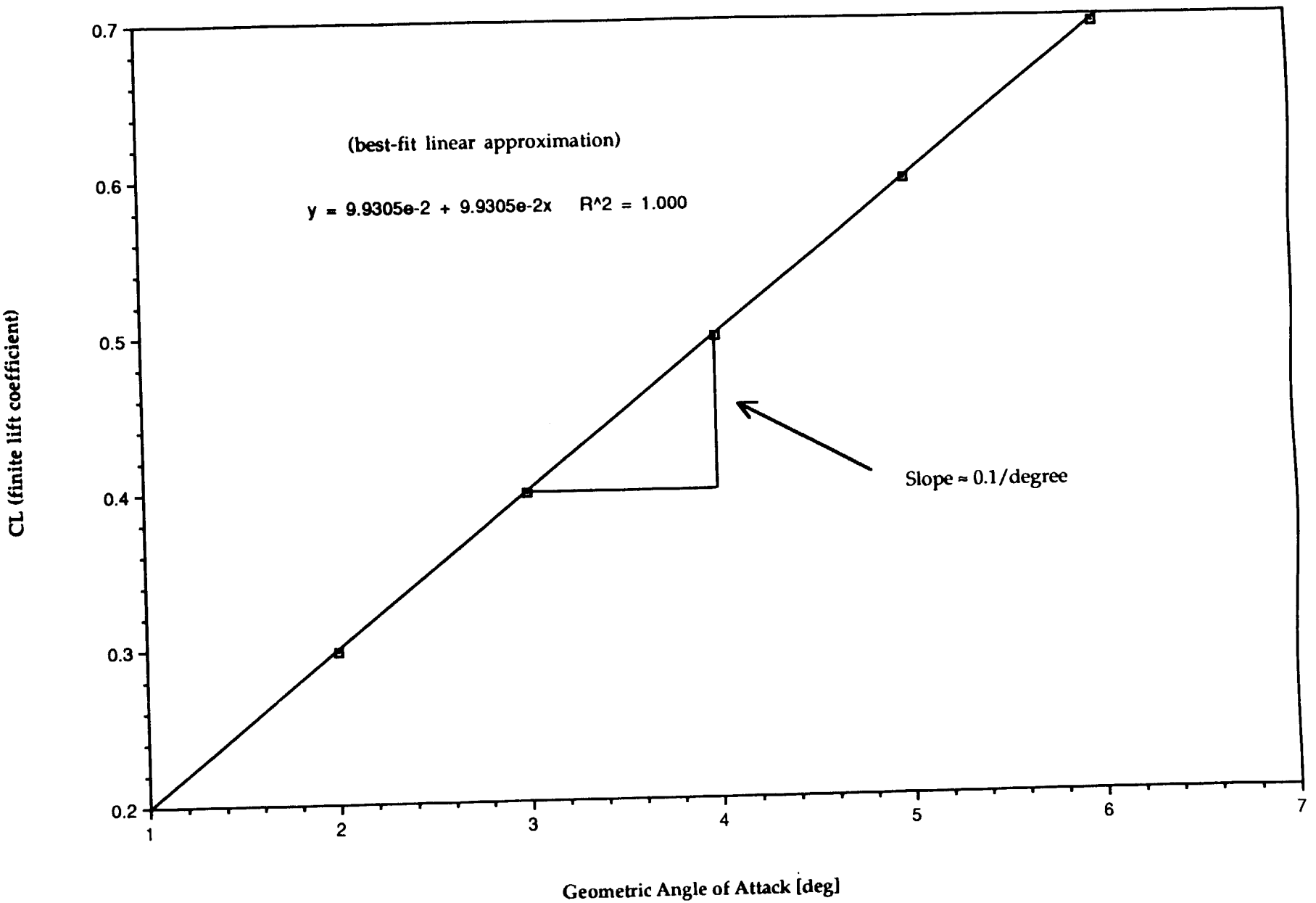

Figure 2-5. NACA 4415 CDi vs. Geometric Angle of Attack

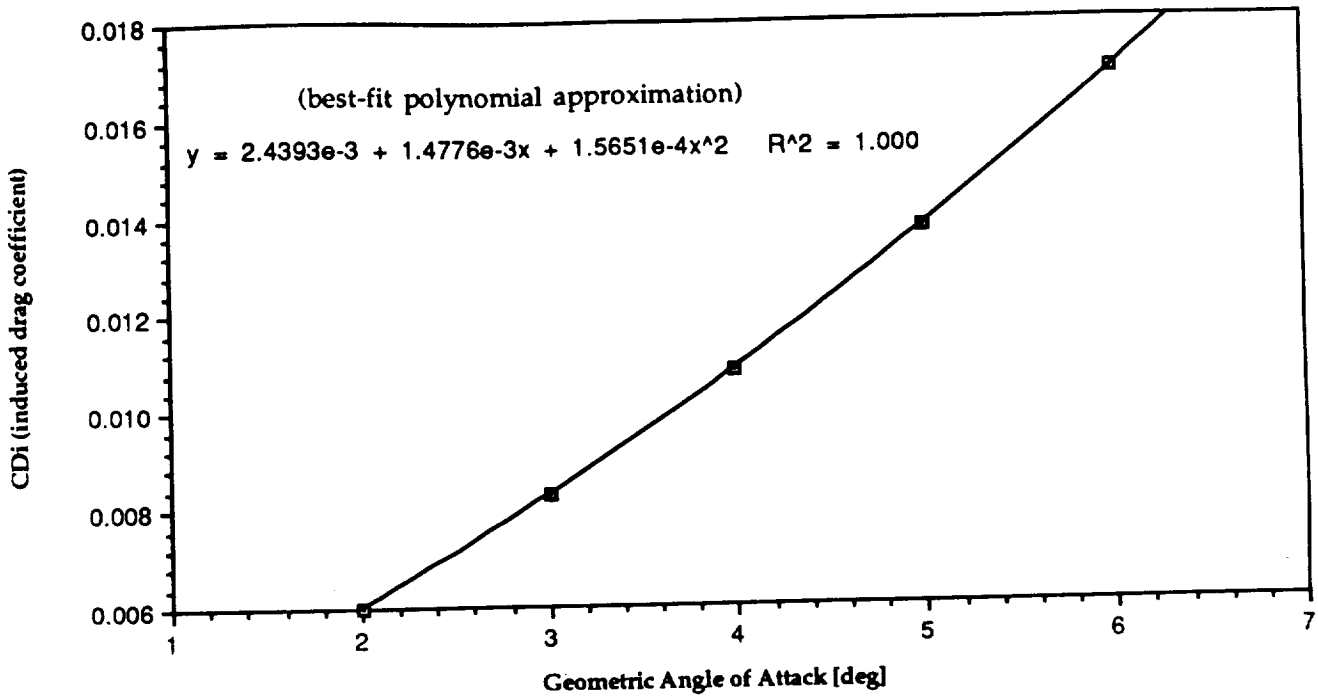

Figure 2-6. NACA 4415 Drag Polar

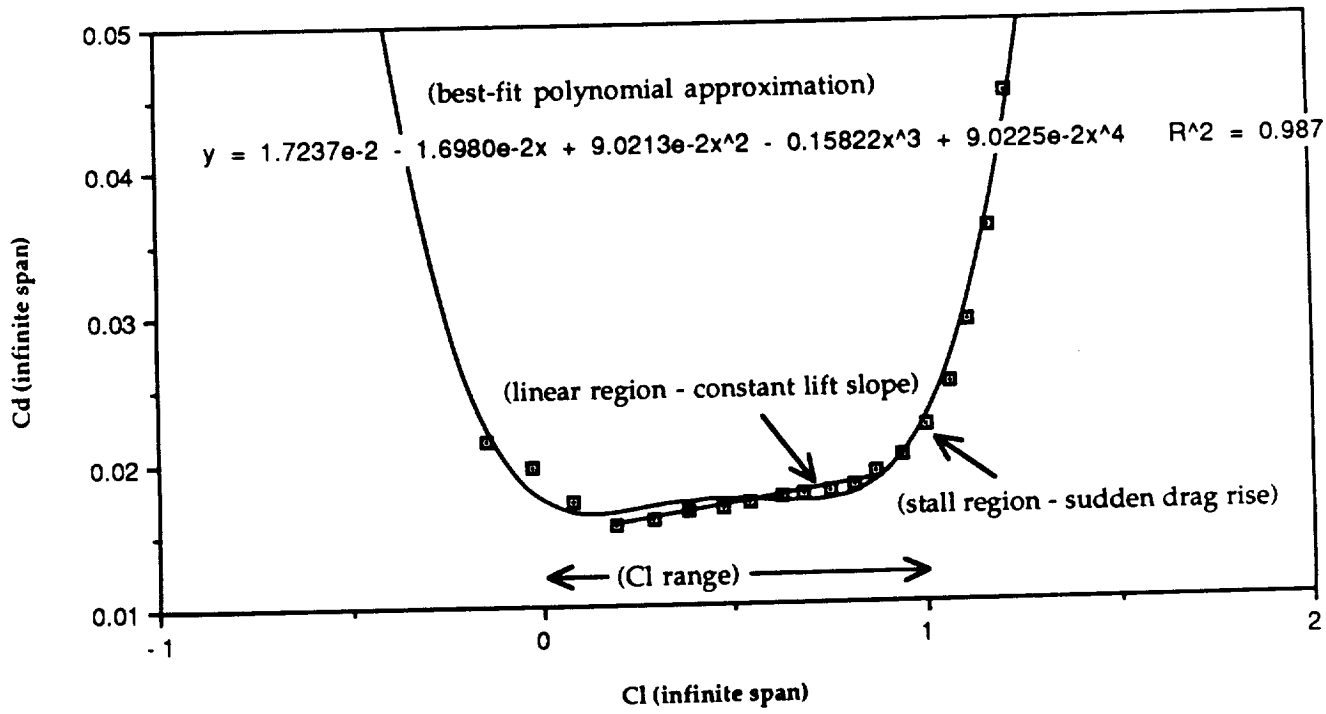

Figure 2-7. AH 79-100C CDi vs. Geometric Angle of Attack

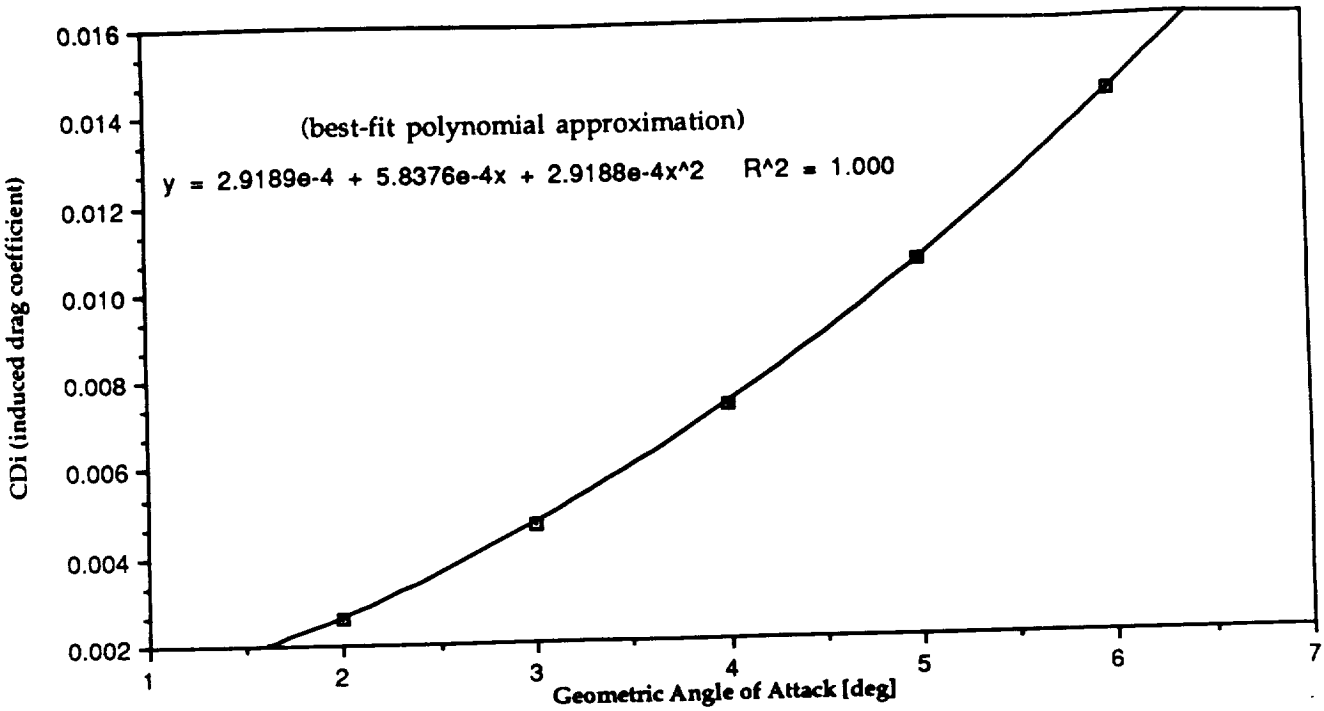

Figure 2-8. AH 79-100C Drag Polar

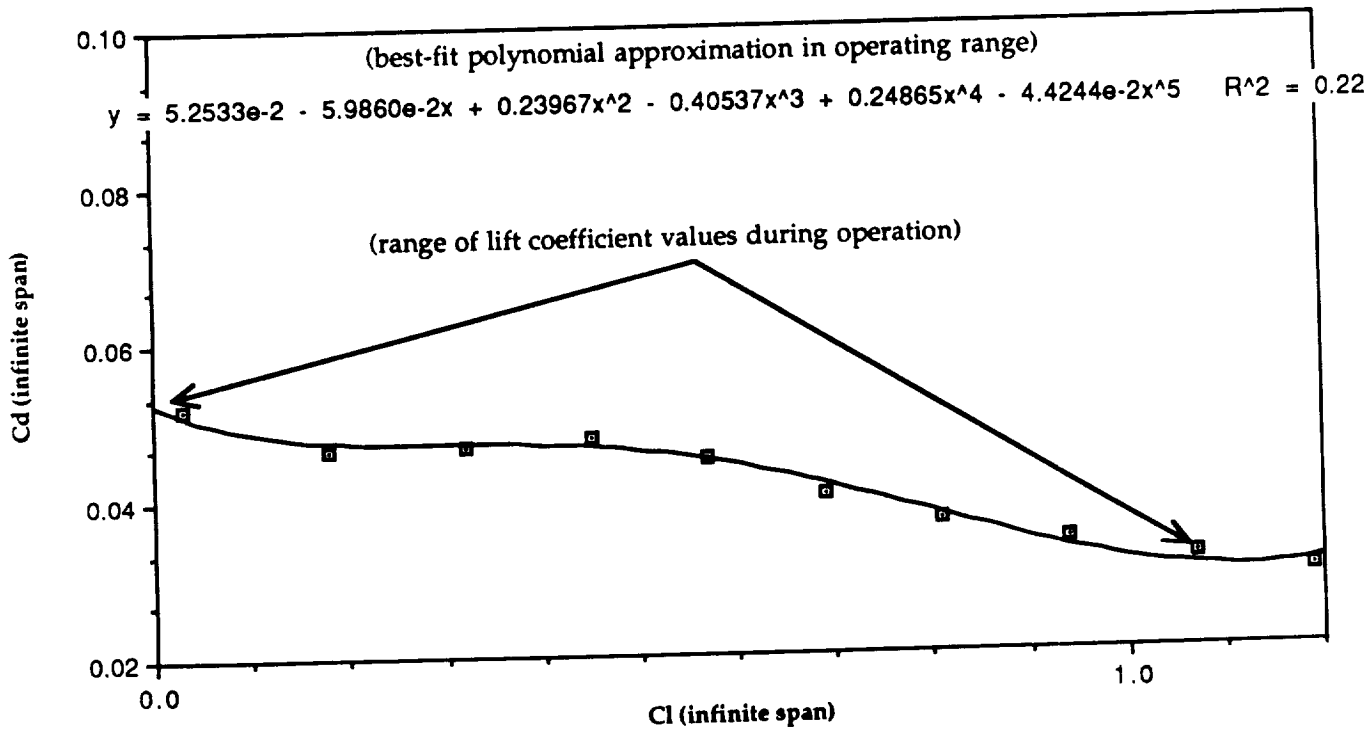

lift characteristics and the measures of merit above, it was not chosen as the main wing airfoil. The fact that it is so thin introduced construction difficulties and posed some concern for the airfoil's structural stability and consistency. Consequently, the AH 79-100C's better performance characteristics were not convincing enough to accept its disadvantages, and the NACA 4415 was selected by default.

Final Selection: The NACA 4415, based on the information available in Reference 12 and interpolated approximations for $Re=10^5$, has the following approximate parameters at infinite span:

Lift curve slope: 3.72 per radian
Zero-lift angle of attack: - 4 degrees
$C_{l_{max}}$: ~ 1.2
L/D_{max} : ~ 15.5

The values for maximum lift coefficient and maximum lift-to-drag ratio did, of course, change when a finite aspect ratio was considered.

B. Wing Geometry

Important Parameters: To specify the wing geometry, the following parameters must be determined:

1. taper
2. span
3. geometric and aerodynamic twist
4. dihedral (discussed in Section III)

These parameters were determined using these fixed (design) values:

1. mean-chord Reynolds number, $Re= 10^5$
2. cruise velocity, $V_\infty= 23$ ft/s
3. freestream density, $\rho\approx 2.37 \times 10^{-3}$ slugs/ft^3
4. freestream viscosity, $\mu\approx 3.76 \times 10^{-7}$ N·s/m^2

The wing span and chord variation together determine the planform [projected] wing area. The mean chord is fixed at a value of 0.68 ft by the cruise velocity and desired Reynolds number.

Measures of Merit: The planform geometry was selected based on the following characteristics:

1. finite lift curve slope
2. stall propagation pattern
3. spanwise lift distribution
4. induced drag
5. structural weight of wing and wing loading

It is desirable to obtain finite lift characteristics commensurate with the performance requirements and overall system weight. To minimize the overall system weight, the planform geometry was selected such that the overall weight of the main wing was at a minimum, given the performance requirements.

To obtain a favorable stall pattern, the planform geometry was selected such that the maximum lift coefficient occurs at the root of the wing. The stall will thus propagate from the root. This is particularly desirable for minimizing bending moments in the wing. This stall pattern is also desirable if control surfaces (i.e., ailerons) are to be located on the outboard wing sections. Although the SCREEM-J4D was designed without these control surfaces, minimizing wing bending moments is still extremely important.

An additional means of minimizing the stresses incurred in the wing is to obtain a lift distribution which, when coupled with the wing surface area, yields a reasonable wing loading. This total wing loading is obtained by integrating the spanwise lift distribution.

Design Constraints and Considerations: As previously mentioned, airfoil selection and wing geometry are influenced by several parameters which were fixed by AETC in the interest of successfully meeting the mission requirements. Table 2-1 is a summary of these fixed parameters.

TABLE 2-1: Design Parameters for Airfoil & Wing Geometry

PARAMETER	VALUE
ρ_∞	2.37×10^{-3} slug/ft^3
V_∞	23.0 ft/s
Re_c	10^5
aircraft gross weight	3.0 lbs

Other constraints and decisions were made during the preliminary design concept (in addition to fixed parameters):

- stall angle - required C_L must be achieved at $\alpha < \alpha_{stall}$
- no taper (taper ratio = 1.0)
- no aerodynamic twist

If a taper ratio is employed on a wing intended for operation at low mean-chord Reynolds numbers, separation effects will cause substantial lift reduction and drag increase at the tip section. This is due to a lower chord than the mean chord and hence the local Reynolds number is smaller than the mean-chord Reynolds number. Therefore, the taper ratio of the wing will remain fixed at 1.0.

Since the mean-chord is fixed by the Reynolds number and cruise velocity, and the chord is constant along the entire span of the wing, the span is determined by a choice of the planform area (or vice versa). Obviously, the choice of airfoil section also directly affects the finite lift characteristics of the wing. The [infinite] airfoil section parameters which affect the finite lift characteristics are the lift curve slope and the zero-lift angle of attack. Because the lift generated by the wing depends on its wetted surface area, the lift is dependent on the choice of wing area or span. In this case, area and twist are the only wing geometry parameters which need to be specified to generate a certain lift force. Aerodynamic twist will not be employed, in the interest of simple wing construction. Thus, our wing geometry options are limited to span and geometric twist configuration. As a result, the independent variables whose effects on lift have been investigated are the planform wing

area, geometric twist configuration, infinite lift curve slope, and infinite zero-lift angle.

An important objective of AETC is to develop a design which is easily constructed, yet capable of successfully meeting the mission requirements. Thus, the independent variables investigated were chosen in part on the basis of their relatively insignificant effects on construction capability. Because aerodynamic twist complicates the wing construction, and (as it turns out) the desired lift performance can be achieved without employing this technique, it has been disregarded as a possibility in the design of the wing. Further, the weight of the wing is an important consideration. Minimal weight of the aircraft is particularly crucial in low-speed flight. Therefore, the wing size must be sufficient to achieve the maximum desired lift force, yet no larger. It is important to remember that because interference effects with the fuselage are not taken into account in the lifting-line wing analysis, the performance predictions of the actual wing will be slightly inferior to those calculated by using finite wing theory.

Assumptions: The analysis that follows is based on several important assumptions:

1. The mean-chord Reynolds number is based on the cruise velocity, which is fixed at 23 ft/s.
2. The angles of attack used in the analysis are sufficiently small for valid applicability of the monoplane [finite wing] equation (Eqn. 2.58 [Ref. 2], Eqn. 5.51 [Ref. 1]).
3. Symmetric load distribution.
4. Effects of fuselage on wing lift performance are not taken into account.

Methods of Analysis and Selection: To determine the span efficiency factor, finite lift curve slope, induced drag vs. geometric angle of attack, and spanwise lift distribution, a finite wing analysis program was employed at geometric attack angles in the range, 1 degree < α < 11 degrees. The finite wing analysis program employs the monoplane equation of Prandtl's lifting line theory [Ref. 2]. This equation is:

$$\alpha(\theta) = \frac{2b}{\pi(c(\theta))} \sum (A_n \sin n\theta + nA_n \frac{\sin n\theta}{\sin \theta}) + \alpha_{L=0}$$

where $\alpha(\theta)$ = geometric angle of attack

$\alpha_{L=0}$ = airfoil zero-lift angle of attack

b = wing span

$c(\theta)$ = functional form of the chord variation (in our case, c(q) is constant)

A_n = Fourier coefficients from the proposed Fourier series representation of the circulation distribution.

To reach a decision regarding the optimum combination of the planform geometry parameters considered, the required lift during the take-off and cruising phases of the flight were determined based on weight estimation, desired rate of climb, and an estimate of the losses incurred due to fuselage-wing interference. The desired C_L for cruise was found according to:

$$C_L = \frac{W}{\frac{1}{2}\rho V_\infty^2 (c)\ (1)}$$

where W is the total aircraft weight, and (c) is the mean chord (which is fixed by the design). The (finite) lift coefficient required during take-off was also computed with this equation replacing W with the required lift during take-off. The required lift was determined from the following equation:

$$L = W\sin\theta,$$

where θ is the desired flight trajectory. To account for the interference effects, a factor of safety was taken to be 1.2 based on an estimate of the effective loss of lift. The values for C_L determined by the above equations were multiplied by this factor to yield realistic requirements. Note that because the induced drag coefficient, $C_{d,i}$, (and therefore the total wing drag coefficient) varies quadratically with C_L, it is desirable to obtain the minimum value of C_L necessary to provide the required takeoff performance and sustain the aircraft

in flight at the desired cruise speed. Thus, a compromise was made between lift coefficient and induced drag coefficient.

Results: Given the measures of merit, the design constraints and the performance characteristics of the NACA 4415 airfoil (see "Airfoil Selection"), Table 2-2 represents the final wing geometric and aerodynamic parameters.

TABLE 2-2: Selected Wing Geometry

Chord, c= 0.683 ft (constant)	Planform area, S= 5.46 ft^2
Span, b= 8.0 ft	Span efficiency factor, e=0.89
Taper ratio, λ= 1.0	Average wing loading = 0.55 lbf/ft^2
Aero. & Geo. twist: none	Finite lift curve slope, a= 0.073/deg

Analysis of Figures: The finite lift curve slope for the NACA 4415 may be estimated from Figure 2-3 as 0.0733/degree. It is evident, also, that the maximum desired lift coefficient which is equal to 1.2 is achieved at an incidence angle of ~11.5 degrees. The desired cruise lift coefficient, 0.87, is achieved at ~7.5 degrees. As expected, the induced drag coefficient varies parabolically with angle of attack. The spanwise lift distribution for the NACA 4415 is shown in Figure 2-9 and Figure 2-10 for angles of attack ranging from 1 to 10 degrees. As is evident from these plots, the distributions are approximately elliptical.

C. Drag Estimation

Paramount in any aircraft's design phase is an accurate estimation of the drag forces produced by the aircraft in flight. Since the power required and many other parameters depend almost exclusively upon the aircraft's drag, this drag estimation needs to be constantly updated as the aircraft nears the production phase. The method used here is a combination of one presented in Mr. Jensen's thesis "A Drag Prediction Methodology for low Reynolds Numbers Flight Vehicles" [Ref. 6] and another presented by Dr. Nelson in Atmospheric Flight Mechanics [Ref. 7].

Figure 2-9. NACA 4415 Finite Wing Lift Distribution

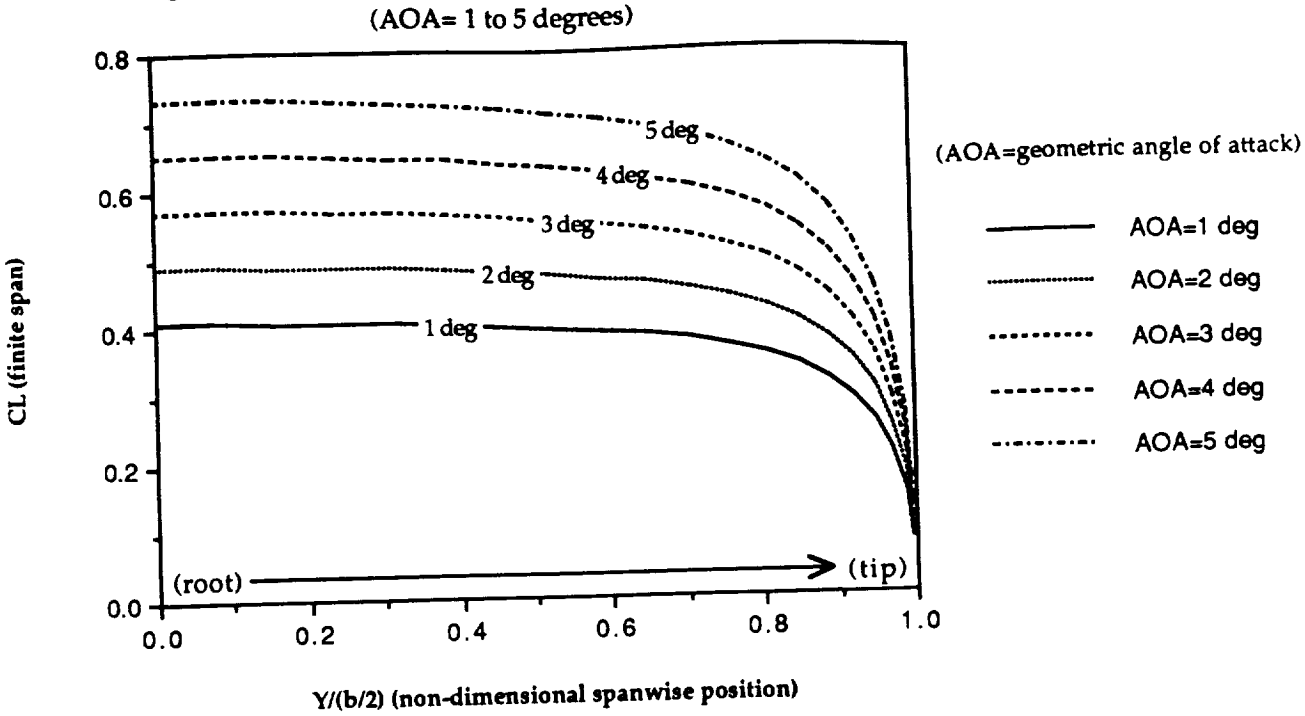

Figure 2-10. NACA 4415 Finite Wing Lift Distribution

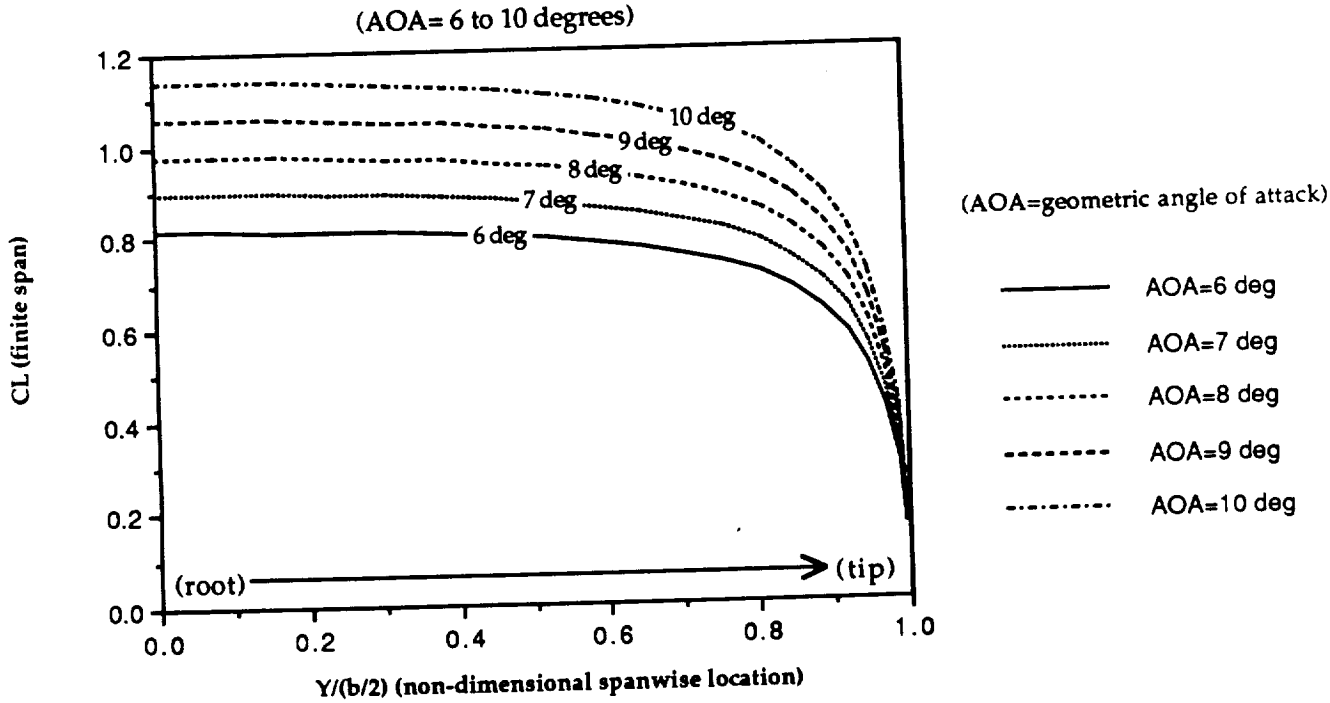

In general, the drag polar for an aircraft is made up of a parasite (or form) drag component and a lift-induced drag component. The general formula for the drag coefficient is then:

$$C_D = C_{Do} + C_L^2/e\pi AR$$

where C_{Do} and e are obtained from a method called the drag breakdown and AR is the aspect ratio of the wing.

Determination of C_{Do}: The value for the parasite drag coefficient, C_{Do}, was determined by summing contributions from all of the aircraft's components and dividing the result by the reference area of the aircraft, in this case wing planform area. In general, this quantity is then boosted by ten percent to include interference effects. The general equation used to calculate C_{Do} is shown here:

$$C_{Do} = \sum(C_{D\Pi} A_\Pi)/S_{ref}$$

The Π's represent the individual components of the aircraft and the C_D and A of each Π are given by certain parameters pertaining to the shape and position of the component. The drag breakdown for the aircraft is summarized in Table 2-3.

TABLE 2-3: Component Contribution to Parasite Drag Coefficient

Component	$C_{D\Pi}$	A_Π	$(C_{D\Pi} A_\Pi)$
Wing	.007	5.46 ft^2	.03822
Fuselage	.110	.111 ft^2	.01221
Vertical Tail	.008	.38 ft^2	.00304
Horizontal Tail	.008	.625 ft^2	.005
Landing Gear	.017	5.46 ft^2	.09282
		Sum $(C_{D\Pi} A_\Pi)$ = .15129	

From this summation, the preliminary C_{Do} value (using the above equation) comes to .0277, and after adding the 15% interference factor, it grows to .0319.

Determination of the Aircraft Efficiency Factor, e: The aircraft efficiency factor, e, can also obtained from a breakdown method. This method uses the following equation:

$$1/e = 1/e_w + 1/e_b + 1/e_o$$

When using this method, e_w and e_b refer to the efficiency factors of the wing and body, respectively, and e_o is a "other" fudge factor to account for interference effects. Using this method, the aircraft's efficiency factor comes to .655. Another method introduced in Reference 6 is based on empirical data and is a function of the aspect ratio only. The formula given for this estimate is as follows:

$$e = 1.78(1 - .045(AR)^{.68}) - .64$$

The value calculated from this empirical formula was .713. Since we have no basis for judgement between these two factors and both come from reputable sources, a decision was made to take the average of these two numbers and use the efficiency factor thus gained. Our complete drag polar is then:

$$C_D = .0319 + C_L^2/.682\pi AR$$

It is interesting to note here that in the calculation of the parasite drag coefficient, the landing gear, because of its large reference area (the same as the wing) and relatively high C_D more than doubles the value of this coefficient. Therefore, if some effort can be made to reduce the drag of the landing gear the aircraft will benefit from a much-reduced drag coefficient.

SECTION III

STABILITY AND CONTROL

A. Horizontal Tail

The primary responsibility of the horizontal tail for this aircraft is to provide longitudinal static stability while allowing the aircraft to be trimmed at a relatively small positive angle of attack. A secondary consideration is that the tail must not make the aircraft so statically stable as to be unresponsive to control input. This section will discuss the process involved with the sizing of the horizontal tail; figures of merit with regard to the primary responsibility are the aircraft's trim angle of attack and total lift generated. The figures of merit with regard to the second consideration are the stick-fixed neutral point and the stick fixed static margin of the aircraft; both of which are measures of the static stability of the aircraft.

Aircraft Moment Coefficients - Trim Angle : The computer program listed as Item 3 in the Appendix was created to study the trends involved with the longitudinal static stability of the aircraft and as such dealt primarily with the moment coefficient of the aircraft about its center of gravity. The program was used to compute the contributions of the wing, fuselage, and horizontal tail to the aircraft's Cm_o and Cm_α. Using the method found in Reference 8, these components are calculated as shown in Table 3-1 (all quantities needed for the following calculations are computed as needed within the program).

TABLE 3-1: Component Contributions to Cm_o and Cm_α

Component	Cm_o Contribution	Cm_α Contribution
Wing	$Cm_{ow} = Cm_{acw} + C_{Lw}(X_{cg} - X_{ac})/c$	$Cm_{\alpha w} = C_{L\alpha w}(X_{cg} - X_{ac})/c$
Fuselage	$Cm_{of} = (k_2-k_1)/36.5Sc\Sigma w_f^2(\alpha_{ow}+i_f)\Delta x$	$Cm_{\alpha f} = 1/36.5Sc\Sigma w_f^2(d\varepsilon_u/d\alpha)\Delta x$
Tail	$Cm_{ot} = \eta VHC_{L\alpha t}(\varepsilon_o + i_w - i_t)$	$Cm_{\alpha t} = -\eta VHC_{L\alpha t}(1 - d\varepsilon/d\alpha)$

After finding the contributions due to all of these components, the Cm_o and Cm_α contributions were summed resulting in the equation for the moment coefficient about the center of gravity of the aircraft:

$$Cm_{cg} = Cm_o + Cm_\alpha \alpha$$

Setting this equation equal to zero will give the angle of attack at which the aircraft is "trimmed":

$$\alpha = - Cm_o / Cm_\alpha$$

Trends & Sensitivities : It should be noted here that the J4D's fuselage contributions to the trim angle of attack are constant and almost negligible, and although the wing's contribution to the moment coefficient is certainly not negligible, it can be treated as a constant for the purpose of the program. By assuming that these values do not change significantly as horizontal tail parameters change, the program was used to examine the tail's influence on the previously mentioned factors. As can be readily seen from the boxed equations above, the contributions due to the horizontal tail factor considerably into the final output of this portion of the program. Specifically, the volume ratio of the tail and the tail incidence angle seem to have a great impact on the tail's contribution to the moment coefficients. At this point in the design phase; structural, weight, and overall size requirements placed the aerodynamic center of the horizontal tail approximately 2 feet behind the center of gravity of the aircraft, which is located at 33% of the mean chord of the wing. This effectively froze the length to the horizontal tail and made the volume ratio of the tail a function of its surface area only. Thus, all of the parameters which were previously strong functions of the volume ratio now become strong functions of the tail surface area.

Once the accuracy of the computer program was checked with a series of hand calculations, it was modified to calculate the trim angles for a number of different tail surface areas and incidence angles. These values generated with this program were then plotted to show the variation of trim angle as a function of different surface areas and tail incidence angles. As is demonstrated in Figure 3-1, the trim angle of attack increases with increasing tail area and decreases with increasing tail incidence angle. The multiple lines on this plot and the ones that follow are for different values of the tail incidence angle. The trim angles shown on the graph are for the fuselage reference line of the aircraft. The wing, due to its incidence angle, will see an effective angle of attack 4.5 degrees higher than this value. The airfoil selected for the wing stalls at approximately 14.5 degrees, so the highest possible angle of attack for the aircraft is 10 degrees. The target trim angle of

Figure 3-1

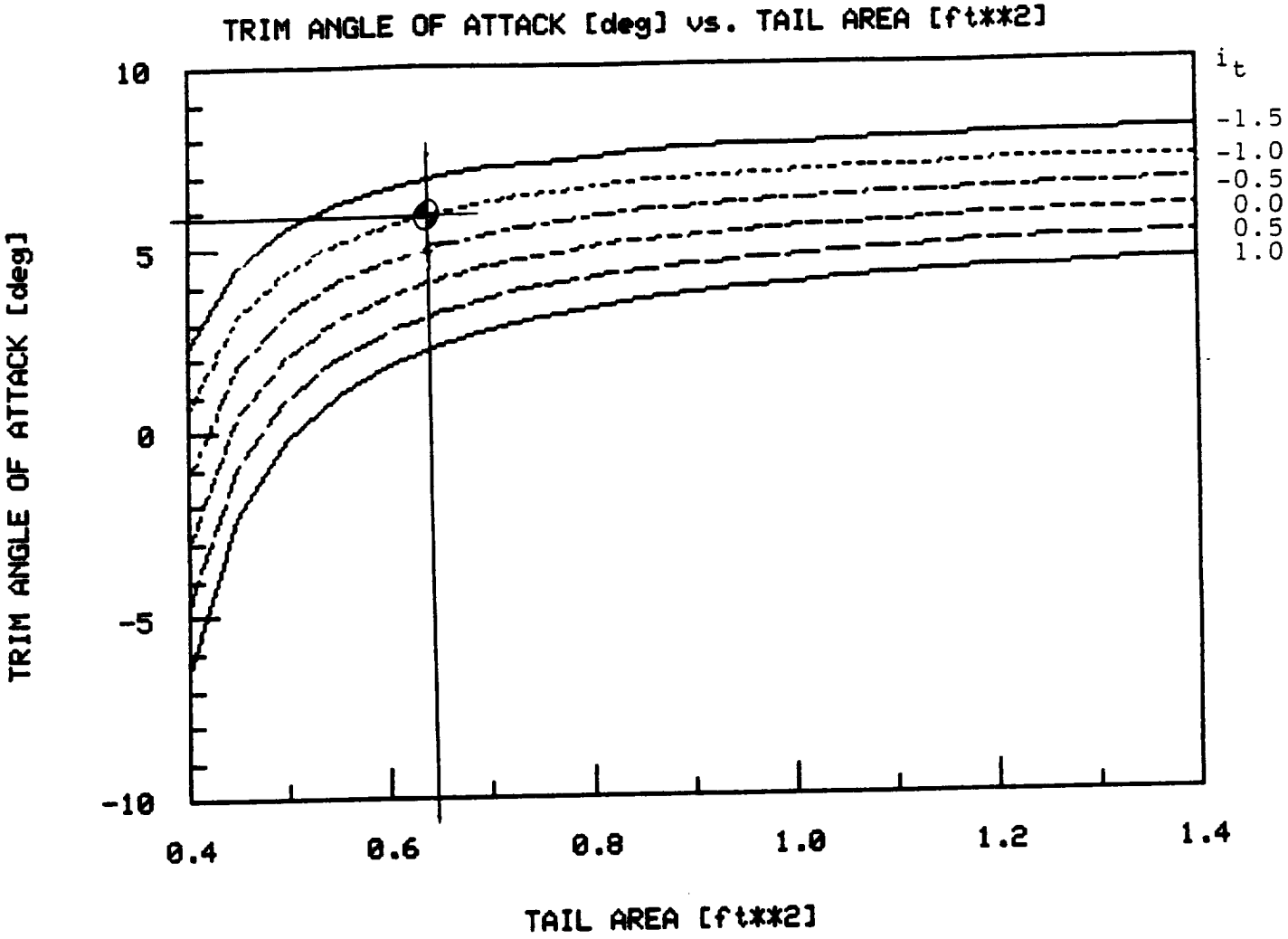
TRIM ANGLE OF ATTACK [deg] vs. TAIL AREA [ft**2]
TRIM ANGLE OF ATTACK [deg]
10
5
0
-5
-10
0.4
0.6
0.8
1.0
1.2
1.4
TAIL AREA [ft**2]
i_t
-1.5
-1.0
-0.5
0.0
0.5
1.0

attack for the aircraft was roughly 6 degrees, allowing close to 4 degrees for in-flight maneuvering before encountering problems with stalling the aircraft.

Horizontal Tail Influence on Lift : The trim angle of attack, though, only tells half of the story. Using this angle of attack as well as the downwash and incidence angles, the lift due to the wing and tail were calculated and summed. Figure 3-2 shows how the tail area and incidence angle influence the lift characteristics of the aircraft. The basic trend is the same: the lift increases with increasing tail area and decreases with increasing tail incidence angle. Since this analysis is dealing only with the the "steady-level" flight phase, the only condition that had to be met here is that the total lift must be equal to 3 pounds. Any excess lift is not needed at this point, and any less lift will not produce a flyable aircraft.

Stick Fixed Neutral Point & Static Margin : The second portion of this analysis deals with the stick fixed neutral point and static margin of the aircraft. The equations for these quantities are given in Reference 8 as:

Stick Fixed Neutral Point:

$$X_{NP}/c = X_{ac}/c - Cm_{\alpha f}/CL_{\alpha w} + \eta V_H C_{L\alpha t}/C_{L\alpha w}(1 - d\varepsilon/d\alpha)$$

Stick Fixed Static Margin:

$$SFSM = X_{NP}/c - X_{cg}/c$$

Although it is difficult to see from the equations standing alone, the variable factor having the most influence on these quantities is the horizontal tail volume ratio. Knowing that the tail length is effectively frozen, the size of the horizontal tail is highlighted as the "most influential factor" in stability considerations.

As a basis for comparison, the horizontal tail surface area was initially sized at 25% of the main lifting surface area (1.367 ft^2) and located 2 ft behind the C.G. This combination created a statically stable aircraft capable of producing the required lift at a 5.5 degree angle of attack. This configuration, however, also produced a Cm_α value of -2.6 per radian, along with a neutral point at 100% of the mean chord (the end of the wing), giving a static margin of 67% of the

Figure 3-2

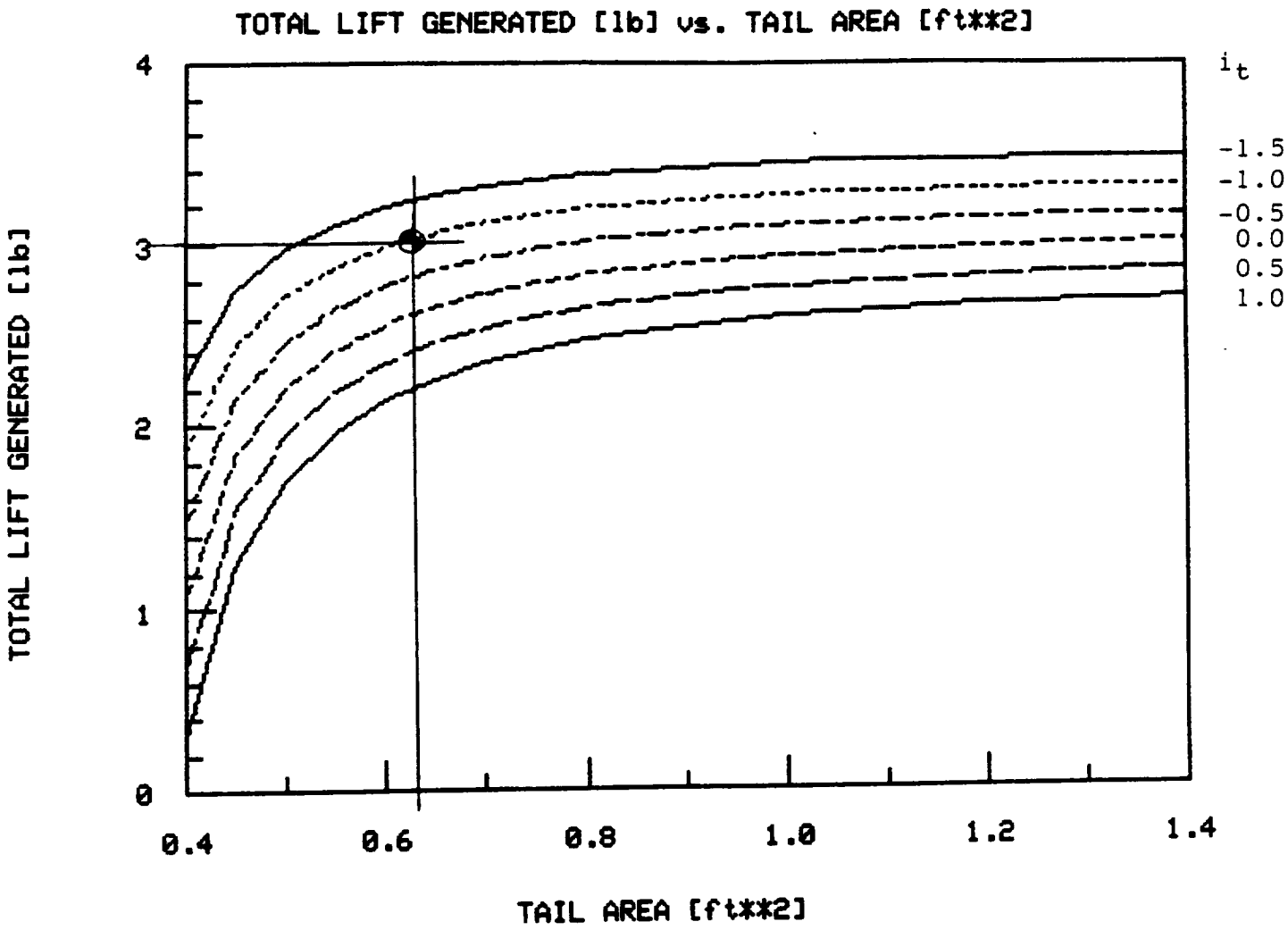
TOTAL LIFT GENERATED [lb] vs. TAIL AREA [ft**2]
TOTAL LIFT GENERATED [lb]
TAIL AREA [ft**2]
i_t
-1.5
-1.0
-0.5
0.0
0.5
1.0
0
1
2
3
4
0.4
0.6
0.8
1.0
1.2
1.4

mean chord. While this would certainly be a stable aircraft, it would probably prove to be very sluggish. In order to make the aircraft more responsive, it is necessary to make the value of Cm_α less negative and to move the neutral point closer to the center of gravity, thus effectively reducing the static margin. Reverting back to the boxed equations, it is easy to see that by decreasing the volume ratio (through the tail surface area) Cm_α will become less and less negative. Figure 3-3 shows the variation of Cm_α with the tail surface area while Figures 3-4 and 3-5 show how the neutral point in percentage of mean chord and static margin are influenced by the same quantity.

Results : With all of these observations in mind, the time for decision approaches. The basic criterion remains the same: produce enough lift at a relatively low angle of attack. But there was a new twist in the form of the Cm_α , neutral point, and static margin values which are actual measures of the aircraft's longitudinal static stability. Certainly, Cm_α must be negative to ensure static stability for the aircraft under consideration. Guidelines from Reference 8 indicate that static margins of 5% of the mean chord are acceptable targets for civilian aircraft. Our preliminary estimate was more than thirteen times that value. More constraints were needed to reduce the number of choices. Further investigation revealed that the drag increases with increasing tail area, and that the lift-to-drag ratio is relatively independent of the tail surface area once it rises above 0.8 square feet for all tail incidence angles (see Figures 3-6 and 3-7). The overriding factor then came from the structures side of the design team, who stated that it would be much easier to mount the horizontal tail if the incidence angle were small than if it were large. With this information in hand, the decisions were made, and the point highlighted on the plots indicate the status of the final design. Table 3-2 is a summary of these characteristics of the J4D:

Figure 3-3

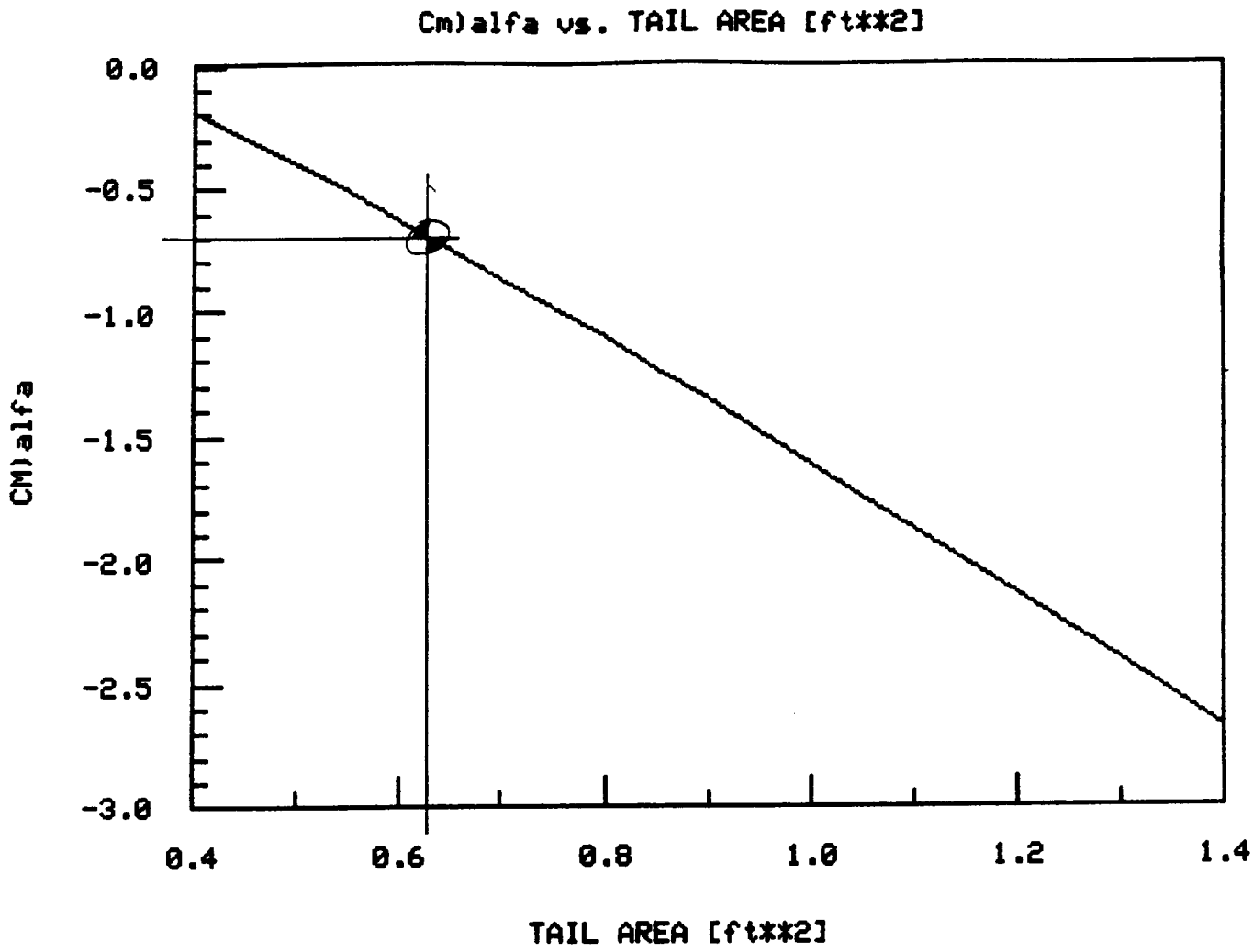
Cm)alfa vs. TAIL AREA [ft**2]
0.0
-0.5
-1.0
-1.5
-2.0
-2.5
-3.0
CM)alfa
0.4
0.6
0.8
1.0
1.2
1.4
TAIL AREA [ft**2]

Figure 3-4

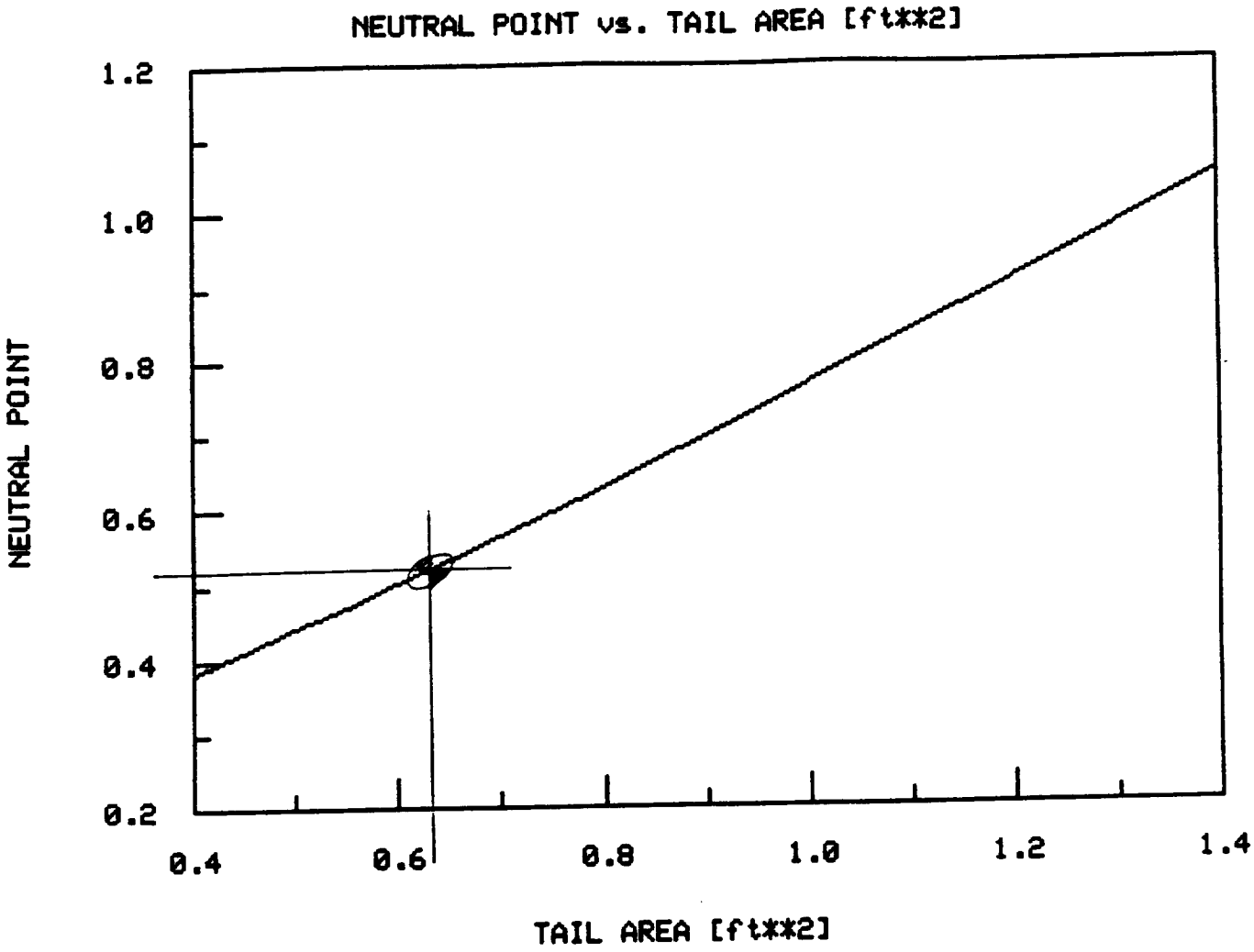
NEUTRAL POINT vs. TAIL AREA [ft**2]
NEUTRAL POINT
1.2
1.0
0.8
0.6
0.4
0.2
0.4
0.6
0.8
1.0
1.2
1.4
TAIL AREA [ft**2]

Figure 3-5

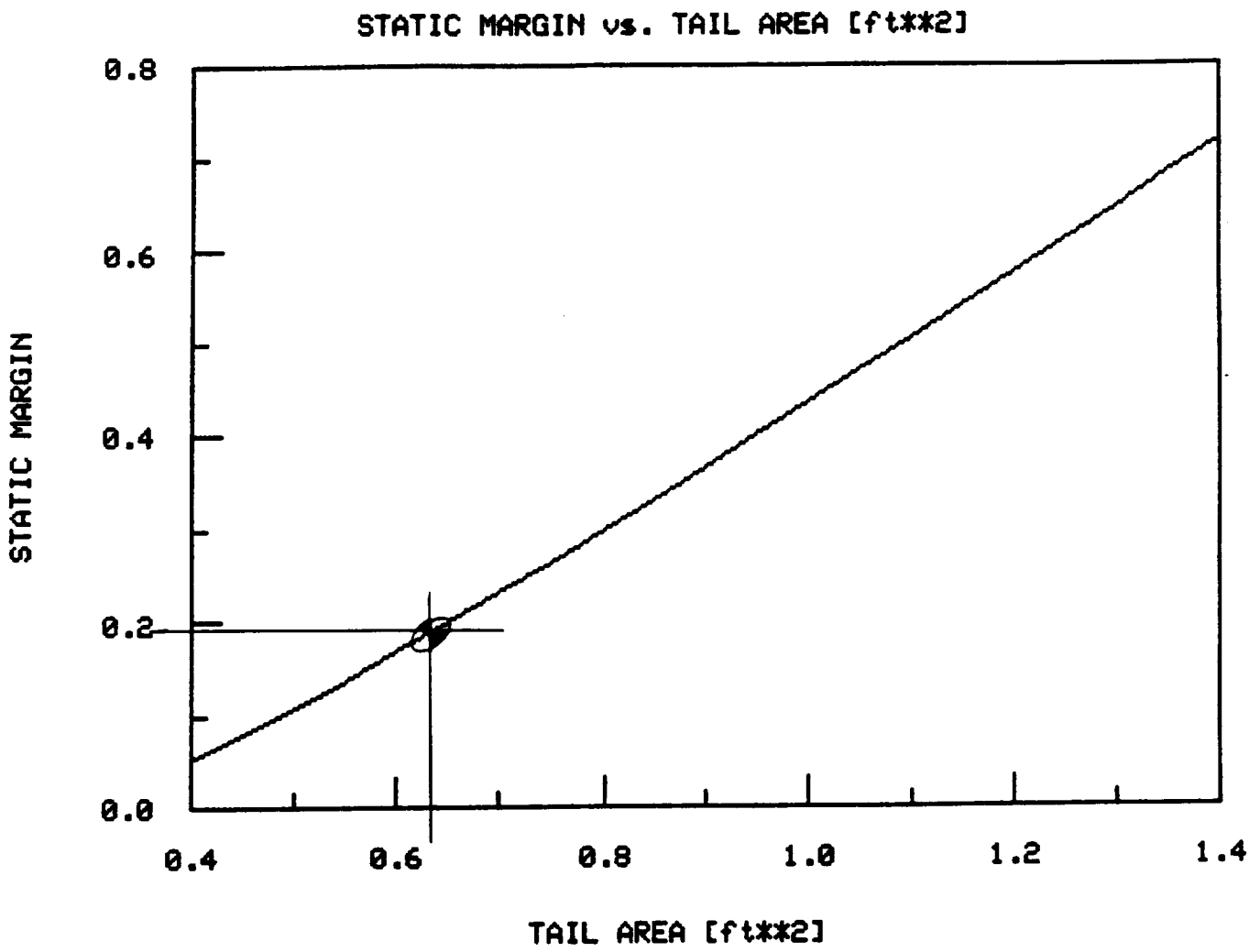
STATIC MARGIN vs. TAIL AREA [ft**2]
STATIC MARGIN
0.8
0.6
0.4
0.2
0.0
0.4
0.6
0.8
1.0
1.2
1.4
TAIL AREA [ft**2]

Figure 3-6

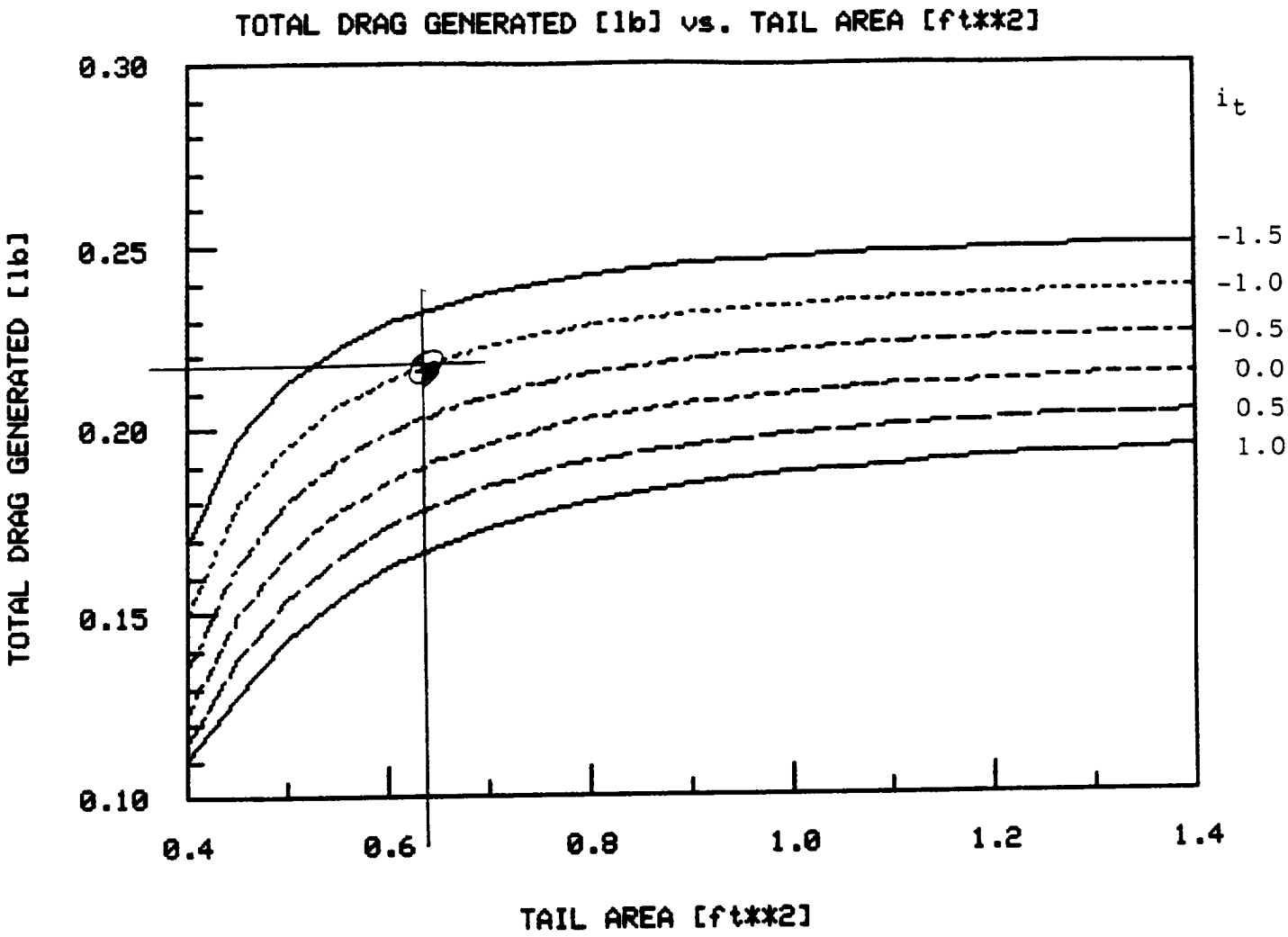
TOTAL DRAG GENERATED [lb] vs. TAIL AREA [ft**2]
TOTAL DRAG GENERATED [lb]
0.30
0.25
0.20
0.15
0.10
0.4
0.6
0.8
1.0
1.2
1.4
TAIL AREA [ft**2]
i_t
-1.5
-1.0
-0.5
0.0
0.5
1.0

Figure 3-7

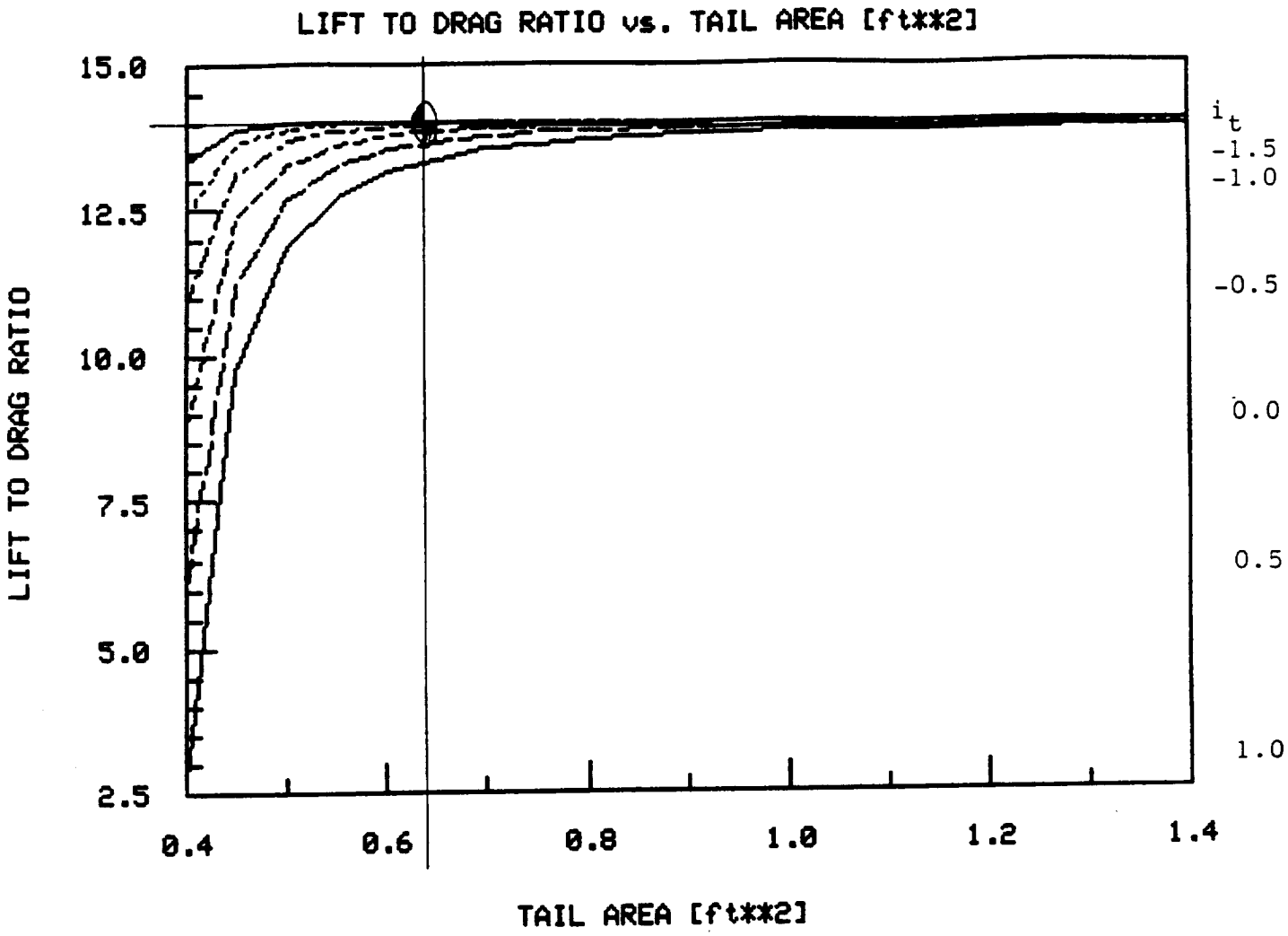
LIFT TO DRAG RATIO vs. TAIL AREA [ft**2]
LIFT TO DRAG RATIO
15.0
12.5
10.0
7.5
5.0
2.5
0.4
0.6
0.8
1.0
1.2
1.4
TAIL AREA [ft**2]
i t
-1.5
-1.0
-0.5
0.0
0.5
1.0

TABLE 3-2: Horizontal Tail Sizing Information

Volume Ratio	.356
Length to Aero Center	2.005 ft
Planform Area	.625 ft^2
Chord	.479 ft
Span	1.304 ft
Incidence angle	-1^o
Cm_α	- .685 rad^{-1}
$X_{NP}/c.$	.514
Static Margin	.184
Aircraft Lift	3.0 lb
Aircraft α	5.87^o

As is seen from this table, the static margin is reduced to 0.184, or just over 3 times the target value of 0.05 set in Reference 8. Additionally, the value of Cm_α has been increased to allow for more control response and less sluggishness. The aircraft produces the required lift and is trimmed at an angle of attack of 5.87 degrees, allowing just over four degrees for maneuvering before stall becomes a problem. Additionally, this tail surface area places the aircraft in the region of relatively low drag and high lift to drag ratio.

Elevator : The elevator consists of roughly one third of the horizontal tail's surface area. Its surface area is .208 ft^2 and $Cm_{\delta e}$ is an acceptable -0.683 rad^{-1}. This elevator area was initially sized based on the rules of thumb found in Reference 5. Once the value of the elevator effectiveness was found to be "large" enough, this value was accepted and finalized for the design.

Dynamic Stability : Under its final configuration, the aircraft is dynamically stable as well; a damping ratio of .88 ensures steady flight and a time to half-amplitude of .105 seconds limits the time the aircraft spends recovering from disturbances. The period of oscillation for these oscillations is 1.86 seconds, meaning that the motion will damp out after less than one oscillation. Clearly this aircraft will be able to perform its station keeping mission in a

stable manner using equation found in Reference 8 modeling the aircraft as a second order differential equation with constant coefficients.

B. Vertical Tail

Lateral stability and control are important considerations in the design of all aircraft. For this rudder and elevator controlled RPV, the vertical tail and wing dihedral were crucial elements influencing its stability, performance and handling. Since the SCREEM-J4D was designed without ailerons, the rudder was required to induce a sufficient yaw angle, β, such that the vertical tail and dihedral would achieve the roll maneuverability usually attributed to the ailerons.

Initial Sizing Analysis: The primary consideration in the sizing of the vertical tail and rudder was the ability to induce a side slip angle, or yaw angle, β (beta). This induced yaw angle, coupled with the design wing dihedral, will provide the lateral control for the J4D. The tail surface area (S_V), flap effectiveness (τ), and the maximum rudder deflection angle (δ_r) were initially selected comparable to typical RPV values. The initial S_V was established through the combination of two "rules of thumb:"

$$S_V / S_h = 0.33 - 0.40$$
$$S_V / S_W = 0.07 - 0.01$$

However, values of S_V outside the range of these typical values were also considered due to the unusual objective of flying at low Reynolds numbers. Table 3-3 contains a further listing of fixed and variable parameters, and the typical RPV values used to select the initial values.

TABLE 3-3: Vertical Tail Sizing Information

Parameter	Value	Reason
Surface Area (S_V)	0.34 - 0.60 ft^2	RPV typical values
Position aft CG (l_V)	1.5 - 2.0 ft	required by horizontal tail
Rudder Deflection (δ_r)	$\leq 25°$	stall and structure stability
Flap Effectiveness (τ)	0.62 - 0.75	tail stability, rule of thumb
Tail Efficiency (n_V)	1.0	low wing in propwash
Lift Curve Slope ($Cl\alpha_V$)	2π	elliptical wing assumption

Lateral Moment Coefficient: The wing-body contribution to $Cn\beta$ was calculated to be -7.21 X 10^{-5}/deg through an empirical equation and is constant throughout the analysis (Eqn. 2.74, [Ref. 8]). This destabilizing contribution was negligible compared to the contribution of the vertical tail:

$$Cn\beta_V = V_V\, n_V\, CL\alpha_V\, (1 + d\sigma/d\beta) \qquad \text{(Eqn. 2.80, [Ref. 8])}$$

The value of $n_V(1+ d\sigma/d\beta)$ was estimated to be 1.135 and directly proportional to S_V (Eqn. 2.81, [Ref. 8]). In addition, since the vertical tail is a flat plate airfoil, the value of the lift curve slope was assumed to equal 2π. The resulting $Cn\beta$ due to the vertical tail was calculated to be 8.4 X 10^{-4} /degree, which is roughly ten times the magnitude of $Cn\beta$ due to the wing-fuselage combination. The total yawing moment coefficient was computed to equal 7.68 X 10^{-4} /deg through:

$$Cn\beta = Cn\beta_V + Cn_{wf}$$

The rudder control power, $Cn\delta_r$, was then calculated:

$$Cn\delta_r = -V_V\, n_V\, \tau\, CL\alpha_V \qquad \text{(Eqn. 2.86, 2.87, [Ref. 8])}$$

The ratio of dynamic pressures of the wing and the vertical tail, n_V, was assumed to remain constant at 1.0, due to the low-wing setting and the positive effects of the propwash. From Figure 2.20 [Ref. 8], the flap effectiveness τ, of 0.72 was selected according the desired ratio of the control surface area to the lifting surface area of 0.55. The rudder was sized at 55% of the overall vertical tail to afford sufficient control power, without

endangering structural stability. The rudder control power, $Cn_{\delta r}$, was thus found to equal -5.33 X 10-4 /degree, at a maximum deflection angle of 25 degrees. From these parameter ranges, the overall yawing coefficient was then determined to vary according to:

$$Cn = Cn_{\beta}\,\beta + Cn_{\delta r}\,\delta r$$

In order to solve for the yaw angle, β, at the trim condition, Cn was set equal to zero. Including the trim condition constraint, Beta becomes directly proportional to the rudder deflection angle; therefore, the optimum β occurs with maximum δr .

This relation verified and the location of the vertical tail aft of the CG, selected in conjunction with the horizontal tail, the vertical tail surface area (S_V) was swept through numerous values using the computer program listed as Item 4 in the Appendix to achieve a satisfactory design. The vertical tail, with tail position l_V=1.9 ft and surface area S_V=.38 ft^2 (which includes a rudder area of .21 ft^2), achieved sufficient yawing power to ensure safe completion of the mission constraints while remaining in agreement with typical RPVs. Numerous values of l_V were analyzed and found to have no significant effect on β. Since it's maximum effect is about +/- 0.1 degrees, it did not take any precedence in the sizing of the vertical tail. The above parameters produced a maximum yaw angle of 17.3 degrees at the maximum rudder deflection angle of 25 degrees.

Roll vs. Yaw : Prior to finalizing the design to the above parameters, an analysis relating the yaw to the roll was completed. The computer program listed as Item 5 in the Appendix was compiled to compute the roll moment due to yaw for various values of dihedral. This code relates the effects of wing tip contour and aspect ratio to the roll moment coefficient through:

$$Cl\beta = (Cl\beta/\Gamma)\,\Gamma \;+\; \Delta Cl\beta \qquad \text{(Table 3.6, [Ref. 8])}$$

Since the maximum ordinates of the wing will lie on the mean line, $\Delta Cl\beta$ is assumed to equal zero. The roll moment coefficient due to yaw angle per

degree, (Cl_β/Γ), was extrapolated from Figure 3.9 in Reference 8, to equal -.00027. Sweeping the dihedral angles from 4 to 12 degrees, over a range of yaw angles of 0 to 30 degrees, a minimum dihedral angle of 7.5 degrees is required, as shown in Figure 3-8. Note, the range of required roll moment coefficients was initially determined by assuming ailerons. The ailerons assumed in the design were selected using "rules of thumb" and RPV's of comparable size. Thus, an estimate of the minimum required Cl of .035 was computed using:

$$Cl = (2\, CL\alpha w\, t\, d\alpha)/Sb \int cy\, dy \qquad \text{(Eqn. 2.96, [Ref. 8])}$$

Before ending this analysis, it is important to note that although a decrease in tail surface area shows an increase in β, the maximum increase is approximately +/- 1.0 degree. Still, a smaller surface area does denote less weight and less skin friction drag. Thus an optimum design would include a high percentage rudder of a smaller tail area (high τ, low Sv). Table 3-4 summarizes the vertical tail as designed for the J4D.

TABLE 3-4: Vertical Tail Summary

Surface Area	0.38 ft^2
Aspect Ratio	1.38
Height	8.0 in
Root Chord	7.2 in
Tip Chord	3.9 in
Taper Ratio	0.54
Sweep	23.2°
Aft CG Position	1.9 ft
Cn_β	7.68×10^{-4}
Rudder Area	0.21 ft^2
Max Rudder Deflection	25°
Flap Effectiveness	0.72
$Cn_{\delta r}$	-5.33×10^{-4}

C. Dihedral

Four wing dihedral configurations were considered for the J4D. These included a V-shape dihedral and three 3-panel polyhedrals, with various

Figure 3-8

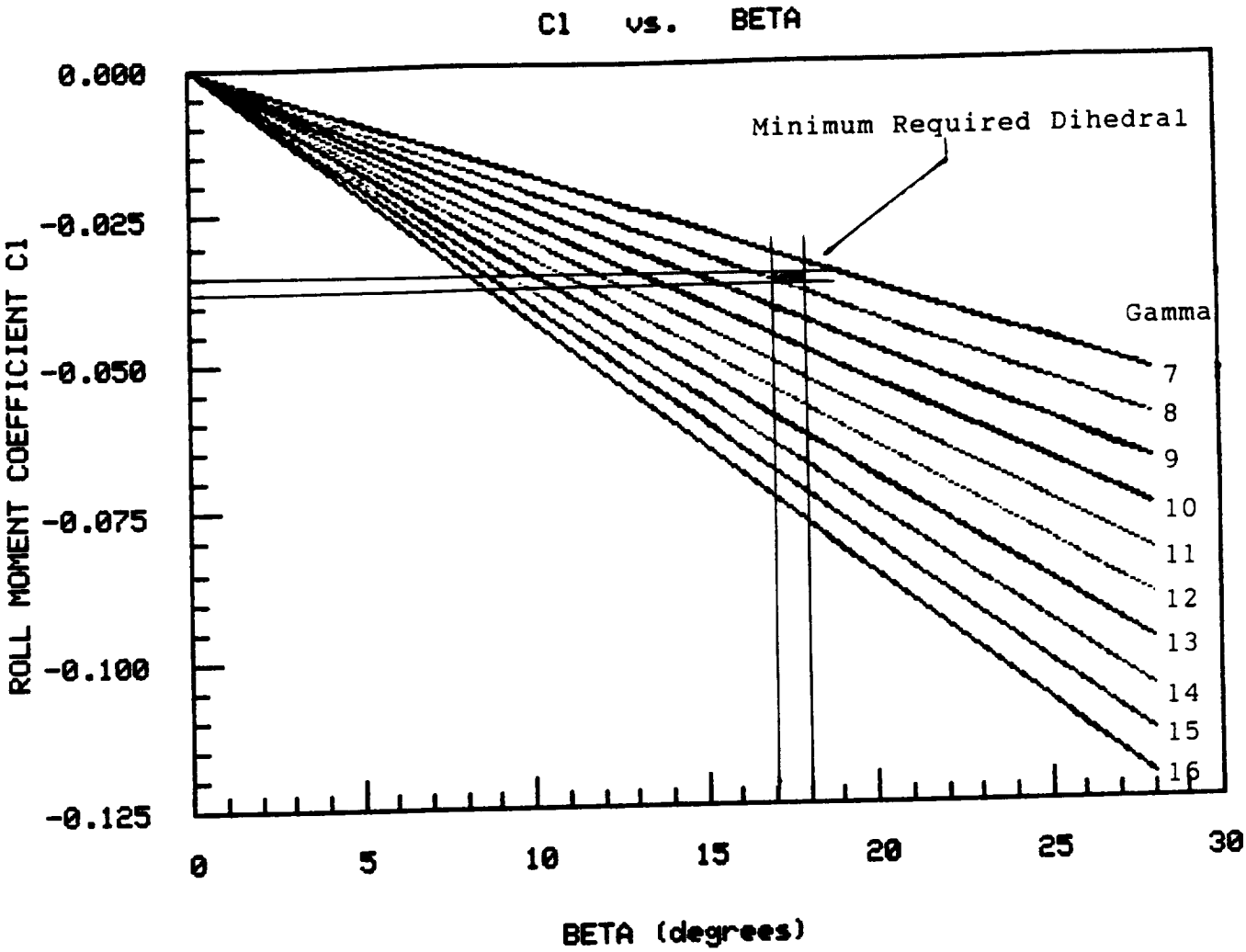
Cl vs. BETA
Minimum Required Dihedral
Gamma
7
8
9
10
11
12
13
14
15
16
0.000
-0.025
-0.050
-0.075
-0.100
-0.125
ROLL MOMENT COEFFICIENT Cl
0
5
10
15
20
25
30
BETA (degrees)

panel break locations, as indicated in Table 3-5 and Figure 3-9. Functionally, the dihedral links the yaw and roll axes of the aircraft, allowing a yaw deflection to cause a rolling moment. This result is due to the increase of angle of attack and thus an increase of lift on the forward wing. A comparable decrease occurs on the aft wing. The net affect creates a wing generated rolling moment. Note however, that the change of angle of attack of the forward wing is equal and opposite to that of the aft wing. This equality provided the wings with a constant total lift within the unstalled region.

TABLE 3-5: Wing Dihedrals

Dihedral Type	Inboard Angle	Outboard Angle	Panel Break
V-shape	10.0 deg.	10.0 deg.	NA
3 panel	0.0 deg.	11.0 deg.	25% (1 ft)
	0.0 deg.	11.9 deg.	37.5% (1.5 ft)
	0.0 deg.	14.3 deg.	50% (2 ft)

Analysis and Results : The change in angle of attack ($\Delta\alpha$), for the wing is a function of the wing dihedral angle and the yaw input angle:

$$\Delta\alpha = \tan^{-1} (\text{SIN Yaw} \times \text{TAN Dihedral}) \qquad \text{([Ref. 4])}$$

The results of the parametric sweep of the yaw angle from 1 to 25 degrees and the dihedral angle from 7 to 21 degrees are plotted in Figure 3-10 (see the computer program listed as Item 6 in the Appendix). The change in angle of attack was plotted verses yaw angle for various Equivalent Dihedral Angles (EDA, discussed below). As demonstrated in Figure 3-10, $\Delta\alpha$ is proportional to both the dihedral angle and the yaw angle. The performance envelope and the design EDA are indicated. The envelop and the selected $\Delta\alpha$ are constrained by the wing's stall angle, the maximum yaw angle of 17.3 degrees and the minimum required dihedral angle of 7.5 degrees (above analysis). The required wing angle of incidence for steady-state cruise is 10 degrees. The stall angle for the wing at a Reynolds number of 100,000 is 14.5 degrees, allowing a maximum $\Delta\alpha$ of 4.5 degrees. Due to the imperfections incurred during manufacture, a maximum $\Delta\alpha$ of 4.0 degrees was selected.

Figure 3-9

Dihedral Configurations Considered

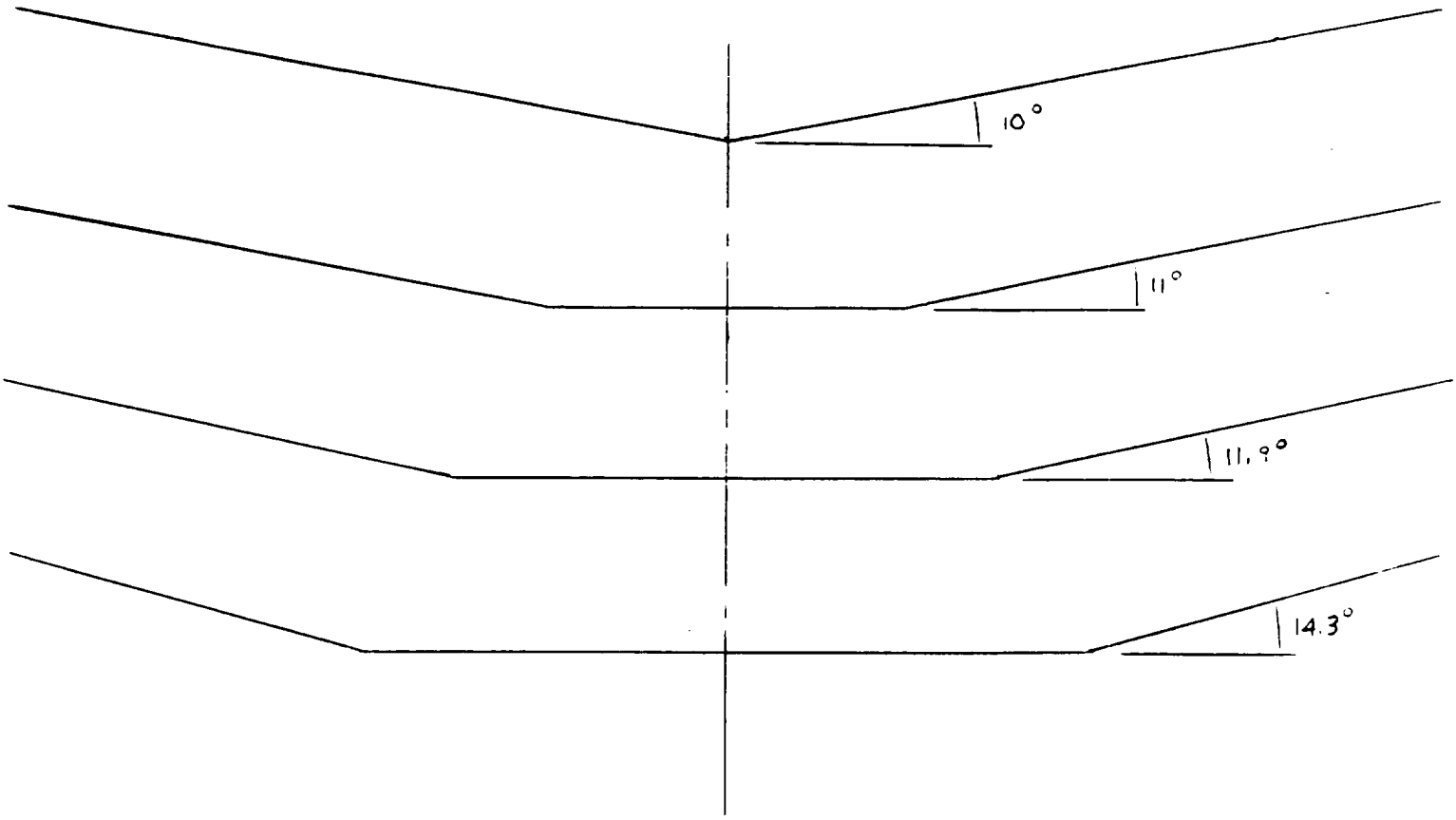

Figure 3-10

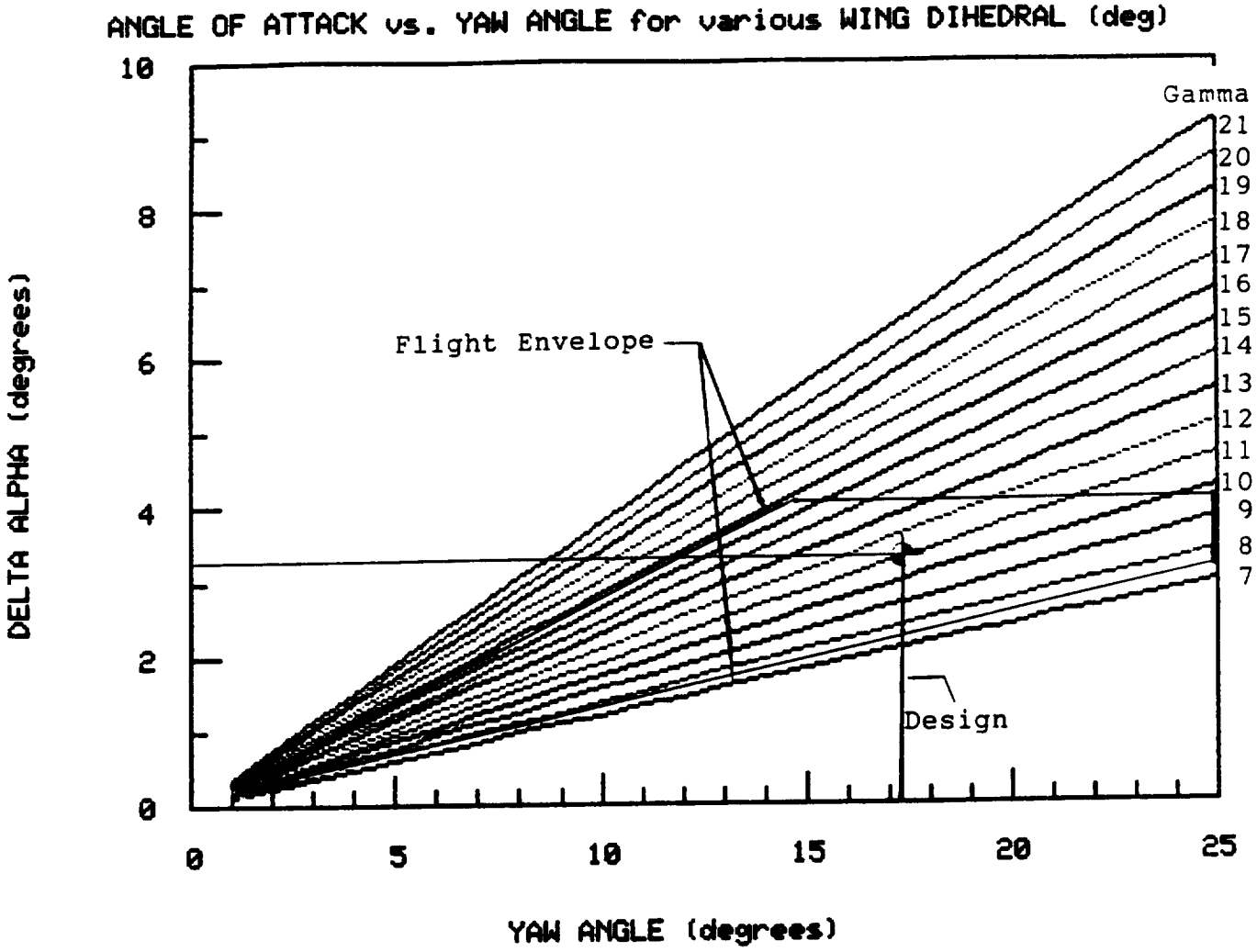
ANGLE OF ATTACK vs. YAW ANGLE for various WING DIHEDRAL (deg)
DELTA ALPHA (degrees)
YAW ANGLE (degrees)
Gamma
21
20
19
18
17
16
15
14
13
12
11
10
9
8
7
Flight Envelope
Design
0
2
4
6
8
10
0
5
10
15
20
25

Given the yaw angle of 17.3 degrees, corresponding to the maximum rudder deflection of 25 degrees, an EDA of 10 degrees was selected from Figure 3-10. EDA's of up to 15 degrees were also considered for this design, since they too, satisfied the envelope constraints. However, the larger EDA's, while slightly increasing the rolling rate, would decrease the wing's lift efficiency slightly and increase the structural instability. The EDA of 10 degrees was also ascetically more pleasing, thus increasing the J4D's marketability. While it would be optimum to reduce the yaw angle, reducing the drag on the vertical stabilizer during maneuvers, with a greater design EDA, 10 degrees was selected to ensure an unstalled wing. Additionally, while the performance requirements necessary for this mission do not "push" the limits of the performance envelop for an EDA of 10 degrees; the V-shape dihedral configuration was selected due to the minimum outboard angle, to reduce the chance of tip stall, should the performance requirements be increased.

Roll Moments and Roll Rates : The maximum $\Delta\alpha$ is shown to be 3 degrees at the maximum yaw angle of 17.3 degrees for a 10 degree EDA. The change in lift over the individual wing was computed, based on a constant lift curve slope of 0.1 /deg within the wing's unstalled region. The total moment was then summed from the section rolling moments computed from the change in lift over 12 panels for an individual wing. Note, due to this dependence on the change in lift, the rolling moment of the dihedral wing is demonstrated to be independent of the overall angle of attack. A parametric sweep of the rolling moment verses the total angle of attack for the leading wing was computed (see the computer program listed as Item 7 in the Appendix). The roll moment generated by the maximum $\Delta\alpha$ of 3.2 degrees is shown to equal 44.8 ft lb.

The rolling moment was then non-dimensionalized by computing the moment fractions at their semi-span locations. Holding the outboard angle (ODA), constant at 10 degrees, for reasons stated above, the rolling moment percentages achievable at a maximum $\Delta\alpha$ were computed for the various configurations (see Table 3-6). These rolling moment percentages correspond directly to the EDA's of the various configurations according to Reference 4:

Rolling Moment (%) x Outboard Dihedral Angle (degrees) = EDA (degrees)

TABLE 3-6: EDA vs. Roll Moment

Dihedral Type	Moment Fraction	EDA	Roll Moment
V-shape	1.0	10.0 deg	44.8 ft lb
3 panel	.91	9.1 deg	40.8 ft lb
	.84	8.4 deg	37.6 ft lb
	.70	7.0 deg	31.4 ft lb

Note, the ODA is equal to the EDA for a V-shaped dihedral, since the panel break occurs at centerline. The rolling moment for the V-shaped dihedral is produced over the entire wing, while the flat center panel of the 3-panel configurations makes no contribution to the roll power, tasking the outboard angles to generate the lift required to roll. Thus, for a constrained wing loading and outboard dihedral angle, the V-shape dihedral, with the largest EDA, will allow the greatest roll power. This is further demonstrated in Table 3-7, where given a constant yaw angle, the wing with the greatest EDA develops the greatest roll rate.

TABLE 3-7: EDA vs. Yaw Angle

Yaw Angle 17.3°		EDA 10°	
EDA	Roll Rate	Yaw Angle	Roll Rate
10 deg	28.8 deg/s	5 deg	7.4 deg/s
9.1 deg	26.2 deg/s	10 deg	16.2 deg/s
8.4 deg	24.2 deg/s	15 deg	25.0 deg/s
7.0 deg	20.2 deg/s	20 deg	31.7 deg/s

The roll rate performance was further analyzed with respect to yaw angle for the design wing dihedral of 10 degrees. The data from this analysis is also included in Table 3-7.

Turning Radius : This coupled relationship was further considered for steady-state turning. Constrained to a 40 ft turning radius at the maximum bank angle of 30 degrees, the aircraft was found to require a yaw angle of 5 degrees. Note, this is the required yaw angle to maintain a steady-state turn at a turning radius of 40 ft. By increasing the yaw angle to its maximum of 17.3 degrees, the turning radius of the J4D can be minimized to 28.6 ft.

SECTION IV

PROPULSION SYSTEM

A. Motor Selection

The first task in sizing a propulsion system was to select a motor. Since design constraints prohibited the emission of particles into the atmosphere, liquid-fueled engines of the piston or ducted-fan type were eliminated as possibilities. Attention then turned to a propulsion system featuring a propeller powered by an electric motor, which met the emissions constraint. The task then was to select an electric motor.

The consideration of electric motors involved the Astro 035, Astro 05, Astro 15, and several generic "others". By generic "others" it is meant those motors for which only the maximum power output, weight, size and RPM range were known. No information regarding their operating characteristics were available. These motors were typically discovered in modelling magazines or manufacturers' literature. The motor selection process to be discussed is summarized in Table 4-1. The first criterion upon which the selection was based was power production. From initial estimates of motor power requirements it was realized that the Astro 035 was inadequate. Its power production was too low and hence eliminated from consideration. The generic "other" engines all appeared attractive in terms of producing enough power to meet requirements. However, since no information as to their operating characteristics was available, any analysis and performance predictions with them would be extremely difficult. This problem could have been resolved through inquiries with the respective manufacturers or tests in a laboratory. Time invested in either of these practices could have been costly and possibly unrewarding. Due to time and practicality considerations, those motors for which the operating characteristics were unavailable were eliminated from consideration.

Attention then focused on the Astro 05 and Astro 15, whose operating characteristics were known and available in tabular form. This allowed for a performance analysis once a motor had been selected. In regards to the selection, both produced an adequate amount of power; in fact, well above that which initial estimates required. The size of both motors was attractive. That is, the dimensions were such that both were compatible with the size of the fuselage and would mount easily to the front of it. The deciding factor

became the motor weight. The Astro 05 weighed an ounce less and its standard (recommended) battery pack weighed 9 ounces less. Using smaller battery packs than those recommended because of lower power requirements would lessen the system weight for both. However, the Astro 05 would still weigh less and therefore it was selected as the motor to power the aircraft.

TABLE 4-1 : Motor Selection Considerations

	Astro 035	Astro 05	Astro 15	"Others"
Power Production :	low	adequate	adequate	adequate
Specifications :	NOT available	available	available	NOT available
Size :	good	good	good	--
Weight : (Motor/System)	4.5 / 11.0 oz	6.5 / 16.0 oz	7.5 / 25.0 oz	--

B. Propeller Data Generation

In order to properly analyze the performance characteristics of different propellers, it was found necessary to generate propeller performance characteristics (thrust and power coefficients, Ct, Cp) as a function of advance ratio J. Since performance estimates on hobby propellers were not available and time did not permit actual wind tunnel testing, a data base was created using a program entitled "Propeller Performance Analysis for Small Computers," written by Barry N. Young [Ref. 11]. This code enabled one to generate theoretical propeller performance characteristics based upon simple blade element theory. Input to the program were airfoil data (of the propeller blade section), estimated flight conditions, and the propeller geometry. These geometrical quantities were the blade angle, chord, and thickness measured at nine radial positions.

Due to the lack of propeller data, it was assumed that all of the propellers used a CLARK Y airfoil section which is used for the TopFlight family of hobby propellers. It was also assumed that all of the propellers studied had a constant blade angle distribution. Which dictated that the only geometrical difference between propellers of the same diameter but different pitch was the blade angle at each radial position. Thus, for a family of propellers with the same diameter, the measurements only had to be performed once, with the blade angle (β) determined by the pitch (P) according to the relation

$$\beta = \tan^{-1} \frac{P}{2\pi r}$$

where r is the radial position measured from the hub (P and r have the same length units).

The propellers studied ranged in diameter (8, 9, 10, 11, 12, and 13 inches) and pitch (4, 6, and 8 inches). Each of these diameters were studied with all three pitches, hence, the total number of diameter-pitch combinations resulted in the analysis of 18 different propellers. A sample of the input geometric characteristics and parameters of Barry Young's program, in addition to a sample of the theoretical performance results are listed as Item 8 in the Appendix.

Simple blade element theory (utilized in this computer program) helped create a data base of performance characteristics for several propellers, but it did not give any indication as to how these theoretical results compared to experimental results. A comparison was made using experimentally derived performance data available for a 13-7, 14-4, and 14-8 propeller. The geometrical parameters were measured for these propellers and input into the performance program to obtain theoretical results. A study of the experimental and theoretical results for the same propellers yielded a definite trend. In general, the theoretical results for the power coefficient were much lower than the "real" experimental results. On the other hand, the theoretical results for the thrust coefficient were much higher than the experimental results. In order to correct the theoretical data, a quantification

of these differences was needed. Correction factors as a function of advance ratio (J) were ascertained for both the power coefficient (Cp) and torque coefficient (Cq). This correction function incorporated the average differences between the theoretical and experimental results for both the thrust and power coefficients over a range of advance ratios from 0.2 to 0.8. This correction function was then added to the theoretical performance characteristics to yield near "real" data. Figures 4-1 and 4-2 compare the theoretical performance curves with the corrected performance curves for the 10-6 propeller. Table 4-2 gives the form of the correction function and the appropriate coefficients.

TABLE 4-2: Correction Functions for Propeller Performance

Functional Form: $CF = CO + C1*J^1 + C2*J^2 + C3*J^3$

Thrust, C_t:	CO = -0.035761	C2 = -0.082838
	C1 = 0.085253	C3 = -0.039541
Power, Cp:	CO = 0.022765	C2 = 0.32328
	C1 = -0.14785	C3 = -0.2654
Efficiency, η:	CO = 0.83487	C2 = 19.653
	C1 = -7.4942	C3 = -17.739

CF is added to theoretical value; J is advance ratio

In correcting the theoretical data, it was assumed that the correction factor was the same for all of the propellers. Experimental results were not available for smaller diameter propellers to validate this assumption. However, the corrected performance data represented a significant improvement in regards to accuracy over the theoretical data. In later analysis, the theoretical performance curves were augmented by these correction functions. This greatly enhanced the accuracy of the propeller selection process.

C. Battery / Propeller Selection

The next task in sizing the propulsion system was to determine the type battery pack and propeller to be used with the Astro 05 motor. These two

Figure 4-1

Thrust coefficient vs. Advance Ratio (10-6)

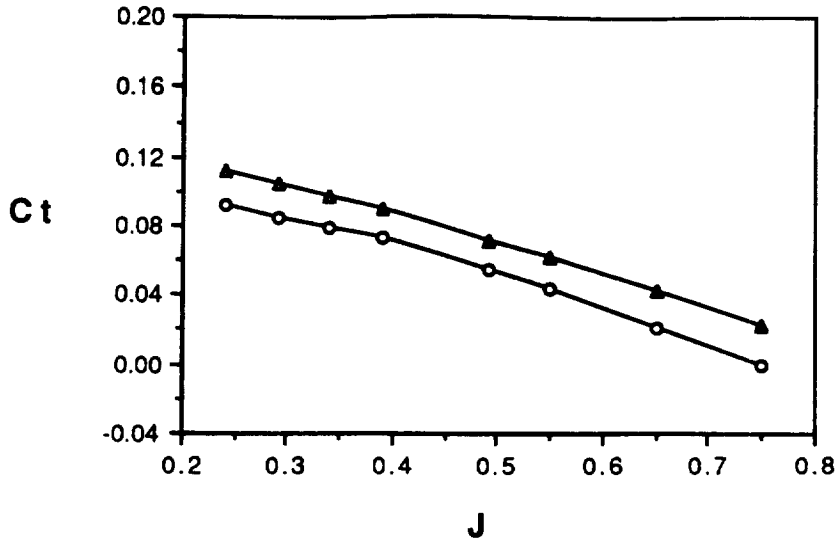

Figure 4-2

Power coefficient vs. Advance Ratio (10-6)

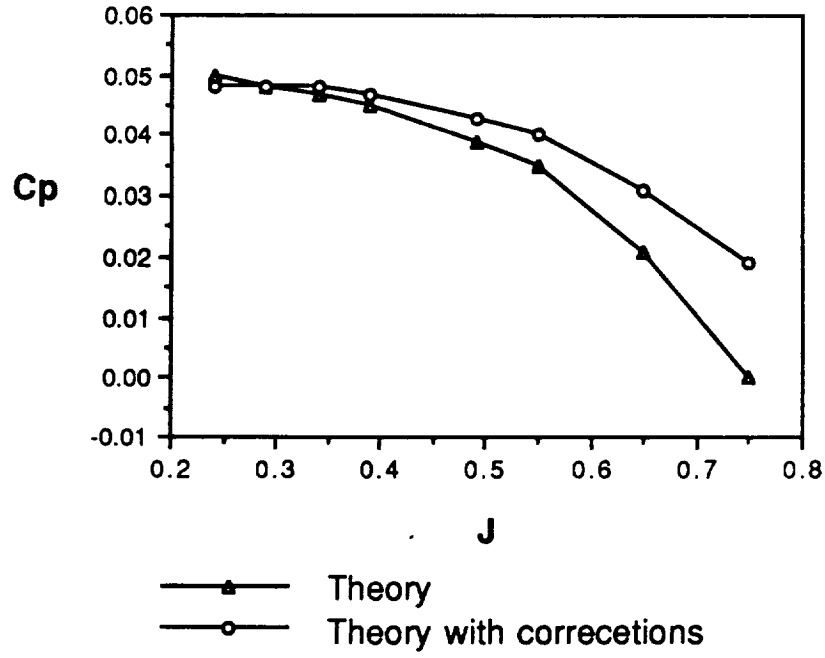

propulsion system components were not independent of each other, rather significantly related. Therefore, the process became one of considering numerous battery pack/propeller combinations. Considered were battery packs ranging from four to ten 1.2 volt Nickel-Cadmium batteries. The battery type would be determined later from a consideration of milliamp-hours needed for endurance purposes.

In selecting the battery pack/propeller combination the three crucial phases of flight -- namely, take-off, climb, and cruise -- were examined. Each of these flight phases were analyzed separately in order to select the battery/propeller combination to yield the best overall performance.

Several constraints governed the selection of the propulsion system. These are summarized in Table 4-3 and are discussed throughout this section in regards to the different components and the processes by which they were selected. Firstly, the maximum distance allowed for ground roll on take-off was 75 feet and was set by the Design Requirements and Objectives study. The maximum current allowed in the circuitry was to be 20 amperes. This arose from the fact that the Astro 05 motor would be damaged if the armature current exceeded this value and it was "enforced" by inserting a 20-amp fuse into the circuitry so that it would blow and safe the motor. It was then obviously undesirable to choose a battery pack/propeller combination that would draw a current exceeding 20 amps at any time during flight because this would cause an immediate loss of all power. Another constraint was a minimum power available output of 37 Watts. This would ensure that the plane climb at the desired rate of climb.

TABLE 4-3 : Constraints Governing Propulsion System

Maximum Take-Off Distance	75 feet
Maximum Current Draw	20 amps
Minimum Power Available	37 Watts
Maximum Battery Pack Weight	11 ounces
Maximum Endurance	78 seconds
Maximum Range	1776 feet

The selection of the battery pack and propeller was accomplished in two related manners. One method examined the take-off phase and the associated constraints. This method examined a wide range of battery pack/propeller combinations and narrowed it down to one which was acceptable. The second method examined the climb phase. It considered fewer propellers and by applying relative constraints eliminated all but two combinations. Considering results of both methods, the battery pack/propeller combination was able to be selected with confidence.

Take-off Phase Method : This analysis proceeded with the take-off performance of the airplane. This phase was aided by the computer program "Take-Off Performance," written by Dr. S. M. Batill [Ref. 3]. It incorporated the previously developed thrust and power coefficients as a function of advance ratio, the lift and drag characteristics of the airplane, the wing area and airplane weight, the ground friction coefficient of the mission flight center, battery voltage and resistance, and the torque and current characteristics for the Astro 05 motor. With these inputs, the program integrated the ground roll performance at 0.05 second intervals and yielded the following output: the distance required to achieve the flight speed; maximum current draw; maximum power required to turn the propeller; time to achieve take-off; and battery power consumed in ground roll. The final selection was based upon take-off distance and maximum current draw, even though we desired that the maximum battery drain not to exceed 5% of the total milliamp-hour capacity. A sample of an input and output data file are presented as Item 9 in the Appendix.

Using the propeller data, each propeller was analyzed for take-off performance in conjunction with 5, 6, 7, and 8 batteries, with each battery representing 1.2 volts. Although the amount of batteries used would have an effect upon the battery pack weight, the weight of the airplane was assumed to remain constant at 3 pounds. This weight estimation is based on 7 batteries, and hence if the number of batteries were less, resulting in a decrease of total airplane weight, the overall take-off performance would improve. This assumption was validated through use of the program and initial hand calculations.

Figures 4-3 through 4-5 represent the results determined through use of the "Take-Off Performance" code. After analyzing the data, it was found that the take-off distance and the maximum current draw defined a definite trend. The grid upon which the curves are drawn represents all combinations of propeller pitch and diameter studied. Each intersection point indicates one such combination with the abscissa indicating the propeller diameter while the ordinate is the propeller pitch. As indicated on the grid, several combinations were eliminated because they did not overcome friction, take-off in under 300 feet, achieve take-off velocity, or produce enough power. These are indicated by the asterisks (*) according to the key at the bottom of the figure.

The take-off distances formed parabolic curves that opened to the right (Figure 4-3), while the maximum current draw formed parabolic curves that opened to the left (Figure 4-4). This trend in data existed for all of the battery pack sizes that were studied. In addition to these results, the battery drain in mahrs is represented for the different propeller sizes (Figure 4-5). The data does not form any analytical trend because the battery drain is a function of current draw as well as total time for take-off.

Referring to Figure 4-3, it is shown that for 7 batteries, there existed the greatest number of propellers which met the take-off distance constraint. These being the 10-6, 10-8, 11-6, 11-8, 12-4, and 12-6, all of which yielded a take-off distance of 50 feet or less. Figure 4-4, however, shows that only three of these propellers fall below the maximum allowable current draw, these being the 10-6, 10-8 and 11-6 drawing approximately 15 amps, 19 amps, and 19 amps respectively. The 10-8 and 11-6 were rejected because they were considered to be within the limit of uncertainty associated with the accuracy of this analysis. Hence, this left only the 10-6 propeller to be examined. The 10-6 yielded a take-off distance of approximately 45 feet which fell well below the maximum allowable take-off distance of 75 feet. In addition to having a relatively short take-off distance, this battery pack/propeller combination drew a maximum of only 15 amps, 25% less than the maximum allowable current draw. It should also be noted that this combination, as shown by Figure 4-5, only consumes approximately 15 mahrs during take-off, which is quite affordable.

Figure 4-3

Take Off Distane (ft)
7 batteries / 8.4 volts

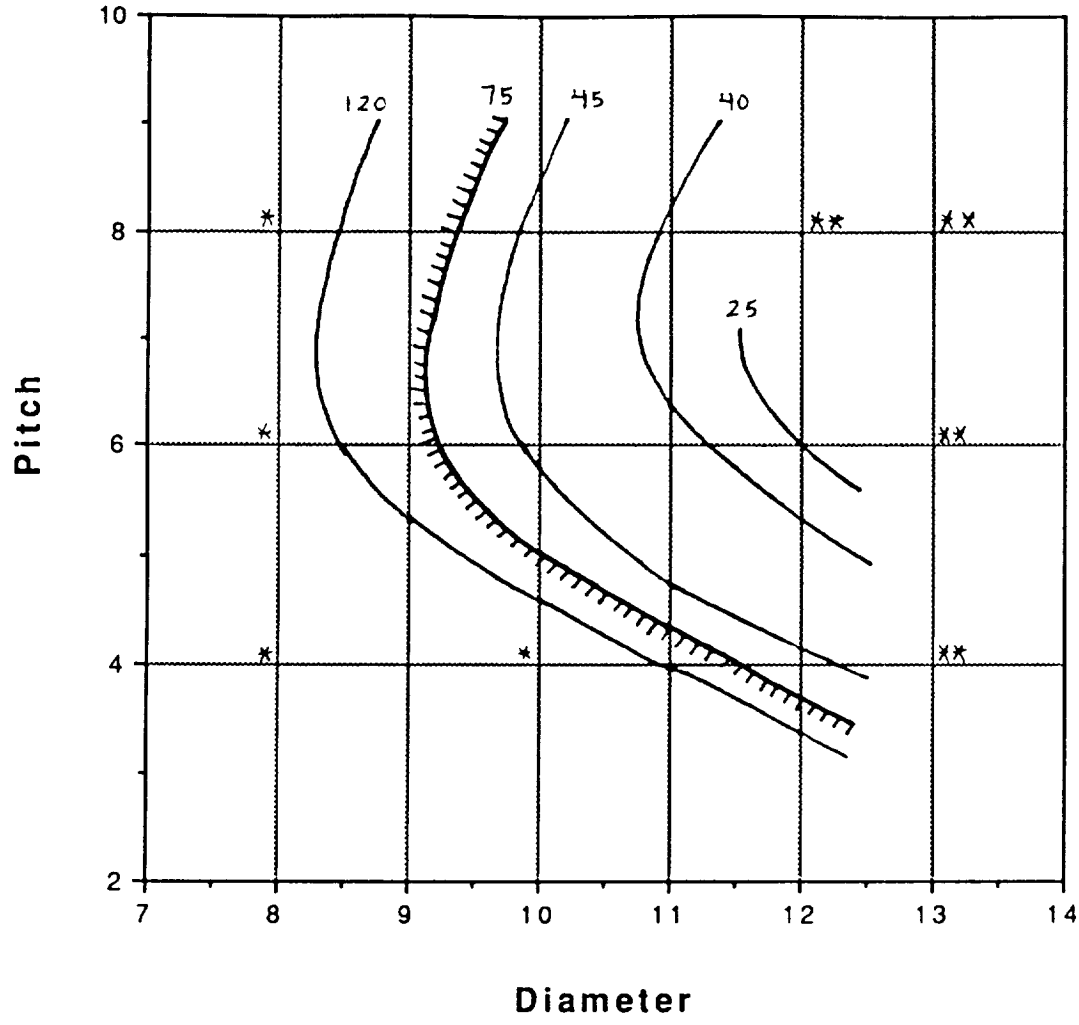

* Friction Exceeds Static Thrust
** Max Power Exceeds Max Allowable

Figure 4-4

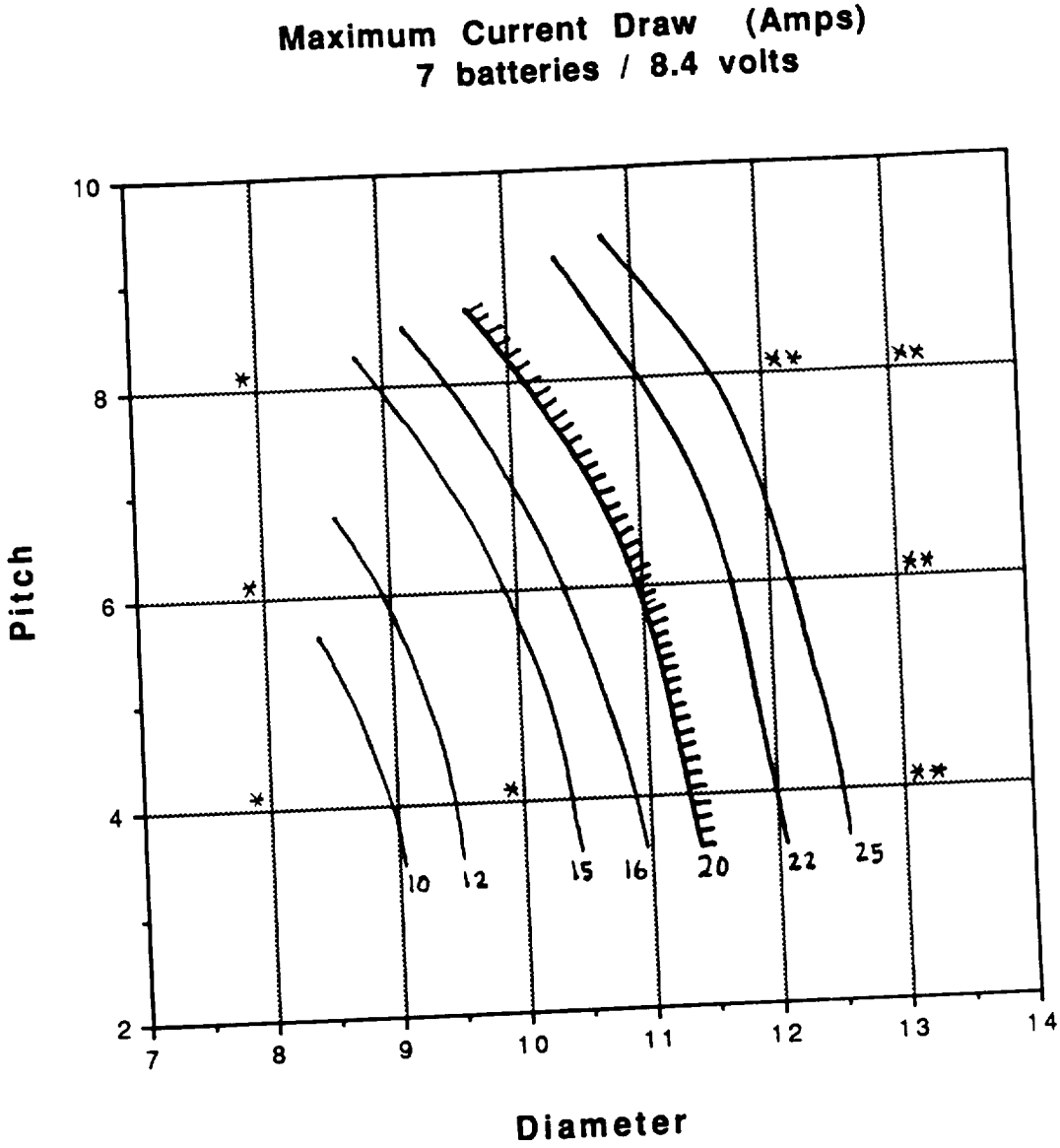

* Friction Exceeds Static Thrust
** Max Power Exceeds Max Allowable

Figure 4-5

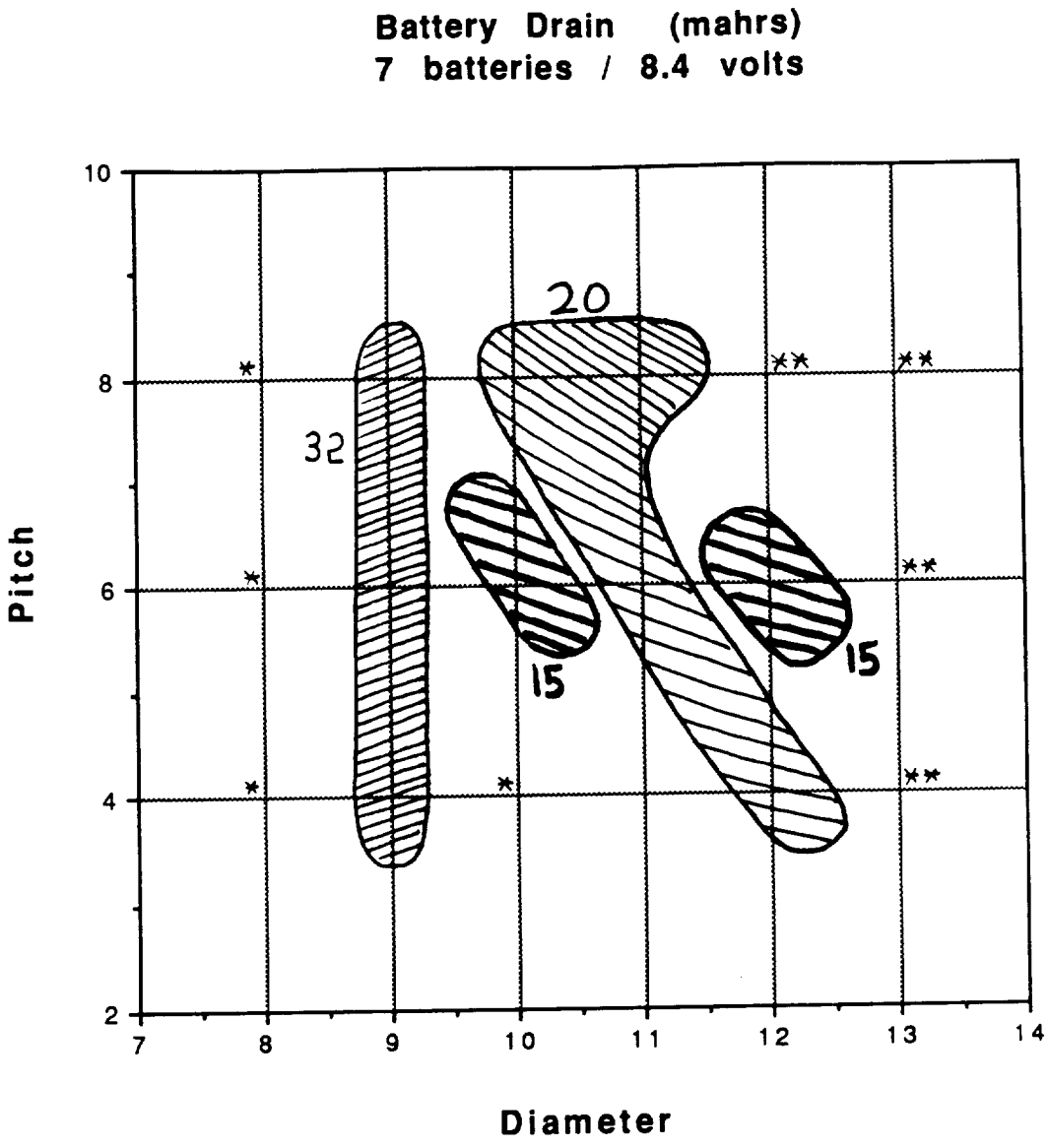

* Friction Exceeds Static Thrust
** Max Power Exceeds Max Allowable

In summary, the take-off performance analysis indicated that the best propeller/battery combination suited for take-off, allowing the airplane to take-off in under 75 feet and drawing less than 20 amps, consisted of the 10-6 propeller.

Climb Phase Method : Initial calculations showed that the climb phase proved to be the most demanding in terms of power requirements. From estimations of cruise power requirements and desired rate of climb, we were able to determine the amount of available power needed to be supplied to the aircraft in order to carry out a successful climb. This needed power available became one constraint which the battery pack/propeller had to fulfill. Another constraint came from the allowable armature current. As mentioned earlier, the Astro 05 motor would be damaged if it experienced a current of greater than 20 amps. For the climb and cruise analysis, an Airscrew 9-6, a Tornado 10-6 and a TopFlight 12-6 were considered so as to represent the desired range of propellers from which to choose.

A plot of power available against the number of batteries for the three choices of propellers is shown in Figure 4-6. From this figure, several combinations are immediately ruled out since they do not provide the 37 watts of available power needed in climb. The Airscrew 9-6 propeller with a battery pack of 7 or fewer batteries fails to produce enough power. Likewise, the Tornado 10-6 with 6 or fewer and the TopFlight 12-6 with 5 or fewer batteries do not meet the power constraint. These combinations were therefore eliminated as possibilities. The armature current constraint served to exclude several other possibilities. Figure 4-7, which shows the relationship between armature current and the number of batteries for the propellers under consideration, illustrates these excluded combinations. The Airscrew 9-6 propeller with a battery pack of 10 batteries violates the current constraint. The combinations involving the Tornado 10-6 with 10 and 9 batteries exceeded the allowable current and were ruled out. This same propeller with 8 batteries was also ruled out since the current draw of 19 amps was, as mentioned earlier, within the limit of uncertainty associated with the accuracy of this analysis. The combinations of the TopFlight 12-6 propeller with 10 to 6 batteries were also eliminated from consideration due to the excessive current draw.

Figure 4-6

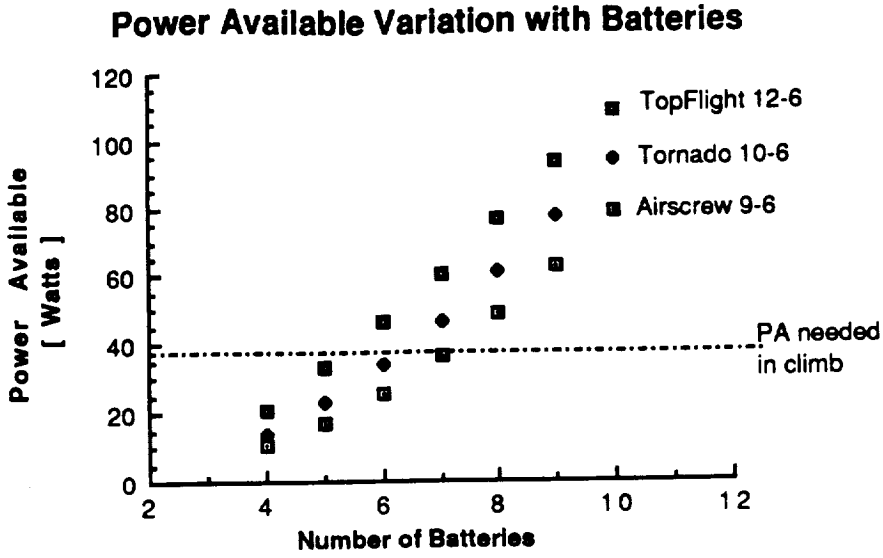

Figure 4-7

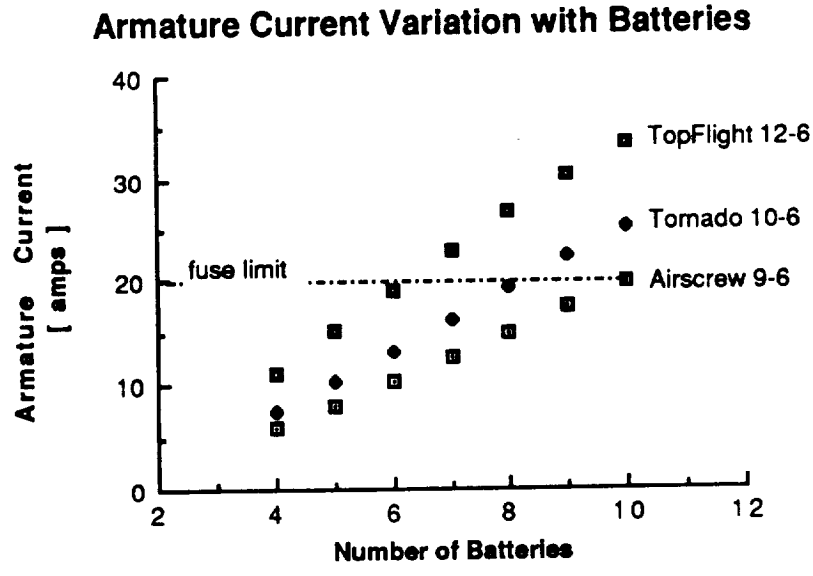

Summarizing the results of these constraints, only two battery pack/propeller combinations satisfied the requirements. These were the Airscrew 9-6 with 8 batteries and the Tornado 10-6 with 7 batteries. The former was eliminated through a take-off analysis since it was unable to generate enough thrust to exceed static friction. This enabled selection the Tornado 10-6 propeller and a battery pack of 7 batteries to be used along with the Astro 05 motor.

The propulsion system had then been specified with the exception of two parameters. These were the battery type (AAA, AA, C, or D) and the manner in which the batteries were arranged (series or parallel). The factors influencing the battery type were capacity (in terms of milliamp-hours) and weight. This discussion will be presented later. The reasons for which the batteries were arranged in series will now be discussed. Since the power produced by the motor is directly proportional to the open circuit voltage it was advantageous to arrange the batteries as to achieve a high voltage. This was accomplished by a series configuration since voltage adds in series. Secondly, the current does not add in series as it would in parallel. Therefore, a series arrangement would keep the current low which is a desirable feature. For these two reasons, the batteries were arranged in series.

Considering the Tornado 10-6 propeller with 7 batteries, Figure 4-7 shows that the current draw during climb at full throttle is approximately 16 amps. For a 4 second climb, the power consumed is approximately 20 mahr, which is quite affordable. Upon reaching a design altitude of 20 feet, the motor was throttled back (by adjusting the voltage with a speed controller) so that the power available would be equivalent to the power required. The power required referred to is that which corresponds to a steady-level turn with a bank angle of 30°. This is so that the airplane would not lose altitude in the turn. Figure 4-8 shows the relationship between armature current and power available for a range of throttle settings. The power required for a steady-level turn was about 8 watts. This figure shows that the corresponding current draw is roughly 6 amps. Although the power required in steady, wings-level flight is slightly less than that required for a steady-level turn, the two powers will be considered equal so as to simplify the calculations and produce a conservative estimate. Considering the power consumed in take-off (15 mahr), the power

Figure 4-8

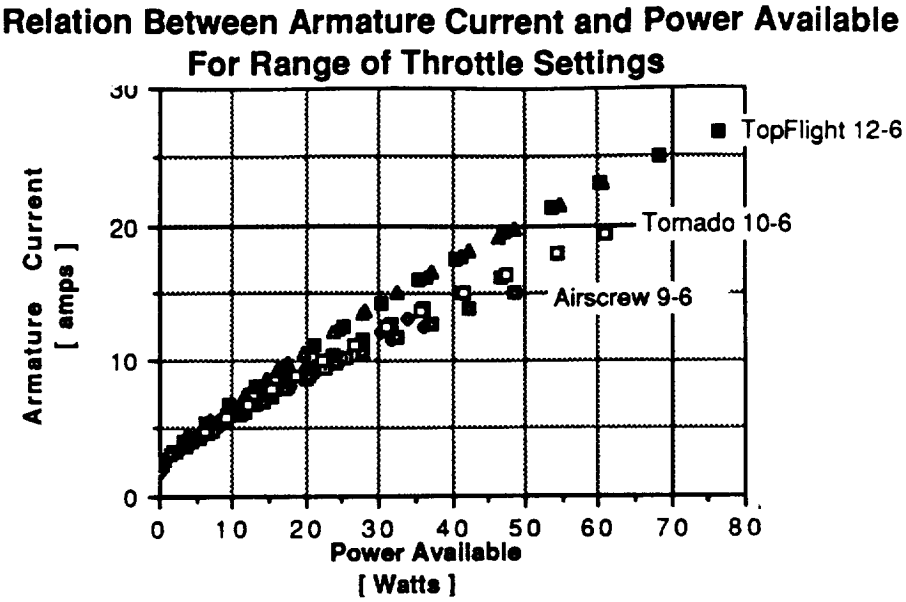

Figure 4-9

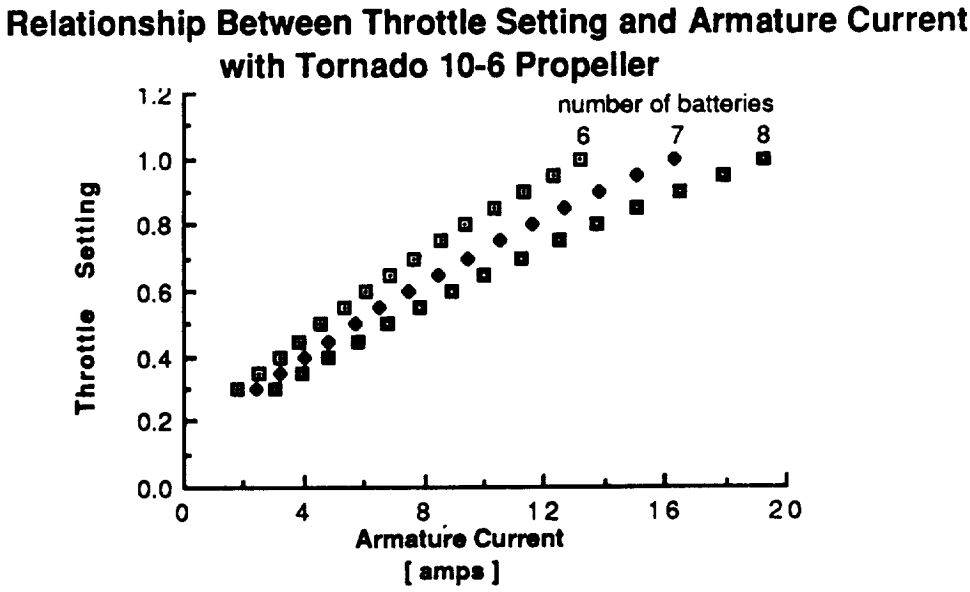

consumed in climb (20 mahr), the current draw in cruise (6 amps), and the aforementioned simplification, the endurance of the aircraft is 221 seconds for a battery pack of AA batteries and 129 seconds for 2/3AA batteries. The AA batteries were chosen because of the large cushion in capacity. Although the 2/3AA batteries provided enough power capacity for the anticipated mission, there were still unknowns that had to be considered. The larger capacity AA batteries were chosen because it provided a margin which would allow for an aborted take-off, ground roll testing prior to flight, and a safe margin to account for standard unknowns. This comfortable increase in capacity with the AA batteries also meant an increase in weight, from 2.94 to 5.46 oz. Weight estimations for the initial design included a battery pack weight of 9-11 ounces. All other parameters in the aircraft design were able to be achieved assuming this battery pack weight. Therefore, by using the seven AA batteries the weight was already well below initial estimations. Though the additional weight savings with the 2/3AA batteries would have been attractive, it was regarded as unnecessary in light of this already "low" battery pack weight achieved with the AA batteries. The small weight penalty was willing to be accepted in light of the increased endurance.

D. Speed Control

As mentioned previously, the propulsion system incorporated a speed controller in order to throttle back the motor for the cruise portion of flight. The take-off and climb phases of flight were performed at full throttle to ensure the desired performance. Throttling back for cruise allowed the pilot to maintain steady level flight through the turns as well as reducing battery consumption in order to increase endurance. Due to the small margin for error in throttling back for cruise, it was desired to obtain some idea of the degree of throttling necessary so that the pilot might be informed. Figure 4-9 shows the relationship between throttle settings and armature current for the chosen Tornado 10-6 propeller. As revealed by the figure, for a cruise armature current of 6 amps (with 7 batteries) the throttle setting was to be approximately 50%. With this information, the pilot knew, upon reaching cruise altitude, to throttle the speed controller to 50% power. From there,

only minor adjustments were required to maintain a steady-level turn and then steady-level flight.

SECTION V

STRUCTURES

A. Structural Configuration

Before estimation of the center of gravity could be completed, the structural configuration of each component was determined. The structural design was based on existing plans of other flight worthy aircraft found in modelling magazines and other such literature. Regular design status reports by the other design groups and aircraft design expert Mr. Joe Mergen also proved quite helpful in determining the structural layout for the SCREEM-J4D.

Fuselage : The fuselage is mainly a truss structure with minimal planking to keep the weight low and to provide added strength. The structure is shown in Figure 5-1. It is comprised of primarily balsa wood with birch plywood used as mounting plates. The fuselage is 37" in length and has a maximum cross section of 4"x 4". The main section of the fuselage was designed in such a fashion as to allow for flexibility in placing the internal components. This was done so that it would be easy to adjust the components if a center of gravity shift was needed.

Wing : The wing is pictured in Figure 5-2. It consists of 3 sections: one 36" inboard and two 30" outboard sections. The wing was designed in this way simply for storage purposes (within a 2'x2'x4' compartment). The design is fairly conventional. False ribs located at the leading edge are used for added support for the skin. The analysis for the spar configuration is discussed in the next section. The main features of the design are the connection of the inboard and outboard wing, and the mounting location of the wing to the fuselage. Initially, a 'micro-bubble/epoxy' matrix with an aluminum or brass rod set in the spar box was considered for this purpose. But a simpler spruce connection was decided upon for lighter weight and ease of construction. 4" spruce beams will be set in the 'box' formed by the spars and webs (see Figure 5-3), one in the inboard section and one in the outboard section. The connection will be secured together with tape wrapped around the wing. Mounting of the wing onto the fuselage will be accomplished using the bolt technique. Bolt locations are at the forward and trailing edge of the wing center. Added support will be provided by securing the wing with a rubber band, if needed.

Figure 5-1

Fuselage Structural Configuration

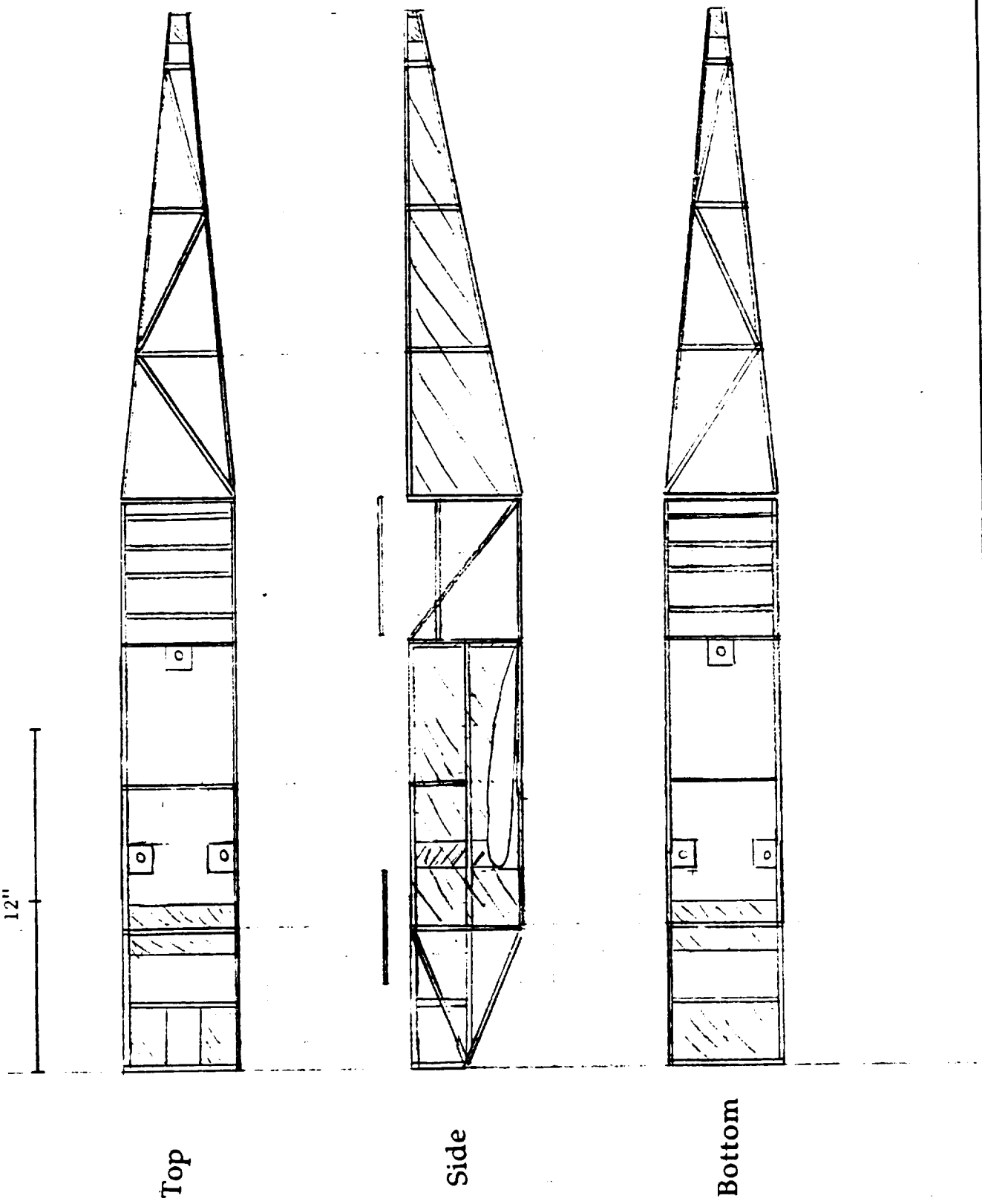

Figure 5-2

Wing Structural Configuration

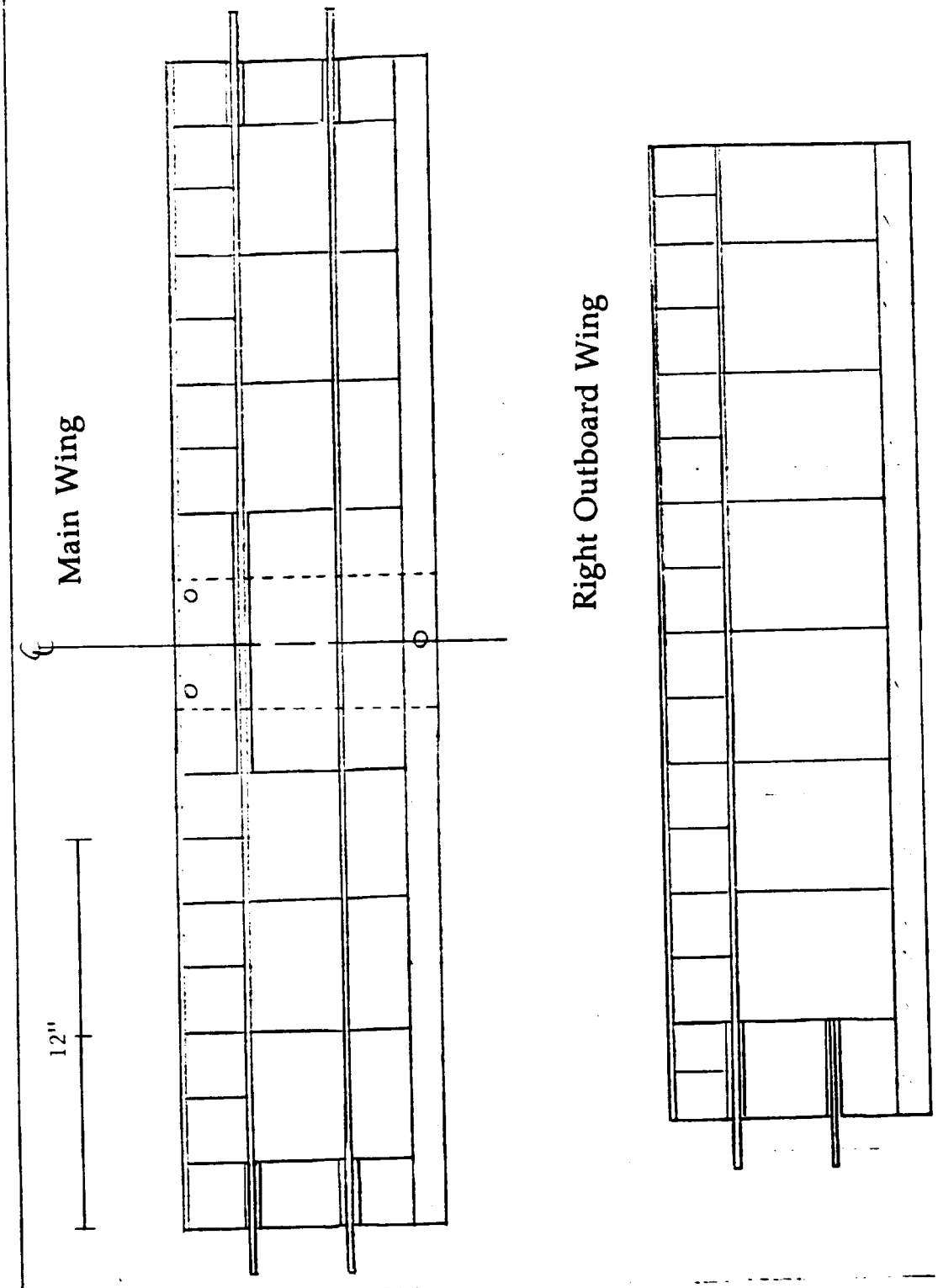

Wing Connection

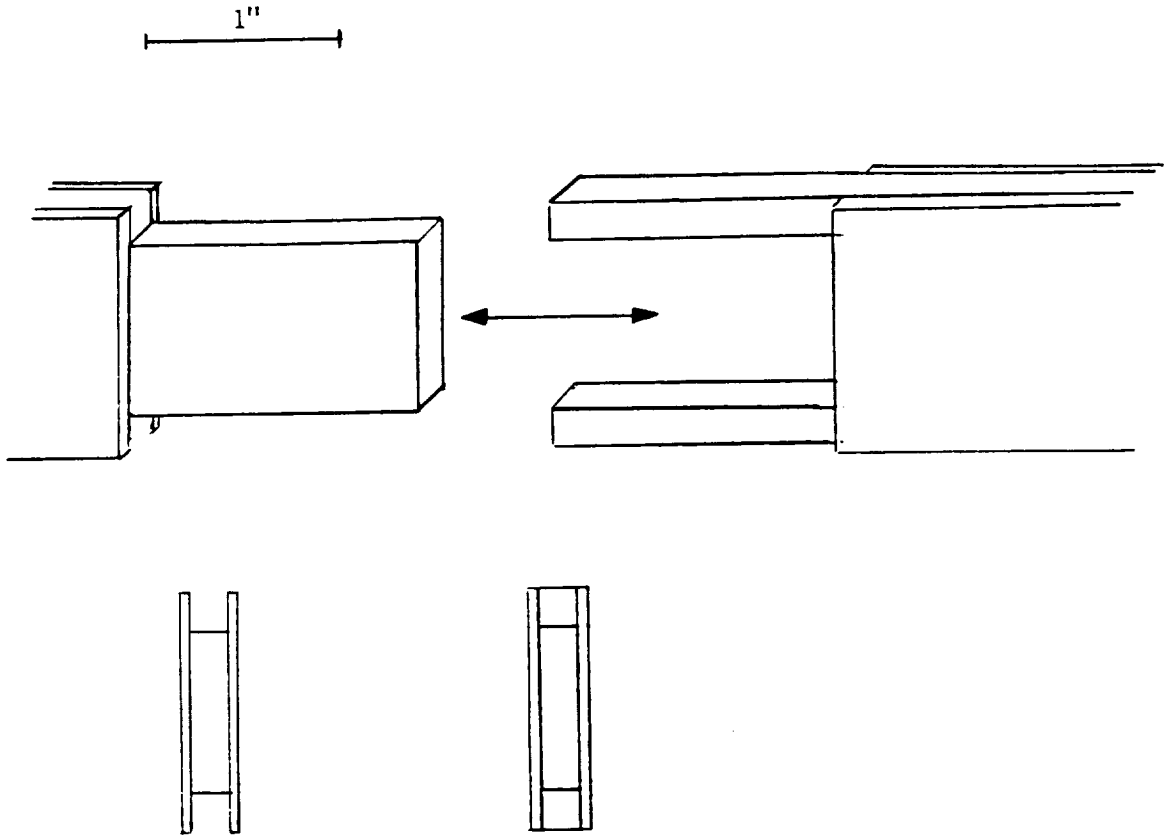

Empennage : The empennage (vertical and horizontal tails) are pictured in Figure 5-4. The design is truss-like to provide strength and low weight. The empennage will be permanently fastened to the fuselage.

B. Spar Configuration

Before analysis of the spar was performed, the spanwise distribution of shear and bending moment for the cruise flight condition was determined. This was done by means of the computer program listed as Item 10 in the Appendix. Input for the computer code included:

a. Wing planform geometry
b. Aerodynamic section properties as a tabular function of spanwise position
c. Structural weight per unit span as a tabular function of spanwise position
d. Aircraft dynamic pressure and angle of attack

which are read from a data file. A second computer program listed as Item 11 in the Appendix was utilized to determine the centroid location, section properties relative to the centroid, and the direct stress due to both bending and axial loads for the idealized airfoil section shown in Figure 5-5. Each component of the airfoil was idealized as a "lumped area". The maximum direct stress, $\sigma = \pm 779$ psi, was located in the main spars (areas 3 and 8) which are spruce. The maximum allowable stress for spruce is 6200 psi which shows that the main spars are safe from failure. Even when considering a factor of safety of 2.0, the maximum direct stress is σ = 1560 psi, which is still safe from failure. Table 5-1 summarizes the section properties, loading conditions, direct and allowable stress for each "lumped area".

Figure 5-4

Empennage Structural Configuration

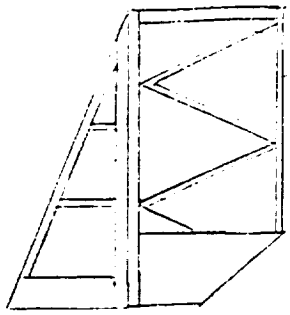

Vertical Tail

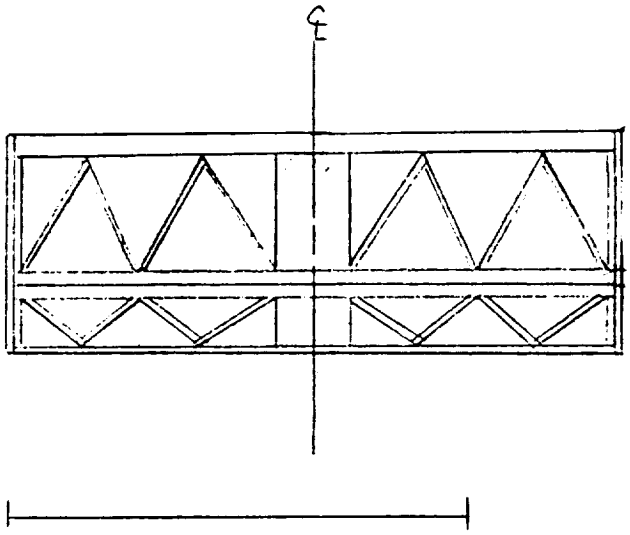

Horizontal Tail

Figure 5-5

Spar Configuration

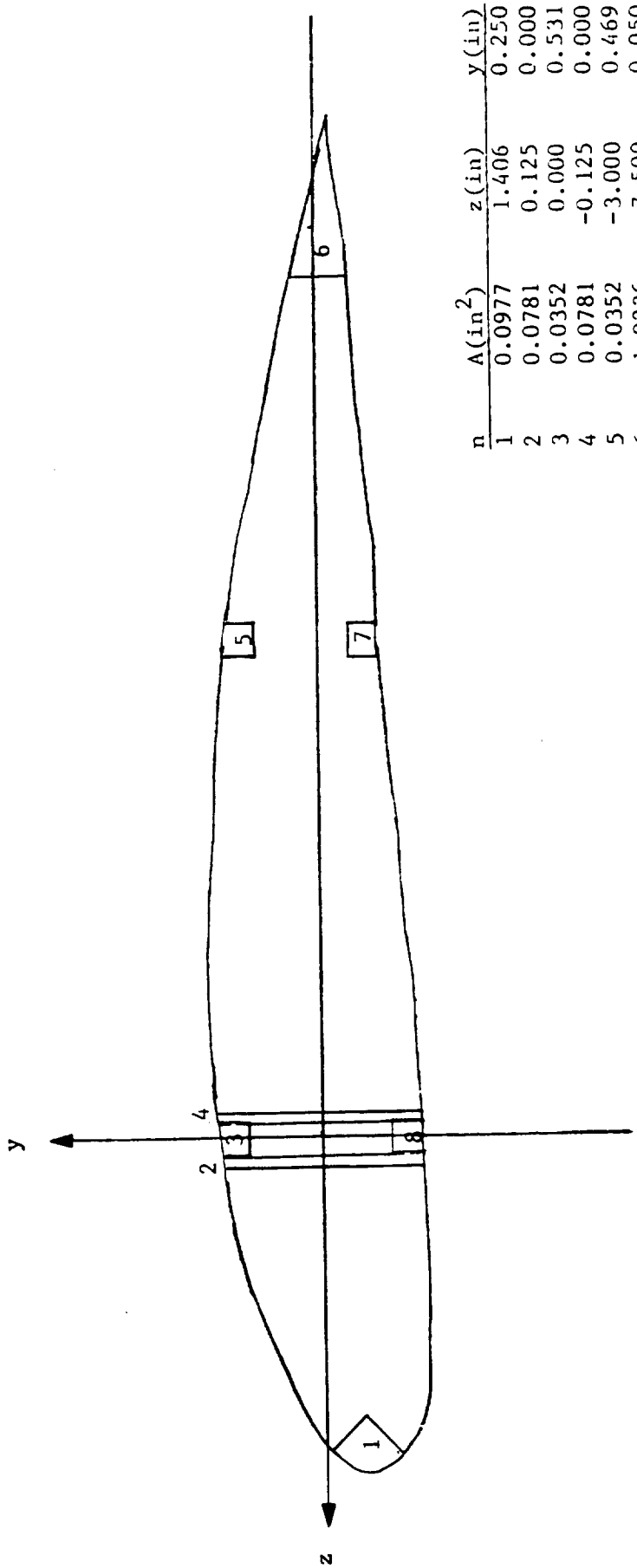

n	$A(in^2)$	z(in)	y(in)
1	0.0977	1.406	0.250
2	0.0781	0.125	0.000
3	0.0352	0.000	0.531
4	0.0781	-0.125	0.000
5	0.0352	-3.000	0.469
6	1.0236	-7.500	-0.050
7	0.0352	-3.000	-0.281
8	0.0352	0.000	-0.531

Figure 5-6 Spar Configuration

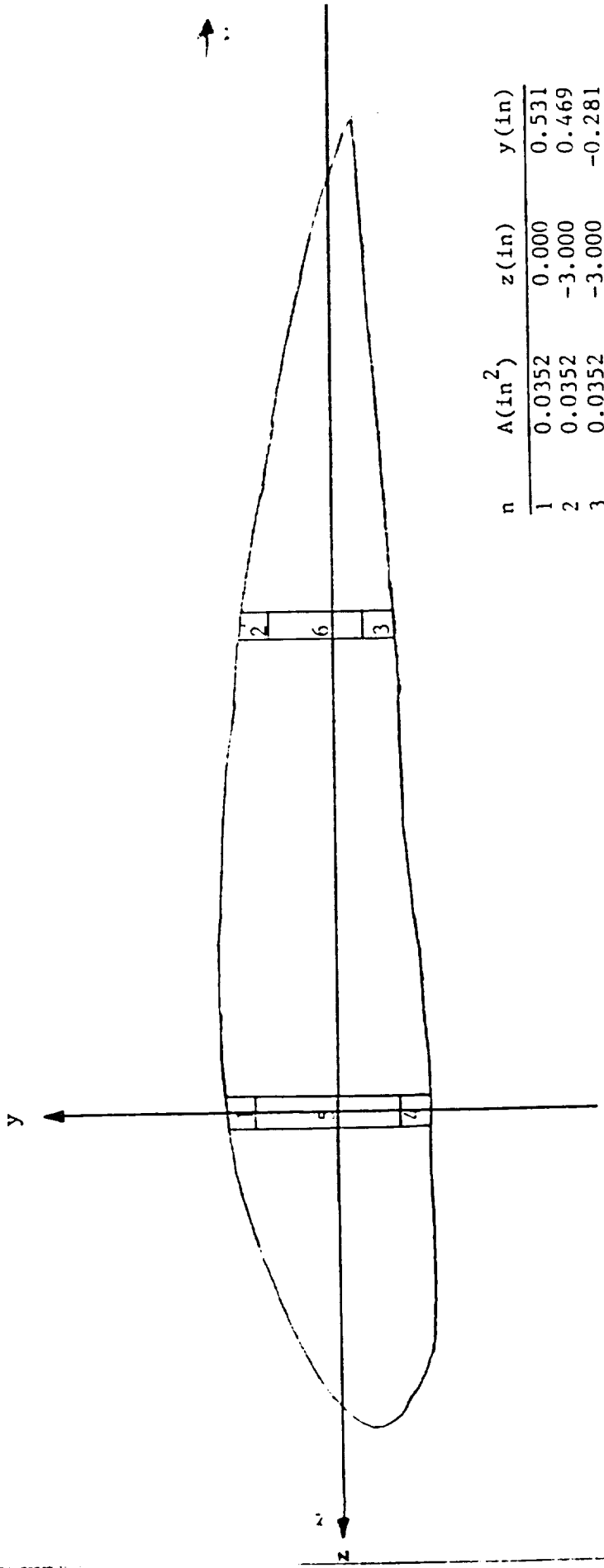

n	$A(in^2)$	z(in)	y(in)
1	0.0352	0.000	0.531
2	0.0352	-3.000	0.469
3	0.0352	-3.000	-0.281
4	0.0352	0.000	-0.531
5	0.1523	0.000	0.187
6	0.1055	-3.000	0.094

TABLE 5-1: Direct Stress Distribution at Wing Root

$Y_{centroid}$ = 0.00 in	I_{yy} = 36.59 in^4	P = 0.00 lb
$Z_{centroid}$ = -2.81 in	I_{zz} = 0.42 in^4	M_y = 2.42 in-lb
	I_{yz} = 0.34 in^4	M_z = 30.24 in-lb

i	σ_{xx}(i) psi	σ_{xx}(all) psi	Material
1	-17.28	±400.00	Balsa
2	0.09	±400.00	Balsa
3	-779.12	±6200.00	Spruce
4	-0.09	±400.00	Balsa
5	-36.62	±400.00	Balsa
6	-1.96	±400.00	Balsa
7	18.37	±400.00	Balsa
8	779.12	±6200.00	Spruce

An analysis of the joints connecting the inboard and outboard wings was also performed. Figure 5-6 shows the configuration of the spars and Table 5-2 summarizes the data. As the table indicates, the maximum allowable stress is not reached in any of the members.

TABLE 5-2: Direct Stress Distribution at Y=18 in

$Y_{centroid}$ = 0.12 in	I_{yy} = 13.14 in^4	P = 0.00 lb
$Z_{centroid}$ = -0.99 in	I_{zz} = 0.44 in^4	M_y = 0.85 in-lb
	I_{yz} = 0.11 in^4	M_z = 10.60 in-lb

i	σ_{xx}(i)psi	σ_{xx}(all)psi	Material
1	-258.07	±6200.00	Spruce
2	-12.20	±400.00	Balsa
3	-7.64	±400.00	Balsa
4	258.07	±6200.00	Spruce
5	-91.08	±6200.00	Balsa
6	-61.78	±6200.00	Balsa

C. Materials Selection

The critical characteristics of the materials under consideration were:

a. Strength
b. Weight
c. Cost
d. Machinability
e. Availability

Wood, metal, composites, and ceramics were considered and the relative rankings of these regarding the critical characteristics are summarized in Table 5-3.

TABLE 5-3 : Relative Material Characteristics

Material	Strength	Cost	Weight	Machinability	Availability
Wood	4	1	2	1	1
Metal	2	2	4	2	2
Composites	1	4	1	3	3
Ceramics	3	3	3	4	4

The table shows that wood is the best material to be used. Though wood ranked last in strength, it still would provided sufficient strength to meet the stress requirements mentioned earlier. The bulk of the structure was comprised of balsa wood with spruce and birch plywood used where extra strength was needed. The skin of the J4D was "Micafilm" manufactured by Coverlite. It is a non-woven fiber that "offers low weight, resistance to tearing, and good modulus" fit for models where weight control is a primary concern.

D. V-n Diagram

The V-n diagram is shown in Figure 5-7. First notice that the gust loads do not affect this diagram because of the indoor operating environment which is free from any significant gusts. There are no negative load factors because the aircraft is not designed to operate at a negative wing incidence. The maximum operating velocity, V_{max}, of the aircraft is 58 ft/s, the minimum

Figure 5-7: V-n Diagram

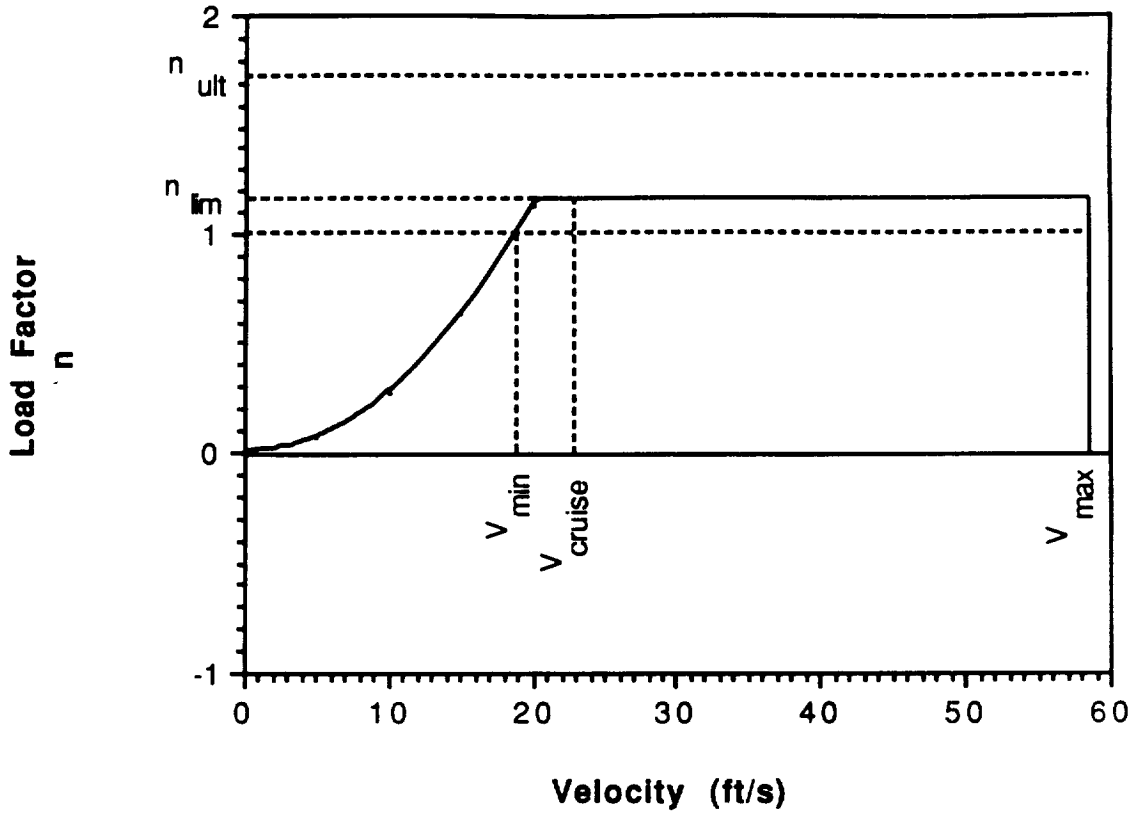

(stall) velocity, V_{min} is 18.9 ft/s, and the cruise velocity, V_{cruise}, is 23 ft/s. The limit load factor, n_{lim}, is 1.15 (from a maximum bank angle of 30 degrees). The positive stalling portion of the curve is found using standard sea-level conditions (ρ = 0.00237 lb/ft^3), a maximum lift coefficient of 1.3 and a wing loading of 0.55 lb/ft^2. The ultimate load factor, n_{ult} = 1.73, is based on a factor of safety of 1.5 ($n_{ult} = 1.5n_{lim}$). Special attention should be made to the fact that the cruise point (n=1.0, $V=V_{cruise}$), pushes the limits of the flight envelope. Therefore, the aircraft must not be flown at an attitude such that disastrous loads are placed on the aircraft. The factor of safety, however, does allow for somewhat significant loads to be placed on the aircraft, if necessary.

TABLE 5-4: Special Flight Conditions Illustrated in V-n Diagram

V_{max}	58	ft/s
V_{min}	19	ft/s
V_{cruise}	23	ft/s
C_{Lmax}	1.3	
n_{lim}	1.15	
n_{ult}	1.73	
β_{max} (bank angle)	30	degrees
W/S (wing loading)	.00237	lb/ft^3
	.0379	oz/ft^3
F.S. (factor of safety)	1.5	

SECTION VI

WEIGHTS ANALYSIS

A. Weights Estimation

An estimation of component weights was initially made based on standard component weight fractions for remote control aircraft of a similar type. These provided the initial goal weights for the components which guided the design of the aircraft. Based on an overall "target weight" for the aircraft of 3 pounds (48 ounces), the component weight fractions were determined. These are summarized in Table 6-1.

TABLE 6-1: Initial Estimation of Component Weights

Component	Weight (oz)	Weight Fraction (%)
Structural Frame	19.2	40.0
Propulsion	17.3	36.0
Avionics	7.2	15.0
Landing Gear	2.1	5.0
Payload	2.0	4.0

After the propulsion system, wing, control surfaces, and fuselage were sized and the material selected, a more refined estimation of component weights was made. The structural weight (fuselage, empennage, wing) were estimated from the structural configuration discussed in Section V. The propulsion system analysis resulted in the selection of the motor, batteries and propeller, and hence the propulsion weight. Avionics weight was known from the knowledge of the servos and speed controller used. The payload was designated to be 2 ounces. The landing gear remained a true estimation since its design had not been determined. The refined component weights and weight fractions are summarized in Table 6-2.

TABLE 6-2: Refined Estimation of Component Weights

Component	Weight (oz)	Weight Fraction (%)
Structures	21.26	44.3
Wing	10.36	21.6
Fuselage/Empennage	6.4	13.3
Skin, Fasteners, Links, etc.	4.50	9.4
Propulsion	16.19	33.7
Propeller	1.00	2.0
Fuel	5.46	11.4
Engine	9.73	20.3
Avionics	4.15	8.6
Landing Gear	2.40	5.0
Payload	2.00	4.0

The avionics components consisted of the receiver, system batteries, and servos, while the engine consists of the motor and speed controller. The "skin, fasteners, links, etc." component is that material which remained for use in construction of the prototype.

B. Internal Layout

In determining the internal arrangement of the aircraft, several factors had to be considered. Those factors of influence were:

- effects on center of gravity location
- proximity requirements
- simplicity of layout: non-interfering components
- cooling paths
- access
- wing mounting space designation

With the above considerations, the internal layout was determined. However, the locations were able to be changed slightly in the event that center of gravity location of the prototype was different from the designed

location. That is, there was some flexibility in this layout to accommodate for the uncertainties of the construction phase.

Table 6-3 is a summary of the internal system components, their respective functional classifications, and the corresponding sizes and weights:

TABLE 6-3: Weights and Sizes of Internal Components

Component	Classification	W [oz.]	L [in]	w [in]	h [in]
Motor	propulsion	6.5	2.25	1.25 **	
Battery Pack (7)*	power supply	5.46	1.95	0.55 **	
Sys. Battery(4)*	power supply	2.0	1.73	0.39 **	
Receiver	control system	0.95	1.31	1.87	0.81
Servos (2)*	control system	0.6	1.06	1.5	1.12
Speed control	control system	3.23	1.875	3.0	1.25
Payload	payload	2.0	2.0	2.0	2.0

value in parenthesis indicates number of such component
* weight and sizes data is given per battery or servo
** indicates diameter

Note that the battery pack is comprised of seven AA batteries, each of which is 1.95 inches in length and 0.5 inches in diameter. Their combined weight, as indicated above, is 5.46 ounces. Also, the system batteries were AAA, 1.73 inches long and .39 inches in diameter. Note that there are two servos: one operates the rudder surface and the other operates the horizontal tail surface.

To determine the relative location of the internal system components, a weight distribution program was utilized (see the computer program listed as Item 12 in the Appendix). With fixed values for the structural center of gravity, the placement of the internal components was selected. With the location of the components already set, the program was used to determine the location of the battery pack (whose weight was considered to be ballast). As mentioned before, the location of the battery pack and other components were allowed to shift slightly so that the overall center of gravity would remain in the design location.

The design locations of the internal components are summarized in Table 6-4 and shown in Figure 6-1.

TABLE 6-4: Design Locations for Internal Components

Component	Center of Gravity Location [in]		
	x	z	y
motor	1.13	2.63	2.0
speed controller	4.0	2.63	2.0
receiver	6.0	0.63	2.0
system battery	6.0	2.28	2.0
servo 1 (rudder)	18.94	2.44	1.0
servo 2 (horiz. tail)	18.94	2.44	3.0
battery pack	9.5	1.5	2.0
payload	9.0	3.0	2.0

x is measured from the nose of the aircraft, increasing toward the tail

z is measured from the bottom of the fuselage, increasing toward the top

y is measured from the middle of the fuselage, increasing toward the right

The servos are placed in the rear so there is no interference with the control lines to the rudder and elevator. They will be mounted on 1/16" balsa wood strips (servo trays), using wood screws. All other internal components, with the exception of the motor and the battery pack, will be similarly mounted. To avoid wood splitting at the screw holes, epoxy will be applied in the holes prior to inserting the screws. The motor will rest on two triangular, balsa wood mounts, and will be secured by elastic straps and screws. The battery pack will be secured by Velcro straps, to allow for quick re-location in the event that additional modifications are made which affect the center of gravity location. Thus, the battery pack provides a means for center of gravity travel.

Figure 6-1 **Internal Layout Configuration**

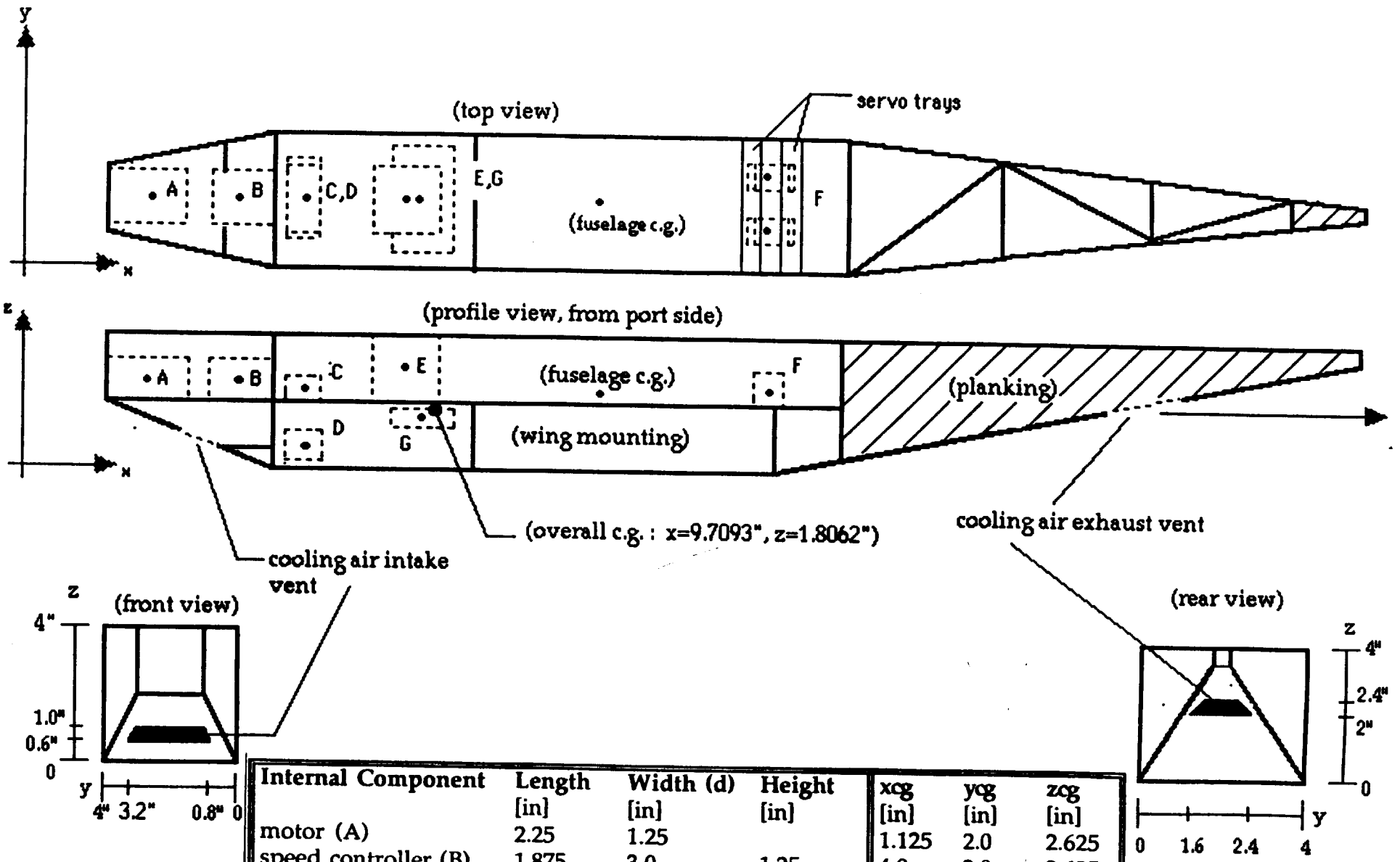

Internal Component	Length [in]	Width (d) [in]	Height [in]	xcg [in]	ycg [in]	zcg [in]
motor (A)	2.25	1.25		1.125	2.0	2.625
speed controller (B)	1.875	3.0	1.25	4.0	2.0	2.625
receiver (C)	1.31	1.87	0.81	6.0	2.0	0625.
system battery (D)	1.18	2.18	0.56	6.0	2.0	2.28
payload (E)	2.0	2.0	2.0	9.0	2.0	3.0
servos-2 (F)	1.06	1.5	1.12	18.94	1.0,3.0	2.44
battery pack (G)	1.95	0.5		9.2	2.0	1.6
fuselage	37.2	4.0	4.0	14.83	2.0	2.1

C. Center of Gravity Estimation

The placement and location of the center of gravity of each component are shown in Figure 6-2. The CG of the overall structure is set at 33% of the chord of the wing and the locations of the vertical and horizontal tail leading edges are set at 31.7" and 33.2", respectively. With these values fixed, the placement of the internal components was selected as outlined in the previous section.

Figure 6-2

Center of Gravity Estimation

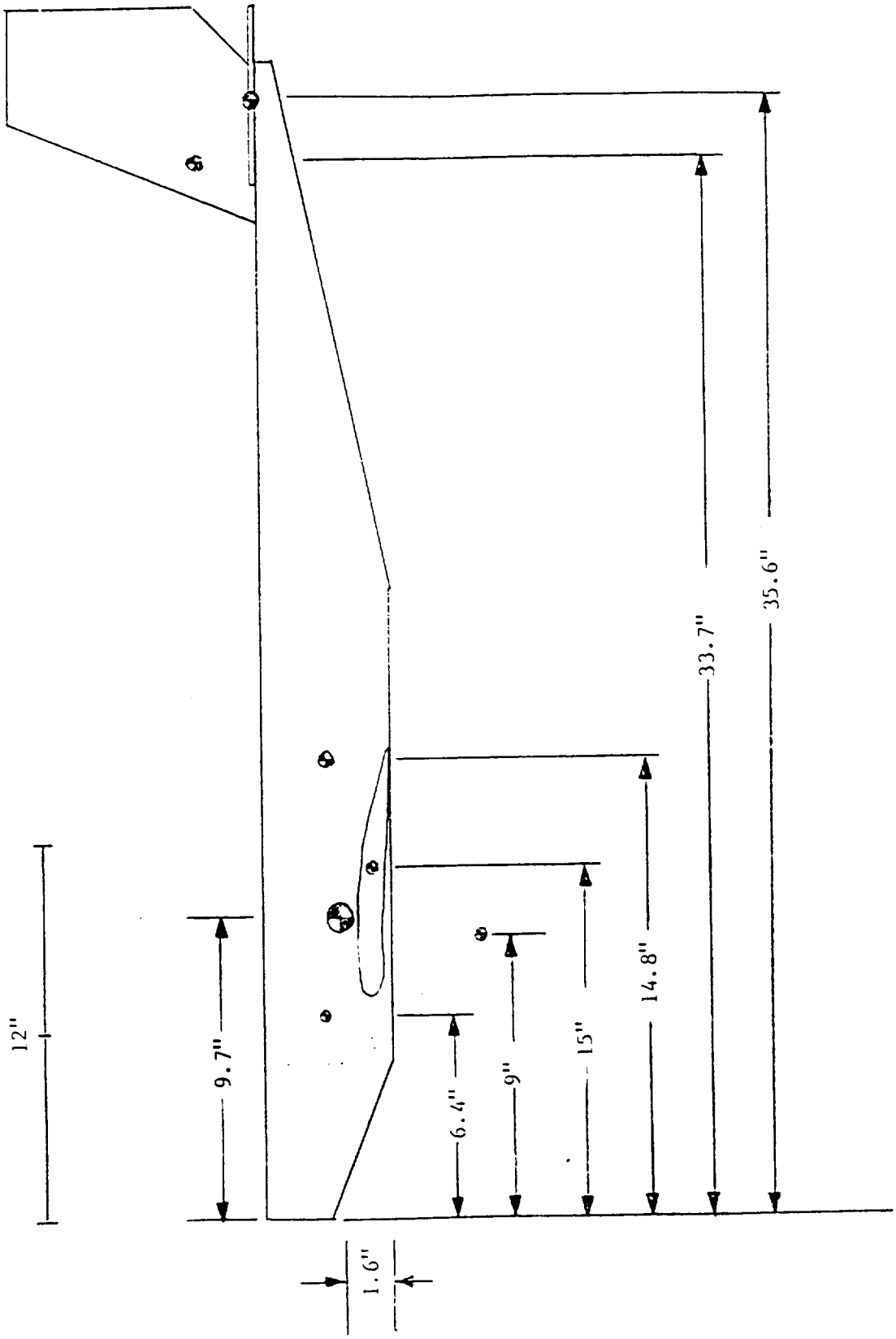

SECTION VII

PERFORMANCE

A. Lift, Drag and Lift/Drag

As for every aircraft, the basic size, weight, and cruise velocity of the aircraft dictate the lift coefficient necessary to sustain steady, level flight. The SCREEM-J4D, with its planform area of 5.46 ft^2, weight of 3 lbs, and cruise velocity of 23 feet per second needs a C_L of 0.874 to maintain steady, level flight. The lift coefficient necessary for flight is plotted as a function of velocity on Figure 7-1. The drag breakdown described in Section II gives a drag polar of $C_D = .0319 + C_L{}^2/.682\pi AR$. Using the SCREEM-J4D's aspect ratio of 11.72 and cruise C_L of .874, the drag coefficient at cruise is then .0564 (see Figure 7-2) for a total drag of .194 pounds. Combining this drag and the cruise velocity, the power required at cruise is 6.05 Watts. While this is not the minimum power required for this aircraft, (which incidentally occurs at 16-18 feet per second, as can be seen in Figure 7-3) it is only 25% higher than this minimum power required. With the lift and drag coefficients thus calculated, the maximum lift/drag ratio is 14.0, and as is evident in Figure 7-4, the SCREEM-J4D is flying at maximum lift to drag ratio at cruise.

B. Take-Off and Turning Flight

The SCREEM-J4D produces a static thrust of 1.186 pounds, which allows for takeoff in 45 feet at a takeoff velocity of 23.8 feet per second and $C_L)_{max}$ of 1.2. The power required to climb at the prescribed rate of 6 feet per second is 37 Watts, and the relatively high power available of 50 Watts means that the SCREEM-J4D will possess the capability to climb at a much higher rate of 15.2 feet per second.

In turning flight at the prescribed turn radius of 40 feet, the SCREEM-J4D must bank to an angle of 23^o, which means that the load factor in the turns rises to 1.1. At a roll rate of 28.8 degrees per second, banking to this angle requires .8 seconds and 18.4 feet to complete the transition to "fully banked." In order to perform this maneuver, the SCREEM-J4D must induce a change in angle of attack on the inboard wing of -3^o and a change of $+3^o$ on the

Figure 7-1

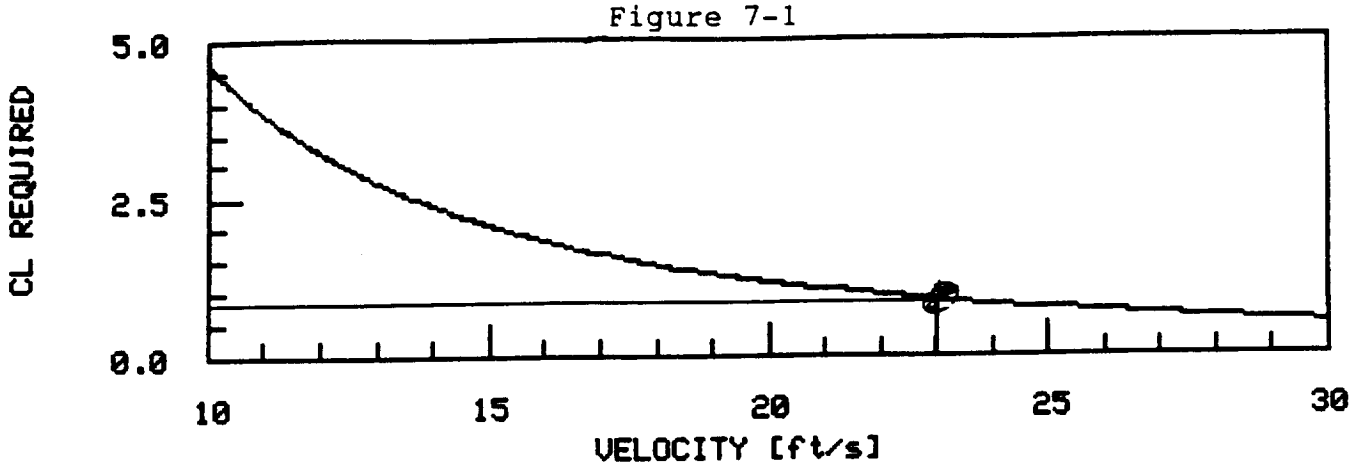

Figure 7-2

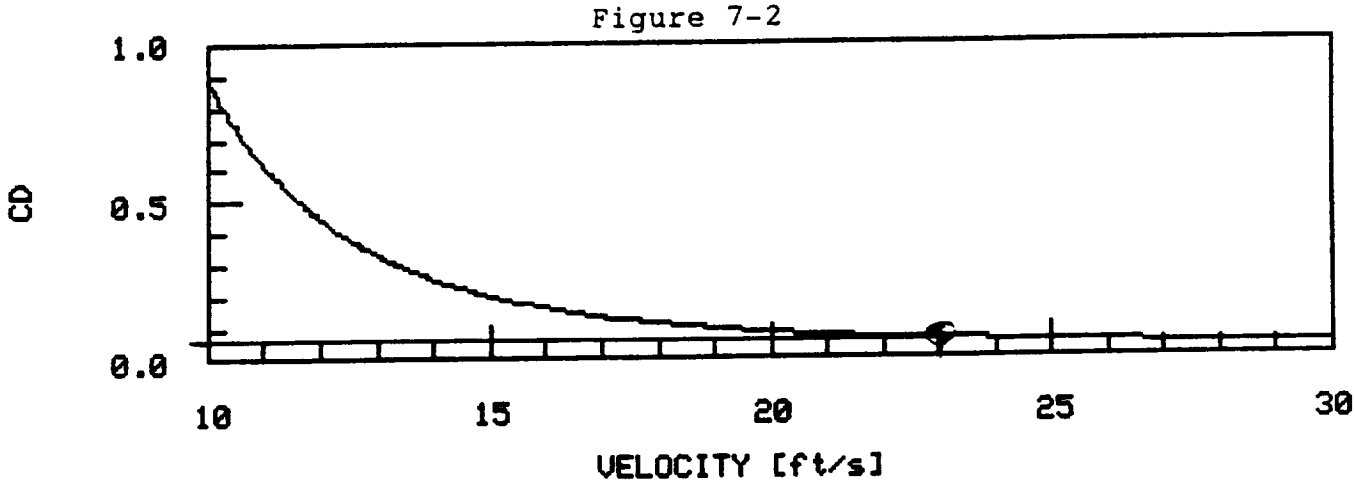

Figure 7-3

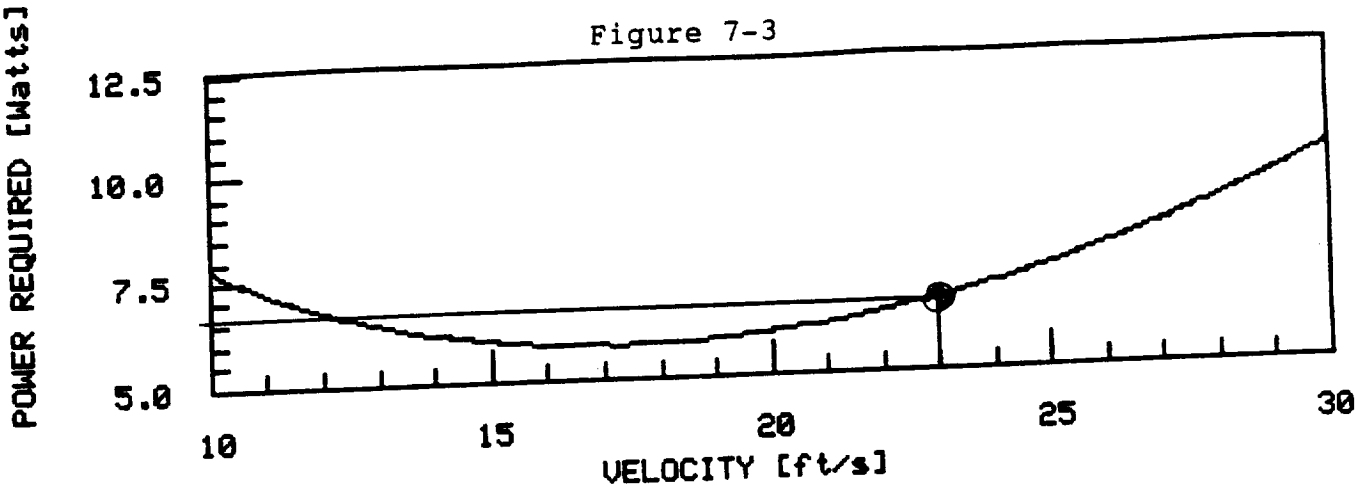

Figure 7-4

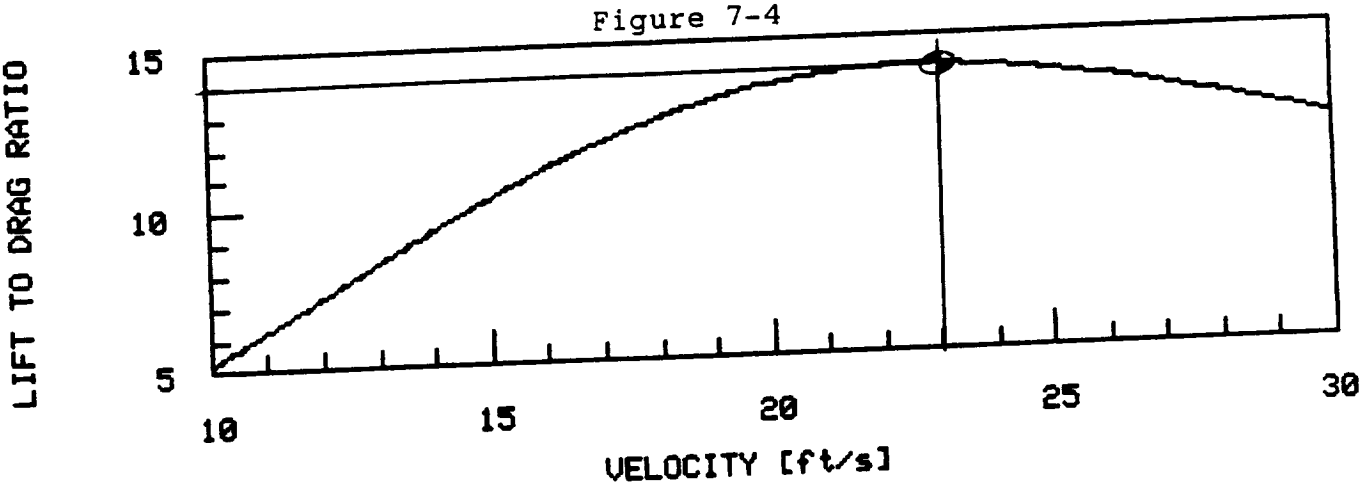

outboard wing. This change is incurred by a maximum rudder deflection of 25°. Reducing the rudder deflection will reduce the roll rate, but even cutting the roll rate in half will not severely inhibit the roll performance of the aircraft.

C. Endurance and Range

Given the battery capacity of 500 mahr the SCREEM-J4D, the maximum endurance is 221 seconds. Broken down into the different sections of the flight, 15 mahr is used in the takeoff phase and 20 mahr is used during the climb phase, leaving 465 mahr for the steady, level phase of the flight. This endurance should be sufficient for the mission, which will only require 78 seconds. Combining this endurance with the cruise velocity of 23 feet per second gives a maximum range of 5500 feet, once again well above the required range of 1800 feet. Parts B and C of this section are summarized in Figure 7-5 while Table 7-1 summarizes all of the critical performance data.

TABLE 7-1: Critical Performance Data

Vcruise	23	ft/s	n_{turn}	1.1	
C_L in cruise	.874		p roll rate	29	°/sec for $\delta_r = 25°$
C_D in cruise	.0564				
L/D max	15.5		E max	221	sec
Pr in cruise	6.05	Watts	R max	5500	feet
Pa	50	Watts	γ_{min} glide angle	4	degrees
Pa needed for climb	37	Watts	R/D	1.6	ft/s
R/C max	15	ft/s			

Figure 7-5

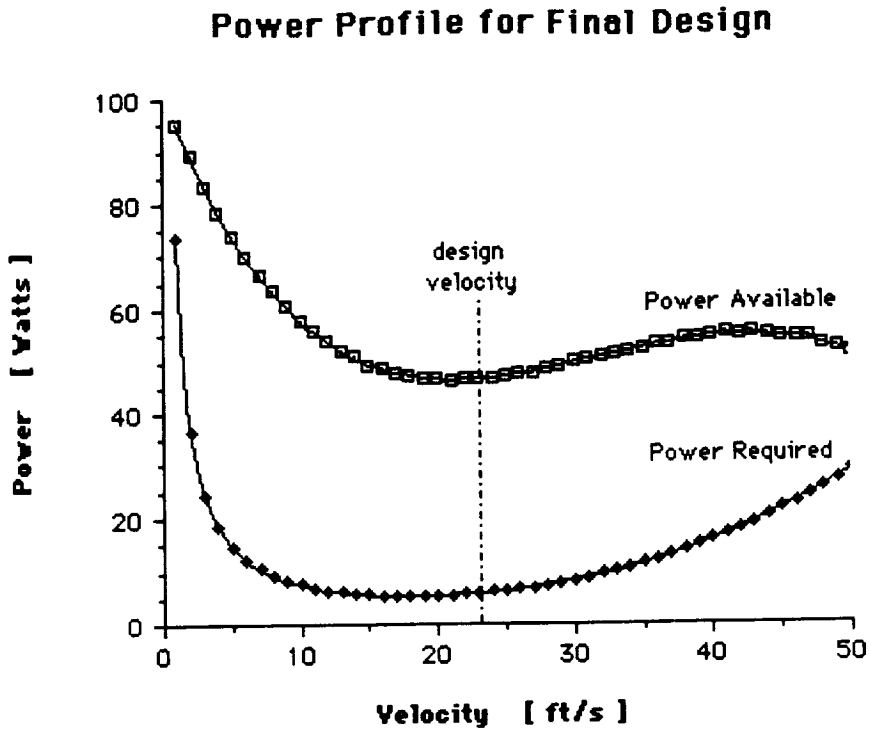

Motor:	Astro 05
Propeller:	Tornado 10-6
Batteries:	7 AA Nickel-Cadmium
Endurance:	221 seconds
Range:	5500 feet
R/C:	6 ft/s
T-O Distance:	45 feet

D. Landing

Because the aircraft will be flying at its maximum lift to drag ratio at cruise, its glide angle will be maximum at cruise. This maximum glide angle is -4^{o}, which will give a minimum rate of descent of 1.6 feet per second. At this rate of descent, the descent phase will take approximately 12.5 seconds, requiring close to 300 feet from the start of the descent phase until touchdown. This distance will be shortened somewhat by descending at a larger angle, with a flare upon touchdown to reduce the impact force. Due to the rough surface of the runway, it is estimated that for a touchdown on the first half of the available runway, the aircraft will come to a complete stop by the end. As a precaution, a net will be available after landing if it is evident from flight tests that the plane requires too much distance to stop.

SECTION VIII

TECHNOLOGY DEMONSTRATOR

A. Construction Phase

The product which emerges from the manufacturing phase is rarely identical to the product of the design phase. The various problems and solutions which were encountered in the construction of the SCREEM-J4D, as well as the resulting variations from the design, are presented in this part.

The aircraft construction was facilitated by the detailed design studies, especially regarding the structural framework. The fabrication process was aided by actual size blue prints which served as templates for the assembly of the fuselage, wing, and empennage. The structure was made of balsa wood, spruce and plywood as designed and held together by epoxy and model glue. The skin was a MonoKote plastic.

The weight of the prototype compared very well with the design weight. Each component of the prototype weighed approximately as it had been designed with the overall weight being .05 pounds less than was designed. This was due to weight saving techniques employed during construction. Holes were punched in non-critical structural components -- airfoils, false ribs, trailing edge -- and the empennage was built using fewer braces than designed to save weight. The MonoKote plastic was also used on the fuselage to eliminate the need for heavier balsa planking.

The prototype did differ from the design in several ways. First, the center of gravity position was designed to be at 33% of the chord. However, the prototype had its center of gravity at 40% of the chord. This was due in part to the internal arrangement being slightly different. After the first flight test it was decided that the CG had to be moved up to the 25% position. This center of gravity shift was accomplished by lengthening the nose of the fuselage by 2.6 inches. This represented a significant difference from the design.

The chord of the main wing was to be 8.2 inches. However, the blue prints were drawn with an 8 inch chord and the trailing edge piece was shortened to adjust to the change.

The prototype possessed a greater endurance than the design. The design batteries were not available for purchase. The batteries that were bought differed only in capacity (700 mahr instead of 500 mahr); the voltage and weight specifications remained the same. This change only affected the endurance, which was significantly increased.

Another striking difference was related to the wing. The design called for the wing to be in three sections with the outboard sections removable for storage. The joint which connected the outboards to the main was not considered to be structurally sound by an expert model builder late in the construction phase. It was suggested that the joint be rebuilt for greater strength. It was at this point that the executive decision was made to relax the requirement that the aircraft fit in a 2'x2'x4' travel box, which restricted any piece from being greater than four feet in length. This enabled AETC to permanently affix the outboard sections to the main wing, greatly increasing the wing's strength and producing a piece 8 feet in length.

B. Flight Tests

The SCREEM-J4D was constantly examined and tested during the construction phase. The motor and control surface actuators were checked as was the strength of the aircraft's structure. It was decided that before the J4D flew its first test flight it should undergo an extensive ground check. Described here are the pre-flight test plan and the actual test flight plan.

Pre-Flight Test Plan : The pre-flight test was intended to check all systems so as to insure a successful flight around the required course. Those capabilities which were examined were: control surface response; ground roll controllability; power production; structural integrity; and lift generation.

Taxi testing was first performed to see how well the aircraft rolled down the runway and was controllable by means of the rear wheel and control surfaces. The power production was partially examined by measuring the speed of the ground roll. The aircraft was held by the wingtips to test their strength. Lastly, the aircraft was allowed to accelerate to take-off velocity and then

flown for a few feet very close to the ground to better understand its in-flight behavior.

This test was carefully observed in order to identify problems which should be addressed before the actual flight.

Flight Test Plan : The course to be flown is shown in Figures 8-1 and 8-2. The course consists of three figure-8 maneuvers preceded by take-off and climb and followed by landing within the shaded area. The ground roll should cover no more than 75 feet with the aircraft becoming airborne by point 1. The aircraft then climbs at a 15° angle until it reaches cruise altitude of 20 feet at the point marked 2. It then banks left and begins its first figure-8 maneuver at point 3. Point 3a indicates the other end of the maneuver whose radius of curvature at the ends is 40 feet. After three figure-8's, the aircraft begins to fly a straight path at point 4, banks around the end of the flight zone and begins decent at point 4a, touches down after a flare maneuver at point 5, and comes to a complete stop by point 6.

The zone allowed for this flight is 300 feet long, 120 feet wide, and 25 feet high. These dimensions are shown in Figure 8-1 and 8-2. The facility used encloses a football field and has physical dimensions larger than the allowable flight zone. This flight is flown in a controlled atmosphere with limited air disturbances.

C. Instructions For Pilot

The pilot was informed of the capabilities and limitations of the aircraft in regards to power, turning capability, bank angles, maximum angle of attack, and cruise velocity. He was also told of the flight plan as described above.

The pilot will position the throttle such that the aircraft will roll at a modest speed, but not take off. He will get a feel for the control surfaces as well as for the turning capabilities of the rear wheel. After he is satisfied with the feel, he will begin the mission flight.

Mission Diagram

Top View

Figure 8-1

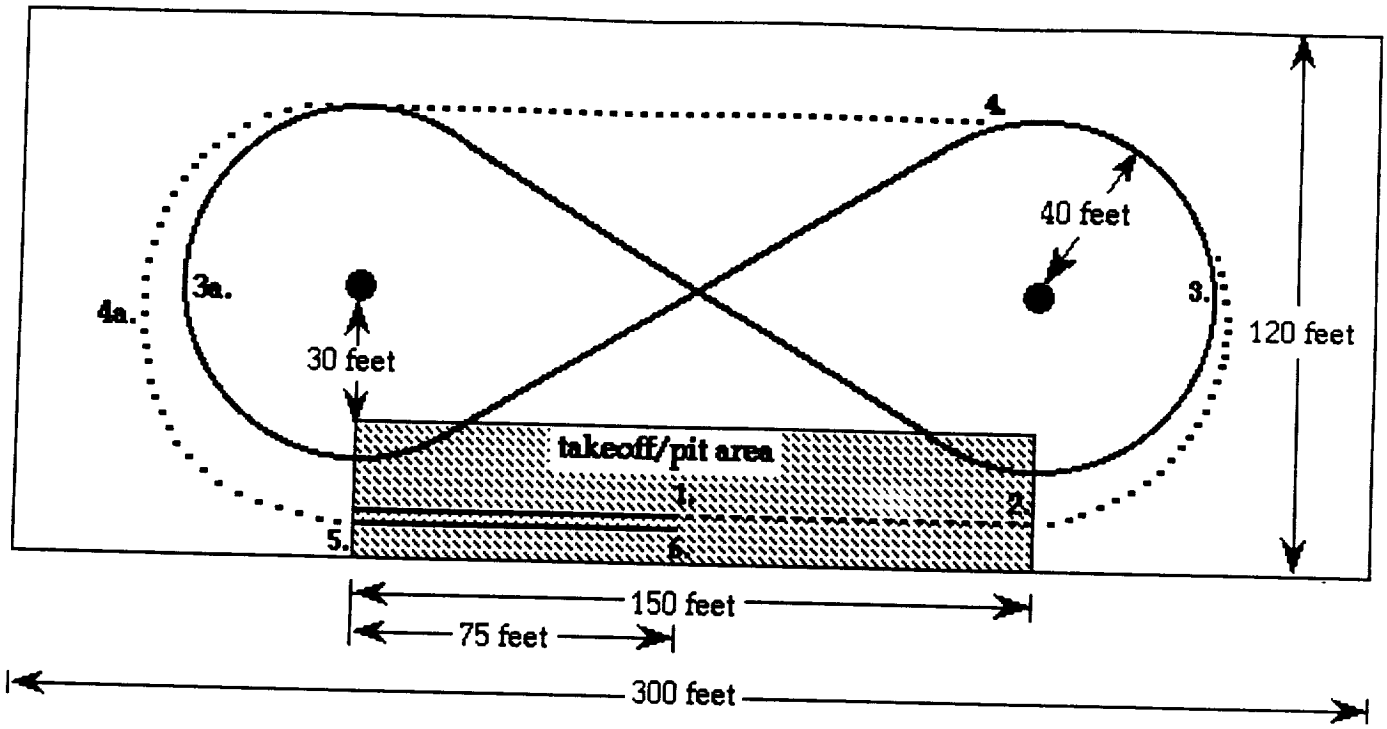

Scale: ⊢——⊣ = 30 feet

Side View

(same scale)

Figure 8-2

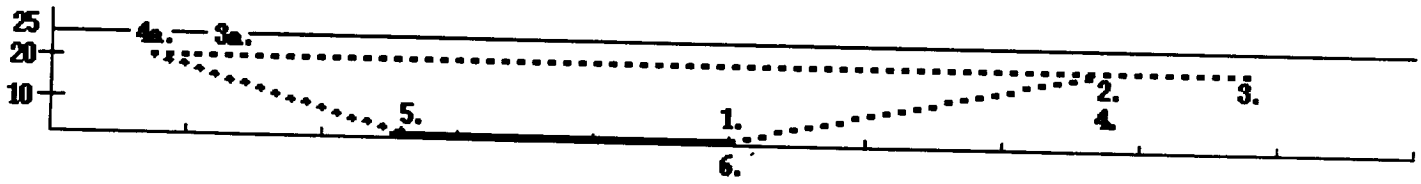

The pilot knows that the maximum take-off distance is 75 feet, which is marked on the runway. He will stand anywhere he feels comfortable and begin the ground roll at full throttle. If for any reason the aircraft fails to achieve flight by the 75-foot mark or it turns out of control, he will abort take-off immediately. For the case of a successful take-off, he will climb at full throttle to an altitude of 20 feet at which point he will throttle down to roughly 50%. When the aircraft is over the end of the runway (even with the pylon, at point 2) he will begin a left turn with approximately a 25° bank angle. However, if for some reason the aircraft does not reach a 20-foot altitude by the pylon, he should begin a turn anyway to avoid leaving the allowable flight zone. In this case, he should maintain a full throttle setting until he is able to reach 20 feet. If an altitude of 20 feet is unattainable, the pilot should land the plane as soon as possible.

Upon successfully climbing and turning, the pilot will proceed to fly three figure-8 maneuvers. The throttle setting for steady, wings-level straight portions of flight is approximately 50%. The pilot will increase the power slightly in the turns so that the aircraft will not loose altitude in the turns. He will fly the straight portions of the flight as accurately as possible so that measurements may be taken by the design team.

If at any time the pilot feels uncomfortable with the qualities of the aircraft -- i.e. stall likely, dynamically unstable, difficult to maintain altitude, unresponsive, ineffective controls, etc. -- he is advised to land it as soon as possible in any safe location. The condition of the aircraft is of higher priority than fulfilling the mission requirements. If the aircraft remains in good condition, it may be modified to fly later and successfully meet the requirements.

After completing the three figure-8's, the pilot will fly the aircraft around the end, throttle down the motor, descend, and land at the beginning of the runway. Upon touchdown, he will completely throttle back the motor and guide it to a safe stop.

D. Safety Considerations

The SCREEM-J4D has not passed any official safety test, therefore it should not be flown except by an experienced RPV pilot. All spectators should be a safe distance from the flight zone and fully attentive in case of a "runaway" aircraft. Members of the design team within the flight zone should be aware at all times. No one should be at the end of the runway as the aircraft takes off or lands or under the aircraft as it makes a turn. The aircraft may stall in these circumstances and fall upon someone.

No one should be within three feet of the aircraft while the motor is running. The propellers are extremely dangerous and often hard to see. No one should ever touch, pick up, or work on the aircraft unless the battery pack is disconnected from the motor.

During the design flight, NO ONE should be in any position which the pilot has designated as unsafe.

The pilot must realize his restrictions flying indoors; hence, he must take protective measures including possibly aborting the mission so as not to jeopardize the facility and/or spectators.

Components inside the aircraft generate heat and may be very hot after flight or taxi test. The aircraft should be handled with the idea that some components may be of high temperatures. The aircraft should be allowed to cool between missions.

F. Cost Analysis

The cost breakdown for the SCREEM-J4D is as follows:

Item or System	Approximate Cost ($)	Notes
Propulsion System		
Motor & Gearing	75.00	
Propeller	2.00	
Batteries	15.75	7 AA NiCad
Speed Controller	100.00	
Avionics		
Transmitter	200.00	
Receiver	40.00	
System Batteries	9.00	4 AAAA NiCad
Servos	88.00	2
Actuation Rods	5.00	
Hinges and Attachments	20.00	
Structures		
Balsa	40.00	
Spruce	5.00	
Glue	15.00	
MonoKote skin	20.00	2 rolls
Labor	536.00	160 hours @ $3.75
Administrative Costs	50.00	copying & binding
Total	**$1220.75**	

G. Critical Data Summary

The final form of the Critical Data Summary is included below.

DESIGN GOALS:	
Re Cruise	100,000
V cruise	23 ft/s
Altitude cruise	20 ft
Turn radius	40 ft
Endurance	78 s
Weight	48 oz
BASIC CONFIG:	
Wing Area	5.46 ft^2
Weight	48 oz
Wing loading	8.79 oz/ft^2
length	37.2 in
span	96 in (8 ft)
height	14 in
WING:	1 (low mount)
Span	8 ft
Aspect Ratio	11.72
Root Chord	8.2 in
taper Ratio	1
Airfoil section	NACA 4415
t/c	15%
Incidence angle	4.5 degrees
C mac - MAC	8.2
Hor. pos of 1/4 MAC	9.017 in
Ver. pos of 1/4 MAC	-4 in
Dihedral	10 degrees
Twist	0
Sweep	0
FUSELAGE:	
Length	37. in
Diameter - max	4 x 4 in
Fineness ratio	9.3
Payload volume	25.17 cu in

EMPENNAGE:	
Horizontal tail:	
Area	.625 ft^2
aspect ratio	2.722 in
root chord	5.75 in
tip chord	5.75 in
taper ratio	1
l.e. sweep	0
incidence angle	0 degrees
hor. pos. of 1/4 MAC	2.9 ft
ver. pos. of 1/4 MAC	0
Airfoil section	flat plate
Vertical Tail:	
Area	.38 ft^2
aspect ratio	1.38
root chord	7.2 in
tip chord	3.9 in
taper ratio	0.54
l.e. sweep	23.2 degrees
hor. pos. of 1/4 MAC	2.749 ft
Airfoil section	flat plate
AERODYNAMICS:	
Cl max	1.2
lift curve slope	3.72/rad
CDo	0.0319
efficiency (e)	0.682
Alpha stall	14.5 (wing)
Alpha zero lift	-4 (wing)
L/D max	15.5

WEIGHTS:	
Weight total	48 oz
C.G. (x-pos)	.33c
Avionics	7.38
Payload	2
Engine	6.5
Propeller	1
Fuel	5.46
Structure	
Wing	10.36
Fuselage/emp.	5.22/1.18
Landing gear	2.4

PROPULSION:	
Type	Astro 05
number	1
placement	front
Pavil max @engine	100W / 50 W
Propeller diameter	10 in.
Propeller pitch	6 in.
Number of blades	2

STABILITY AND CONTROL:	
Neutral point	.514 c
Static margin %MAC	18.40%
Hor tail volume ratio	0.356
Vert tail volume ratio	0.016
Elevator area	.208 ft^2
Elevator max deflection	15 degrees
Rudder Area	.21 ft
Rudder max deflection	25 degrees
Aileron Area	none
Aileron max deflection	none
Cm alpha	-0.685 [1/rad]
Cn beta	7.68 E-4
Cl alpha tail	3.73
Cn delta r tail	5.33 E-4 (neg)
Cm delta e	-0.683 [1/rad]

PERFORMANCE:	
Vmin	18.9 ft/s
Vmax	58.6 ft/s
Vstall	18.9 ft/s
Range max	5500 ft
Endurance Max	3.9 min
ROC max	6.3 ft/s
Min Glide angle	4.1 degrees
T/O distance	42 ft
T/O rotation angle	11 degrees
Landing Distance	50 ft
Bank Angle	30 degrees
Turn Radius	28.6 ft

SYSTEMS:	
Landing gear type	tail dragger
Main gear position	wings
Main gear length	5 in
Main gear tire size	1 in diameter
tail gear position	rudder
tail gear length	.5 in
tail tire size	.5 in diameter
engine speed control	yes
Control surfaces	Rudder/elevator

TECH DEMO:	
Weight total Take off	49 oz
Weight empty	49 oz
Wing Area	5.23 ft^2
Hor. Tail Area	.625 ft^2
Vert Tail Area	.38 ft^2
C.G. position	.27 c
1/4 MAC position	9.0 in
Static margin %MAC	18 %
V takeoff	30 ft/s
Range	8000 ft
Endurance	240 s
V cruise	33 ft/s
Re cruise	128,000
Turn radius	30 ft

SECTION IX

CONCLUSIONS

A. Disadvantages and Advantages

While the SCREEM-J4D will accomplish the proposed mission with a margin of safety, there are a few short comings to the design. The allowable payload is limited to a volume of 25.17 cubic inches and a weight of 2 ounces, to meet our design requirements. The J4D has also been designed to meet the specific requirements of this proposal. This greatly restricts the design flight envelop as compared to general aviation RPVs. In addition to the restriction on the flight envelop, the J4D was design to fly indoors, in a controlled environment. While this will not restrict the SCREEM-J4D to indoor flights, it has not been design to handle hostile environments, including wind gusts and adverse weather conditions. This does not preclude the SCREEM-J4D from all inclement weather; however, further analysis of its durability is suggested.

The SCREEM-J4D is not without its advantages. Due primarily to the constraints imposed on the design by AETC and the initial request for proposal, the J4D has been designed as low speed, lightweight, highly maneuverable RPV. In addition, it has been design for disassemble and transportation within an 2 x 2 x 4 cubic foot volume. A further advantage of the disassembly, is the ability to interchange parts. This facilitates the replacement of broken or damaged parts. The disassembly will also aid in the modification of the J4D for other missions.

B. Applications

From the analysis presented in this proposal, the SCREEM-J4D will perform the the required station keeping mission within the design constraints as set by AETC, with a reliable margin of safety. Due to the stringent constraints, as set by AETC, the SCREEM-J4D can be a formidable option for numerous other missions. Due to the goals of this mission, the battery pack and thus the endurance are held to a minimum. Through an increase in the milliamp-hours, corresponding to an increase in battery size, the endurance of the J4D can be increased to meet the requirements of a prolonged station keeping mission. Unfortunately, the increase in battery size will increase the weight

and required cruise velocity. Prolonged station keeping mission may include low altitude surveillance or electronic cloaking for military operations. Since the SCREEM-J4D has been designed to perform its mission at low speeds, it may be flown at speeds comparable to Navy ships. An electronic device may then be loaded on board to emit artificial waves that simulate electromagnetic emission of a Naval vessel.

Since the SCREEM-J4D is designed with a non-airbreathing engine, it may be easily adapted to work as an atmospheric sampler, in both toxic and non-toxic environments. Due to the design cruise velocity, the J4D may be modified for function as a high altitude long duration station keeping mission. The SCREEM-J4D was initially designed to complete a station keeping mission; thus, it has been designed to optimize steady-state circling. The required modifications for a prolonged flight mission were discussed above. Recall, that these modifications will increase the cruise velocity. The cruise velocity will be further increased for applications at high altitudes, due to a decrease in density. This decrease in density will correspond to a decrease in lift for a constant velocity. Thus, a high altitude mission will require an increase in cruise velocity. While it may be necessary to select another engine to meet these requirements, the present design only mandates 50% of the design engine torque. This short discussion has presented a few of the numerous missions that the SCREEM-J4D may be modified to accomplish

C. Final Word From The Design Team

This project has progressed rapidly from beginning to end, no doubt to the dedication and incessant efforts of the team members. The design has evolved from a rough sketch and a lot of hand waving into a polished aircraft more than capable of performing the mission for which it was intended. The SCREEM-J4D has a singular mission at this time; but its basic design, as we have already seen, can be easily modified into one capable of performing a number of far-reaching surveillance and reconnaisance missions. Its basic airframe is lightweight and durable, lending itself well to effortless transportation and on-site assembly. In addition to being extremely quiet, its electric motor is perfect for missions in atmospherically hostile

environments. We, the members of AETC, support the SCREEM-J4D fully and have no doubt that it will be successful in its intended mission and any other applications that follow.

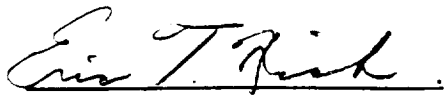

Eric T. Fick

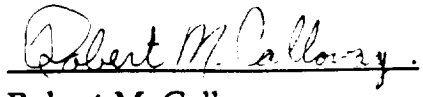

Robert M. Calloway

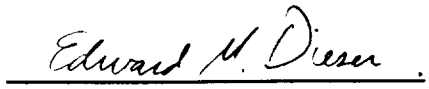

Edward M. Dieser

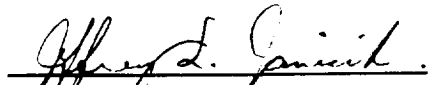

Jeffrey L. Janicik

Michael J. Park

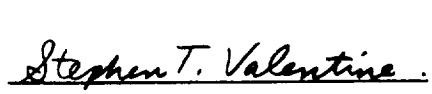

Stephen T. Valentine

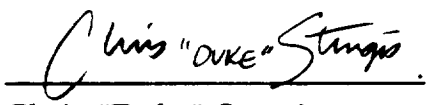

Chris "Duke" Sturgis

REFERENCES

REFERENCES

1. ANDERSON, John D. Jr., Introduction to Flight, New York: McGraw-Hill Book Company, 1985.

2. ANDERSON, John D. Jr., Fundamentals of Aerodynamics, New York: McGraw-Hill Book Company, 1984.

3. BATILL, Dr. Stephen M., "Take-Off Performance," Computer Code, University of Notre Dame, 1990.

4. BERON-RAWDON, Blaine, Model Aviation, "Dihedral," four-part series, August, September, October, and December 1989.

5. DUNN, Dr. Patrick F., "Design Rules of Thumb," University of Notre Dame, 1989.

6. JENSEN, Daniel T., "A Drag Prediction Methodology for Low Reynolds Number Flight Vehicles," University of Notre Dame, January, 1990.

7. NELSON, Dr. Robert C., Atmospheric Flight Mechanics, University of Notre Dame, Spring, 1989.

8. NELSON, Dr. Robert C., Flight Stability and Automatic Control, New York: McGraw-Hill Book Company, 1989.

9. STINTON, Darrol, The Design of the Aeroplane, New York: Van Nostrand Reinhold Company, 1983.

10. USAF Stability and Control DATCOM, Flight Control Division, Air Force Flight Dynamics Laboratory, Wright-Patterson AFB, OH.

11. YOUNG, Barry N., "Propeller Performance Analysis for Small Computers," University of Notre Dame, May, 1984.

12. NATIONAL TECHNOLOGY INFORMATION SOURCE, "A Catalog of Low Reynolds Number Airfoil Data for Wind Turbine Applications," College Station, TX, February 1962.

APPENDIX

ITEM 1

COMPILER OPTIONS: LISTING INTL DCLVAR NOMAP CHECK NOBIG LOGL DYNM NOOFFSET LGO NOAN
NOFRN FPN NOLUNFREC NOSILENT NO_OPTIMISE NOIMPURE

```
0001       C                    AE 441:   AEROSPACE DESIGN
0002       C                              GROUP D
0003       C                     PARAMETRIC SWEEP NUMBER 1
0004       C                           24 JAN 1990
0005       C
0006       C      ***** INITIALIZE VALUES *****
0007       C
0008             REAL PI,RE,V,CBAR,RHO,VIS,KINVIS,PHI,G,RADIUS,N
0009             PI=4.*ATAN(1.)
0010             G=9.81
0011       C
0012       C      ***** SET OUTPUT CODE *****
0013       C
0014             WRITE(1,*) 'ENTER OUTPUT CODE: "1" FOR SCREEN, "6" FOR PRINTER'
0015             READ(1,*) IWR
0016       C
0017       C      ***** INPUT PRELIMINARY DATA *****
0018       C
0019             WRITE(1,*) 'ENSURE THAT ALL QUANTITIES ARE IN METRIC UNITS!!!'
0020             WRITE(1,*) 'ENTER TARGET REYNOLDS NUMBER'
0021             READ(1,*) RE
0022             WRITE(1,*) 'ENTER LOCAL DENSITY'
0023             READ(1,*) RHO
0024             WRITE(1,*) 'ENTER LOCAL FLUID VISCOSITY'
0025             READ(1,*) VIS
0026       C     WRITE(1,*) 'ENTER DESIRED TURN RADIUS'
0027       C     READ(1,*) RADIUS
0028       C
0029       C      ***** PRELIMINARY CALCULATIONS *****
0030       C
0031             KINVIS=VIS/RHO
0032       C
0033       C      ***** LOOP THE MEAN CHORD VALUES AND SOLVE THE REMAINING *****
0034       C      *****          EQUATIONS FOR THE OTHER QUANTITIES          *****
0035       C
0036             WRITE(IWR,*) 'REYNOLDS NUMBER =',RE
0037             DO 20 D=0.,12.
0038.01          RADIUS=6.+D
0039.01          WRITE(IWR,*) ' '
0040.01          WRITE(IWR,*) ' '
0041.01          WRITE(IWR,*) 'RADIUS =',RADIUS,'[M]'
0042.01          WRITE(IWR,*) ' '
0043.01          WRITE(IWR,85)
0044.01          WRITE(IWR,87)
0045.01          WRITE(IWR,*) ' '
0046.01          DO 10 C=0.,38.
0047.02             CBAR=.02+(C*.01)
0048.02             V=(RE*KINVIS)/CBAR
0049.02             PHI=ATAN(V**2./(G*RADIUS))
0050.02             N=1./COS(PHI)
0051.02             PHI=PHI*180./PI
0052.02             WRITE(IWR,86) CBAR,V,PHI,N
0053.02       10 CONTINUE
0054.01       20 CONTINUE
0055.01    C
0056.01    C      ***** FORMATS *****
0057.01    C
0058             85 FORMAT(5X,'MEAN CHORD',5X,'VELOCITY',5X,'BANK ANGLE',5X,'LOAD FAC
                +OR')
0059             86 FORMAT(7X,F7.3,6X,F8.3,7X,F7.3,8X,F7.3)
0060             87 FORMAT(8X,'[M]',11X,'[M/S]',8X,'[DEG]')
0061
0062       C
0063       C      ***** STOP AND END *****
0064       C
0065             STOP
0066             END
```

END OF COMPILATION CLOCKED .372 SECONDS

ITEM 2

```
C     Stephen T. Valentine (Design Group D)
```

```
C     Stephen T. Valentine (Design Group D)
C     AE 441: AEROSPACE SYSTEMS DESIGN
C     written 02-15-90
C     LIFTING-LINE WING ANALYSIS (Program B)
C
C     LIBRARY 'PLOTLIB'
C
C     ********************** variable declarations ****************
C
      REAL THETA(8),THETAP(20),ALPHA(11),ALPHAa(11),COEFM(8,8)
      REAL SOLN(8,11),ALPHMU(8,11),CL(11),CDI(11),Y(20,1)
      REAL GAMMA(20,11),LIFT(20,11),DRAG(20,11),CLT(20,11),CDT(20,11
      REAL CDO(20,11),L,LCS,MU
      INTEGER WK1(8),WK2(8),NP(11)
C
C     ************************ initial input ************************
C
      WRITE (1,*) 'enter output port number:'
      READ (1,*) IWR
      WRITE (1,*)
C     WRITE (1,*) 'enter airfoil zero-lift angle of attack:[deg]'
C     READ (1,*) AOL
C
C     ********************* initial output ***************************
C
      WRITE (IWR,*) '                LIFT DISTRIBUTION DATA'
      WRITE (IWR,*)
      WRITE (IWR,1)
    1 FORMAT (6X,'ALPHA',14X,'CL',12X,'CDI',12X,'Lift')
      WRITE (IWR,4)
    4 FORMAT ('       [deg]                          ',21X,'[lb]')
C
      IOPT=-111
C
C     ********************** constants declarations ***************
C
C ***** freestream *****
      DENSTY=2.3769E-3
      VELCTY=23.0
      Qinf=0.5*DENSTY*(VELCTY**2)
C ***** wing *****
      CHORD=0.6833333
C     SPAN=8.0
C     AR=11.72
C     WAREA=SPAN**2/AR
      WAREA=5.5
      SPAN=WAREA/CHORD
C ***** airfoil *****
C     LCS=5.02
      LCS=5.5
      AOL=-4.0
C
      PI=4.*ATAN(1.)
      DEGRAD=PI/180.
C
C     ************************ initialization of variables *********
C
      MU=CHORD*LCS/(4.*SPAN)
      AOL=AOL*DEGRAD
C
      DO 10 I=1,8
        THETA(I)=(90./8.)*REAL(I)*DEGRAD
   10 CONTINUE
C
      ALPHA(1)=6.0*DEGRAD
      ALPHAa(1)=ALPHA(1)-AOL
      NP(1)=20
      DO 20 J=1,10
        NP(J+1)=20
        ALPHA(J+1)=DEGRAD*(ALPHA(J)/DEGRAD+0.2)
        ALPHAa(J+1)=ALPHA(J+1)-AOL
   20 CONTINUE
C
C     ********* determine matrix of Fourier coefficients **********
C
      DO 40 I=1,8
```

```
C     Stephen T. Valentine (Design Group D)

(      77)           DO 30 J=1,8
(      78)             L=2.*REAL(J)-1.
(      79)             COEFM(I,J)=(SIN(L*THETA(I)))*(1.+L*MU/SIN(THETA(I)))
(      80)  30       CONTINUE
(      81)  40     CONTINUE
(      82)
(      83)         DO 60 J=1,11
(      84)           DO 50 I=1,8
(      85)             ALPHMU(I,J)=(ALPHAa(J))*MU
(      86)  50       CONTINUE
(      87)  60     CONTINUE
(      88)
(      89)           CALL INVRT (COEFM,8,8,WK1,WK2)
(      90)           CALL MULT (COEFM,ALPHMU,SOLN,8,8,11,8,8,8)
(      91)
(      92) C       ******************** calculate lift parameters ***************
(      93)
(      94)         DO 80 I=1,11
(      95)           CL(I)=PI*AR*SOLN(1,I)
(      96)           SUM=1.0
(      97)           DO 70 J=2,8
(      98)             L=2.*REAL(J)-1.
(      99)             SUM=SUM+L*(SOLN(J,I)/SOLN(1,I))**2
(     100)  70       CONTINUE
(     101)           CDI(I)=((CL(I)**2)/(PI*AR))*SUM
(     102)           E=1./SUM
(     103)  80     CONTINUE
(     104)
(     105) C       ***************** calculate circulation distribution ********
(     106)
(     107)         DO 110 I=1,20
(     108)           THETAP(I)=REAL(I)*(90./20.)*DEGRAD
(     109)           Y(I,1)=COS(THETAP(I))
(     110)           DO 100 J=1,11
(     111)             SUM=0.0
(     112)             DO 90 K=1,8
(     113)               L=2.*REAL(K)-1.
(     114)               SUM=SUM+SOLN(K,J)*SIN(L*THETAP(I))
(     115)               GAMMA(I,J)=2.0*SPAN*VELCTY*SUM
(     116)               LIFT(I,J)=GAMMA(I,J)*DENSTY*VELCTY
(     117)               CLT(I,J)=LIFT(I,J)/(0.5*DENSTY*(VELCTY**2)*CHORD)
(     118)             CDO(I,J)=1.7237E-2-(1.698E-2)*CLT(I,J)+(0.09021)*(CLT(I,J
(     119)             CDO(I,J)=CDO(I,J)-(0.15822)*(CLT(I,J)**3)
(     120)             CDO(I,J)=CDO(I,J)+(9.0225E-2)*(CLT(I,J)**4)
(     121)               CDT(I,J)=CDO(I,J)+(CLT(I,J)**2)/(PI*E*AR)
(     122)               DRAG(I,J)=0.5*DENSTY*(VELCTY**2)*WAREA*CDT(I,J)
(     123)  90           CONTINUE
(     124)  100        CONTINUE
(     125)  110    CONTINUE
(     126)
(     127) C       ****************** final output ******************************
(     128)
(     129)         DO 120 I=1,11
(     130)           WRITE (IWR,*) ALPHA(I)/DEGRAD,CL(I),CDI(I),Qinf*WAREA*CL(I)
(     131)  120    CONTINUE
(     132)
(     133)         WRITE (IWR,*)
(     134)         WRITE (IWR,*) 'Span Efficiency Factor is ',E
(     135)         WRITE (IWR,*)
(     136)         WRITE (IWR,*) 'Spanwise Lift Distribution:'
(     137)         WRITE (IWR,*)
(     138)         DO 140 I=1,11
(     139)           WRITE (IWR,*)
(     140)           WRITE (IWR,*) 'Incidence=',ALPHA(I)/DEGRAD,' degrees'
(     141)           WRITE (IWR,*)
(     142)           WRITE (IWR,2)
(     143)           WRITE (IWR,*) '                    [lb/ft]                [lb]'
(     144)           WRITE (IWR,*)
(     145)           DO 130 J=1,20
(     146)             WRITE (IWR,3) Y(J,1),LIFT(J,I),DRAG(J,I),CLT(J,I),CDT(J,I
(     147)  130      CONTINUE
(     148)  140    CONTINUE
(     149)
(     150)  2      FORMAT (2X,'Y/(b/2)',7X,'LIFT/unit span',5X,
(     151)     +          'DRAG',9X,'CLT',12X,'CDT')
(     152)  3      FORMAT (2X,F7.5,8X,F7.5,8X,F7.5,8X,F7.5,8X,F7.5)
```

```
C       Stephen T. Valentine (Design Group D)

(       153)
(       154) C      CALL TPLOT  (IOPT,Y,CLT,20,20,5)
(       155) C      CALL TLABEL  ('Y/(b/2)','Lift Coefficient')
(       156) C      CALL TITLE  ('SPANWISE LOAD DISTRIBUTION (aOL= -4 degrees)')
(       157)
(       158) C      PAUSE
(       159)
(       160) C      CALL TPLOT (IOPT,Y,CDT,20,20,5)
(       161) C      CALL TLABEL ('Y/(b/2)','Drag Coefficient')
(       162) C      CALL TITLE  ('SPANWISE DRAG DISTRIBUTION (aOL= -4 degrees)')
(       163)
(       164)        STOP
(       165)        END
```

ITEM 3

```
**************************************************

 1) C      ***************************************************
 2) C      ***** LONGITUDINAL STATIC STABILITY ANALYSIS *****
 3) C      *****              ERIC T. FICK               *****
 4) C      *****              4 MARCH 1990               *****
 5) C      *****            DESIGN GROUP D               *****
 6) C      ***************************************************
 7) C
 8) C      CLOW=LIFT COEFFICIENT AT ZERO ANGLE OF ATTACK              (WING)
 9) C      CLAW=LIFT CURVE SLOPE [1/rad]                              (WING)
10) C      CMACW=MOMENT COEFFICIENT ABOUT THE AERODYNAMIC CENTER      (WING)
11) C      XACW=X-POSITION OF THE AERODYNAMIC CENTER [ft]             (WING)
12) C           {mesured from the origin of the coordinate system}
13) C      XACCB=AERODYNAMIC CENTER DIVIDED BY MEAN CHORD             (WING)
14) C      IW=INCIDENCE ANGLE [deg]                                   (WING)
15) C      S=PLANFORM AREA [ft**2]                                    (WING)
16) C      ARW=ASPECT RATO                                            (WING)
17) C      CBAR=MEAN CHORD [ft]                                       (WING)
18) C      CMOW=ZERO LIFT MOMENT COEFFICIENT                          (WING)
19) C      CMAW=MOMENT CURVE SLOPE [1/rad]                            (WING)
20) C-------------------------------------------------------------------------
21) C      IT=INCIDENCE ANGLE [deg]                                   (TAIL)
22) C      ST=PLANFORM AREA [ft**2]                                   (TAIL)
23) C      BT=SPAN [ft]                                               (TAIL)
24) C      LT=DISTANCE FROM TAIL A.C. TO CENTER OF GRAVITY            (TAIL)
25) C      ART=ASPECT RATIO                                           (TAIL)
26) C      CBART=MEAN CHORD                                           (TAIL)
27) C      XACT=X-POSITION OF THE AERODYNAMIC CENTER [ft]             (TAIL)
28) C          {measured from the origin of the coordinate system}
29) C      CLOT=LIFT COEFFICIENT AT ZERO ANGLE OF ATTACK              (TAIL)
30) C      CLAT=LIFT CURVE SLOPE [1/rad]                              (TAIL)
31) C      CMOT=ZERO LIFT MOMENT COEFFICIENT                          (TAIL)
32) C      CMAT=MOMENT CURVE SLOPE [1/rad]                            (TAIL)
33) C-------------------------------------------------------------------------
34) C      CMOF=ZERO LIFT MOMENT COEFFICIENT                    (FUSELAGE)
35) C      CMAF=MOMENT CURVE SLOPE [1/rad]                      (FUSELAGE)
36) C-------------------------------------------------------------------------
37) C      XCGCB=CENTER OF GRAVITY POSITION DIVIDED BY MEAN CHORD
38) C           {measured from the leading edge of the wing}
39) C      RHO=FREESTREAM DENSITY
40) C      VEL=FREESTREAM VELOCITY
41) C      Q=FREESTREAM DYNAMIC PRESSURE
42) C      E=DOWNWASH ANGLE
43) C      EO=DOWNWASH ANGLE AT ZERO ANGLE OF ATTACK
44) C      DEO=CHANGE IN DOWNWASH ANGLE WITH ANGLE OF ATTACK
45) C      CMO=MOMENT COEFFICIENT AT ZERO ANGLE OF ATTACK
46) C      CMA=CHANGE IN MOMENT COEFFICIENT WITH ANGLE OF ATTACK
47) C      SFNP=STICK FIXED NEUTRAL POINT/MEAN CHORD
48) C           {measured from the leading edge of the wing}
49) C      SFSM=STICK FIXED STATIC MARGIN
50) C           {as a fraction of the mean chord}
51) C      ALFA=TRIM ANGLE [rad]
52) C      ALFD=TRIM ANGLE [deg]
53) C      CLW=WING LIFT COEFFICIENT
54) C      CLT=TAIL LIFT COEFFICIENT
55) C      CLTOT= TOTAL AIRCRAFT LIFT COEFFICIENT
56) C      LW=WING LIFT GENERATED
57) C      FT=TAIL LIFT GENERATED
58) C      LTOT=TOTAL LIFT GENERATED
59) C      CDO=FORM DRAG COEFFICIENT
60) C      CDTOT=TOTAL DRAG COEFFICIENT
61) C      DTOT=TOTAL DRAG GENERATED
62) C      LODTOT=TOTAL LIFT TO DRAG RATIO
63) C
64) C-------------------------------------------------------------------------
65) C
66)        REAL IW,IT(21),CMOW(21,21),VH(21,21),CMOT(21,21),ALFA(21,21)
67)        REAL CMAW(21,21),CMAT(21,21),CMA(21,21),ALFD(21,21),CMO(21,21)
68)        REAL EO,DEO,ST(21),BT(21),ART(21),CLAT(21),LT(21,21),CLOT
69)        REAL CLW(21,21),CLT(21,21),LW(21,21),FT(21,21),LTOT(21,21)
70)        REAL E(21,21),CDO(21,21),CLTOT(21,21),CDTOT(21,21),DTOT(21,21)
71)        REAL LODTOT(21,21),XCGCB(21),SFNP(21),SFSM(21)
72) C-------------------------------------------------------------------------
73) C      INITIALIZE "HARD" VALUES
74) C-------------------------------------------------------------------------
75)        CLOW=.2596
76)        CLAW=3.7199
```

```
**************************************************

  77)         CMACW=-0.093
  78)         XACCB=.25
  79)         S=5.46
  80)         ARW=11.72
  81)         CBAR=.68333
  82)         XACT=2.935
  83)         CLOT=0.0
  84)         CBART=.4792
  85)         CMOF=-0.0002
  86)         CMAF=0.0341
  87)         RHO=.0023769
  88)         PI=4.*ATAN(1.)
  89)       1 CONTINUE
  90)         WRITE(1,*) 'ENTER OUTPUT CODE: [1] FOR SCREEN, [6] FOR PRINTER'
  91)         READ(1,*) IWR
  92)         WRITE(1,*) 'ENTER WING INCIDENCE ANGLE [DEGREES]'
  93)         READ(1,*) IW
  94)         WRITE(1,*) 'ENTER X-POSITION OF AERODYNAMIC CENTER OF WING [FT]'
  95)         WRITE(1,*) '(measured from the origin of the coordinate system)'
  96)         READ(1,*) XACW
  97)         WRITE(1,*) 'ENTER FREESTREAM VELOCITY [FT/S]'
  98)         READ(1,*) VEL
  99)         Q=.5*RHO*VEL**2
 100)
 101)  C
 102)
 103)         WRITE(IWR,95) IW
 104)         WRITE(IWR,96) XACW
 105)         WRITE(IWR,97) XACT
 106)         WRITE(IWR,99) VEL
 107)  C
 108)         DO 10 I=1,6
 109)            IT(I)=-1.5+REAL(I-1)*.5
 110)            WRITE(IWR,*) ' '
 111)            WRITE(IWR,*) ' '
 112)            WRITE(IWR,91) IT(I)
 113)            WRITE(IWR,92)
 114)            WRITE(IWR,*) ' '
 115)         DO 20 J=1,21
 116)            XCGCB(J)=.3333
 117)            ST(J)=.4+REAL(J-1)*.05
 118)            BT(J)=ST(J)/CBART
 119)            ART(J)=BT(J)**2./ST(J)
 120)            CLAT(J)=(2.*PI)/(1.+(2./ART(J)))
 121)  C
 122)  C--------------- 'O' VALUES FOR THE MOMENT COEFFICIENT ----------------
 123)  C
 124)            CMOW(J,I)=CMACW+CLOW*(XCGCB(J)-XACCB)
 125)            LT(J,I)=(XACT-XACW)+(XACCB-XCGCB(J))*CBAR
 126)            VH(J,I)=(ST(J)*LT(J,I))/(S*CBAR)
 127)            EO=((2.*CLOW)/(PI*ARW))*180./PI
 128)            DEO=(2.*CLAW)/(PI*ARW)
 129)            CMOT(J,I)=VH(J,I)*CLAT(J)*(EO+IW-IT(I))*PI/180.
 130)            CMO(J,I)=CMOW(J,I)+CMOT(J,I)+CMOF
 131)  C
 132)  C--------------- 'A' VALUES FOR THE MOMENT COEFFICIENT ----------------
 133)  C
 134)            CMAW(J,I)=CLAW*(XCGCB(J)-XACCB)
 135)            CMAT(J,I)=-VH(J,I)*CLAT(J)*(1.-DEO)
 136)            CMA(J,I)=CMAW(J,I)+CMAT(J,I)+CMAF
 137)  C
 138)  C-------------------- STICK FIXED NEUTRAL POINT ----------------------
 139)  C
 140)            SFNP(J)=XACCB-(CMAF/CLAW)+VH(J,I)*(CLAT(J)/CLAW)*(1.-DEO)
 141)            SFSM(J)=SFNP(J)-XCGCB(J)
 142)  C
 143)  C------------ FINDING ANGLE OF ATTACK TO TRIM AND LIFT FORCES------------
 144)  C
 145)            ALFA(J,I)=CMO(J,I)/(-CMA(J,I))
 146)            ALFD(J,I)=ALFA(J,I)*180./PI
 147)            CLW(J,I)=CLOW+CLAW*(ALFA(J,I)+(IW*PI/180.))
 148)            E(J,I)=(2.*CLW(J,I))/(PI*ARW)
 149)            CLT(J,I)=CLOT+CLAT(J)*(ALFA(J,I)-(IW*PI/180.)-E(J,I)
 150)         +  +(IT(I)*PI/180.))
 151)            LW(J,I)=CLW(J,I)*Q*S
 152)            FT(J,I)=CLT(J,I)*Q*ST(J)
```

```
**************************************************

153)           LTOT(J,I)=LW(J,I)+FT(J,I)
154)           LTOT(J,I)=LTOT(J,I)*.966
155)           CLTOT(J,I)=LTOT(J,I)/(Q*S)
156)  C
157)  C---------------------- CALCULATING DRAG FORCES -------------------------
158)  C
159)           CDO(J,I)=(.14885+(ST(J)*.008))/S
160)           CDO(J,I)=1.15*CDO(J,I)
161)           CDTOT(J,I)=CDO(J,I)+(CLTOT(J,I)**2/(.6815*PI*ARW))
162)           DTOT(J,I)=CDTOT(J,I)*Q*S
163)           LODTOT(J,I)=CLTOT(J,I)/CDTOT(J,I)
164)  C
165)  C---------------------- PRINTING STATEMENTS -----------------------------
166)  C
167)           WRITE(IWR,90) ALFD(J,I),LTOT(J,I),VH(J,I)
168)       +,LODTOT(J,I),SFNP(J),SFSM(J),CMA(J,I),ST(J)
169)  C
170)     20 CONTINUE
171)     10 CONTINUE
172)  C
173)  C---------------------- PLOTTING STATEMENTS -----------------------------
174)  C
175)      2 CONTINUE
176)        WRITE(1,*) 'ENTER PLOTTING OPTION: [1] = LIFT, [2] = DRAG, [3] = L
177)       +/D RATIO, [4] = CM)alfa, [5] = TRIM ANGLE OF ATTACK, [6] = NEUTRAL
178)       +POINT, [7] = STATIC MARGIN'
179)        READ(1,*) NUM
180)        IF(NUM.EQ.1) THEN
181)        CALL TPLOT(-011,ST,LTOT,21,21,6)
182)        CALL TITLE('TOTAL LIFT GENERATED [lb] vs. TAIL AREA [ft**2]')
183)        CALL TLABEL('TAIL AREA [ft**2]','TOTAL LIFT GENERATED [lb]')
184)        ELSE IF(NUM.EQ.2) THEN
185)        CALL TPLOT(-011,ST,DTOT,21,21,6)
186)        CALL TITLE('TOTAL DRAG GENERATED [lb] vs. TAIL AREA [ft**2]')
187)        CALL TLABEL('TAIL AREA [ft**2]','TOTAL DRAG GENERATED [lb]')
188)        ELSE IF(NUM.EQ.3) THEN
189)        CALL TPLOT(-011,ST,LODTOT,21,21,6)
190)        CALL TITLE('LIFT TO DRAG RATIO vs. TAIL AREA [ft**2]')
191)        CALL TLABEL('TAIL AREA [ft**2]','LIFT TO DRAG RATIO')
192)        ELSE IF(NUM.EQ.4) THEN
193)        CALL TPLOT(-011,ST,CMA,21,21,1)
194)        CALL TITLE('Cm)alfa vs. TAIL AREA [ft**2]')
195)        CALL TLABEL('TAIL AREA [ft**2]','CM)alfa')
196)        ELSE IF(NUM.EQ.5) THEN
197)        CALL TPLOT(-011,ST,ALFD,21,21,6)
198)        CALL TITLE('TRIM ANGLE OF ATTACK [deg] vs. TAIL AREA [ft**2]')
199)        CALL TLABEL('TAIL AREA [ft**2]','TRIM ANGLE OF ATTACK [deg]')
200)        ELSE IF(NUM.EQ.6) THEN
201)        CALL TPLOT(-011,ST,SFNP,21,21,1)
202)        CALL TITLE('NEUTRAL POINT vs. TAIL AREA [ft**2]')
203)        CALL TLABEL('TAIL AREA [ft**2]','NEUTRAL POINT')
204)        ELSE IF(NUM.EQ.7) THEN
205)        CALL TPLOT(-011,ST,SFSM,21,21,1)
206)        CALL TITLE('STATIC MARGIN vs. TAIL AREA [ft**2]')
207)        CALL TLABEL('TAIL AREA [ft**2]','STATIC MARGIN')
208)        ELSE
209)        ENDIF
210)        WRITE(1,*) 'MORE PLOTS ? [1] FOR YES, [NOT 1] FOR NO'
211)        READ(1,*) NUMMM
212)        IF(NUMMM.EQ.1) GOTO 2
213)        WRITE(1,*) 'CONTINUE ? [1] YES, [NOT 1] FOR NO'
214)        READ(1,*) NUMM
215)        IF(NUMM.EQ.1) GOTO 1
216)  C
217)  C---------------------- FORMAT STATEMENTS -------------------------------
218)  C
219)     90 FORMAT(2X,F7.4,2X,F6.4,2X,F6.4,2X,F8.4,2X,F8.4,2X,F8.4,2X,F8.4,2X,
220)       +F8.4)
221)     91 FORMAT(2X,'TAIL INCIDENCE ANGLE IS ',F8.4,' [DEGREES]')
222)     92 FORMAT(4X,'ALFA',4X,'LIFT',3X,'VolRat',5X,'LoD)t',5X,'SFNP',
223)       +6X,'SFSM',5X,'CM)alfa',4x,'Stail')
224)     95 FORMAT(2X,'WING INCIDENCE ANGLE          = ',F8.4)
225)     96 FORMAT(2X,'WING AERODYNAMIC CENTER       = ',F8.4)
226)     97 FORMAT(2X,'TAIL AERODYNAMIC CENTER       = ',F8.4)
227)     99 FORMAT(2X,'FREESTREAM VELOCITY [FT/S]    = ',F8.4)
228)  C
```

ITEM 4

```
C     ***********************************************

      C     ***********************************************
      C        SIZING THE VERTICAL TAIL & RUDDER
      C           GROUP D -- JEFFREY JANICIK
      C     ***********************************************
      C
            REAL SV(110),LV(110),BETA(110,110)
            WRITE(1,*)  'ENTER IWR: '
            READ(1,*) IWR
      C
      C     ******** FIXED PARAMETERS *********
            PI=4.*ATAN(1.)
            SW=5.46
            B=8.0
            ARW=11.72
            ETAV=1.0
            CLAV=(2.*PI)/2.45
            CNBWF=-.0000721
      C     ************************************
      C
      C     ******* VARYING PARAMETERS ********
      C        -- CONSTRAINTS SET BY GROUP DESIGN AND "RULES OF THUMB"
      C     lv = 1.5 ft  -  2.0 ft
      C     Sv = .38 ft^2  -  .60 ft^2
      C     tao = .62 - .72  figure 2.20 Nelson
      C     delta rudder max = 25 degrees
      C     ************************************
            WRITE(1,*) 'ENTER VALUE OF TAO : '
            READ(1,*) TAO
            WRITE(1,*) 'ENTER VALUE OF DELTA RUDDER : '
            READ(1,*) DELTAR
      C
      C
            DO 10 I=37,42,1
               SV(I)=REAL(I)/100.
                  DO 20 J=18,20,1
                     LV(J)=REAL(J)/10.
      C
      C     ***** CALCULATING CNB OF VERTICAL TAIL  --eqn. 2.80 NELSON *****
      C        --- SDEF = SIDEWASH & TAIL EFFICIENCY FACTOR (EMPIRICAL FORMUL
                     VV=SV(I)*LV(J)/(SW*B)
                     SDEF=.724+3.06*((SV(I)/SW)/2.)+0.2+0.009*ARW
                     CNBV=VV*CLAV*SDEF*PI/180.
      C
      C     ***** CALCULATING CNB OF ENTIRE AIRPLANE *****
                     CNB=CNBWF+CNBV
      C
      C     ***** CALCULATING CN-DELTA-R    --eqn.s 2.86 & 2.87 NELSON *****
                     CNDELR=-ETAV*VV*CLAV*TAO*PI/180.
      C
      C     ***** CALCULATING BETA (THE HEADING ANGLE) *******
      C          --  THIS IS DONE BY SETTING CN = 0 FOR TRIM CONDITION IN
      C              EQUATION  CN = CNB*BETA  +  CNDELR*DELTAR
                     BETA(J,I)=-CNDELR*DELTAR/CNB
            WRITE(IWR,*) CNB,CNDELR
       20          CONTINUE
       10    CONTINUE
      C
      C
            WRITE(IWR,*) 'TAO = ',TAO,'DELTA RUDDER =',DELTAR
            WRITE(IWR,*) ' '
            WRITE(IWR,*) '     Sv   (ft^2) ',',      Lv   (ft) ',',    BETA (DEGREE
           *'
            DO 30 I=37,42,1
               DO 40 J=18,20,1
                  WRITE(IWR,*) SV(I),LV(J),BETA(J,I)
       40       CONTINUE
       30    CONTINUE
      C     ************************
      C     CALL TPLOT(-011,SV,BETA,100,100,6)
      C     CALL TITLE('BETA  vs.  Sv')
      C     CALL TLABEL('Sv (ft^2)','BETA (degrees)')
      C
            STOP
            END
```

ITEM 5

```
C     ****************************************

      1) C      ****************************************
      2) C       PROGRAM TO GENERATE Cl vs BETA GRAPH
      3) C         -- GROUP D  JEFFREY L. JANICIK
      4) C      ****************************************
      5)        REAL BETA(40),CL(40,40),GAMMA(40)
      6)        WRITE(1,*) 'INPUT IWR:'
      7)        READ(1,*) IWR
      8) C
      9) C      ****  ASPECT RATIO EFFECT ON CLB FOUND BY FIGURE 3.9  ****
     10)        CLBGAM=-.00027
     11) C
     12) C      **** VARYING PARAMETER --DIHEDRAL *****
     13) C         --- "RULE OF THUMB"  GAMMA = 5 DEGREES - 8 DEGREES
     14) C
     15)        DO 10 I=1,10
     16)           GAMMA(I)=6.+REAL(I)
     17)           DO 20 J=9,28,1
     18)              BETA(J)=REAL(J)
     19)              CL(J,I)=CLBGAM*GAMMA(I)*BETA(J)
     20) C            WRITE(IWR,*) GAMMA(I),BETA(J),CL(J,I)
     21)   20      CONTINUE
     22)   10   CONTINUE
     23) C
     24) C      ******     PLOTTING ROUTINE     *******
     25)        CALL TPLOT(-011,BETA,CL,40,40,10)
     26)        CALL TITLE('Cl    vs.    BETA')
     27)        CALL TLABEL('BETA (degrees)','ROLL MOMENT COEFFICIENT Cl')
     28) C      ****************************************
     29)        STOP
     30)        END
```

ITEM 6

EDWARD DIESER

```
 1) C      EDWARD DIESER
 2) C       AERO DESIGN
 3) C       TRADE STUDY
 4) C      22 MARCH 1990
 5)
 6)        REAL IC(15),JC(25),DIHED(15),YAWA(25),DAL(25,15)
 7)
 8)        PI=4.*ATAN(1.)
 9)
10) C      YAWA= YAW ANGLE
11) C      DAL=  DELTA ALPHA
12) C      DIHED=DIHEDRAL ANGLE
13)
14)        WRITE(1,*) 'ENTER IWR (1=TERMINAL, 6=PRINTER)'
15)        READ(1,*) IWR
16)
17)        DO 10 I=1,15
18)        IC(I)=6.+REAL(I)
19)        DIHED(I)=IC(I)*PI/180.
20)
21) C      WRITE(IWR,*) 'DIHEDRAL ANGLE=', IC(I) ,'DEGREES'
22) C      WRITE(IWR,*) 'YAW ANGLE (DEGREES)  DELTA ALPHA (DEGREES)'
23)
24)        DO 15 J=1,25
25)        JC(J)=REAL(J)
26)        YAWA(J)=JC(J)*PI/180.
27)        DAL(J,I)=ATAN(SIN(YAWA(J))*TAN(DIHED(I)))
28)        DAL(J,I)=DAL(J,I)*180./PI
29)
30)     15 CONTINUE
31) C   15 WRITE(IWR,*)'    ',JC(J),'          ',DAL(J,I)
32)     10 CONTINUE
33)
34)        CALL TPLOT(-011,JC,DAL,25,25,15)
35)        CALL TITLE('ANGLE OF ATTACK vs. YAW ANGLE for various WING DIHEDRA
36)       +L (deg)')
37)        CALL TLABEL('YAW ANGLE (degrees)','DELTA ALPHA (degrees)')
38)
39)        STOP
40)        END
```

ITEM 7

EDWARD DIESER

```
C       EDWARD DIESER
C        AERO DESIGN
C        TRADE STUDY
C       22 MARCH 1990

        REAL ROLMO(15),ROLI(15),ALPHA(15),LI(15),LIP(15),RIP(15),CL(15)

        Q=.5*.00237*23.**2
        S=4./12.*.683
        PI=4*ATAN(1.)
        PC=0.

        WRITE(1,*) 'ENTER IWR (1=TERMINAL. 6=PRINTER)'
        READ (1,*) IWR

C       DO 5 K=1,11
C    5  ROLMO(K)=0.0
        ROLMO(1)=0.0

        LI(2)=2
        DO 7 K=3,13
      7 LI(K)=2+REAL(K-2)*4.


        DO 10 I=1,15
        ALPHA(I)=6.+REAL(I)
        CL(I)=.6+ .1*REAL(I)
C       WRITE(IWR,*) 'ANGLE OF ATTACK=',ALPHA(I),'(deg)'
C       WRITE(IWR,*) 'PANEL SECTION #     LENGTH        SECT. ROLL MOMENT'
        PC=0.

        DO 20 J=2,13
           PC=PC+1
           ROLI(J)=CL(I)*Q*S*LI(J)
           ROLMO(J)=ROLMO(J-1)+ROLI(J)

           LIP(J)=LI(J)/48.
           RIP(J)=ROLI(J)
C          DO 30 K=1,11
C  30      RIP(J)=RIP(J)/ROLMO(11)

    20  CONTINUE
C   20  WRITE(IWR,*) ' ',PC,'    ',LI(J),'    ',ROLI(J)
C       WRITE(IWR,*) 'ROLL MOMENT=', ROLMO(12)
C   10  WRITE(IWR,*) '                '
    10  CONTINUE

        CALL TPLOT(-011,ALPHA,ROLMO,15,15,1)
        CALL TITLE('ROLL MOMENT vs. ANGLE OF ATTACK')
        CALL TLABEL('ALPHA (degrees)','ROLL MOMENT (ft.-lb.)')

        STOP
        END
```

ITEM 8

TORNADO 10—6 PROPELLER

Performance Estimate

DATA MEASURED 2-27-90

Analysis by simple blade element theory.

DESCRIPTION: 2 Blades; 10 In. Dia.; CLARK Y Airfoil; Blade set at 24.2 Degrees at 2.1 Inch Station
FLIGHT CONDITIONS: Calculations adjusted for neither Mach nor Reynolds numbers at 15 MPH and .02 thousand Feet.

Blade Measurements

Fractional Radius,	X:	.3	.45	.6	.7	.75	.8	.85	.9	.95
Radial Position,	r:	1.5	2.2	3	3.5	3.8	4	4.3	4.5	4.7
Blade Chord,	C:	.8	.9	.9	.8	.8	.7	.7	.6	.4
Thickness,	In.	.2	.2	.1	.1	.1	.1	.1	.1	.1
Thickness Ratio,	T:	.25	.18	.15	.14	.14	.14	.12	.11	.15
Blade Angle,	Beta:	32.4	23	17.7	15.3	14.3	13.4	12.7	12	11.3
Geometric Pitch,	GP:	6	6	6	6	6	6	6	6	6
Solidity,	S:	.102	.114	.121	.108	.099	.091	.085	.075	.054

Thrust, Power, Efficiency, and Velocities

J:	.24	.29	.34	.39	.44	.49	.55	.6	.65	.7	.75
Ct:	.142	.135	.127	.118	.107	.095	.082	.069	.056	.043	.029
Cp:	.044	.047	.049	.051	.052	.051	.048	.045	.04	.033	.023
eta:	.783	.846	.882	.904	.917	.923	.925	.922	.913	.896	.857
Mt:	.257	.219	.192	.169	.151	.137	.115	.106	.098	.091	.085
RPM:	6541	5612	4616	4023	3546	3202	2905	2659	2451	2273	2119

Angles of Attack (Degrees)

X	J:	.24	.29	.34	.39	.44	.49	.55	.6	.65	.7	.75
.3		18	15.2	12.4	9.7	7.2	4.7	2.4	.1	-2	-4.1	-6
.45		13.3	11.3	9.3	7.4	5.5	3.7	1.9	.1	-1.6	-3.2	-4.9
.6		10.3	8.8	7.3	5.9	4.4	3	1.5	.1	-1.3	-2.6	-4
.7		9	7.7	6.4	5.1	3.8	2.6	1.3	.1	-1.1	-2.3	-3.5
.75		8.4	7.2	6	4.8	3.6	2.4	1.3	.1	-1.1	-2.2	-3.3
.8		7.9	6.8	5.6	4.5	3.4	2.3	1.2	.1	-1	-2.1	-3.1
.85		7.5	6.4	5.3	4.3	3.2	2.2	1.1	.1	-.9	-2	-3
.9		7.1	6.1	5.1	4.1	3.1	2.1	1.1	.1	-.9	-1.9	-2.8
.95		6.7	5.7	4.8	3.8	2.9	1.9	1	0	-.9	-1.8	-2.7

Reynolds Number (Millions)

Y	J:	.24	.29	.34	.39	.44	.49	.55	.6	.65	.7	.75
.3		.04	.03	.03	.02	.02	.02	.02	.02	.02	.02	.02
.45		.06	.05	.04	.04	.03	.03	.03	.03	.03	.02	.02
.6		.09	.07	.06	.05	.05	.04	.04	.04	.03	.02	.02
.7		.09	.08	.06	.06	.05	.05	.04	.04	.04	.03	.03
.75		.09	.07	.06	.06	.05	.04	.04	.04	.03	.03	.03
.8		.09	.07	.06	.05	.05	.04	.04	.04	.03	.03	.03
.85		.09	.07	.06	.05	.05	.04	.04	.04	.03	.03	.03
.9		.08	.07	.06	.05	.04	.04	.04	.03	.03	.03	.03
.95		.05	.04	.04	.03	.03	.03	.02	.02	.02	.02	.02

Advance ratio values limited by available Cl and Cd data for selected airfoil section.

PROPELLER DATA SHEET

A) Propeller Designation: TORNADO 10-6

B) Number of Blades: 2 Diameter: 10 (Inches)

C) Select one of the following airfoil sections:
1) INVISCID FLAT PLATE
2) THIN FLAT PLATE
3) SYMMETRICAL
--> 4) CLARK Y
5) RAF-6

D) Blade thickness may be entered as either:
1) Fraction of chord
--> 2) Inches

E) Blade data may be entered at radial locations specified as:
1) Fractional Radius
--> 2) Inches

F) Radius* at which blade setting is measured: 2.125

G) Blade setting (i.e. ref angle for whole blade): 24.2

H) Enter the number of radial data positions: (3-9): 9

I)

Data Point	Radius*	Chord	Thickness*	Angle
1:	.625	.625	.305	56.8
2:	1.125	.75	.225	40.33
3:	1.625	.8125	.191	30.44
4:	2.125	.875	.165	24.2
5:	2.625	.9375	.147	19.99
6:	3.125	.9375	.134	16.99
7:	3.625	.8125	.114	14.76
8:	4.125	.6875	.091	13.03
9:	4.625	.5	.058	11.67

J) Select desired refinment of analysis:
--> 1) Analysis by simple blade element theory.
2) Analysis including induced velocity.
3) Analysis including induced velocity and tip losses.

K) These Cl/Cd coefficient adjustments may be selected
--> 1) No Cl/Cd adjustments
2) Mach number adjustment
3) Reynolds number adjustment
4) Mach and reynolds number adjustments

L) Select altitude in thousands of feet: .02

M) Specify one of the following:
--> 1) Airspeed FIXED at: 15 MPH
2) Propeller RPM FIXED at:

N) Range of Advance Ratio to be used in calculations:
J min: 0 J max: 1

NOTES: First data point must be less than 30% radius; others must progress outward.
Designation must start with a letter and may not contain a comma.
For square tip blades only, use tip as last data point.
Angles must be specified in degrees, lengths in inches.
* Units must be as specified in lines D and E.

ITEM 9

```
CASE - GROUPD
WGT = 3.000
SREF = 5.460
RHO = 2.3780E-03
CLTO = .3000
CDTO = 4.0000E-02
CLMAX = 1.200
SMAX = 300.0
MU = .2000
DIA = .8333
BVOLTS = 8.400
KT = .5500
KV = 5.0000E-04
RARM = 6.0000E-02
RBAT = 4.7000E-02
FUSAMP = 20.00
GEARAT = 2.210
DT = 5.0000E-02
TMAX = 60.00
NJ = 10


 .0000 .1040 7.0000E-02
 .2400 9.2000E-02 5.0000E-02
 .2900 8.5000E-02 7.9000E-02
 .3400 7.9000E-02 4.7000E-02
 .3900 7.2000E-02 4.5000E-02
 .4900 5.4000E-02 3.9000E-02
 .5500 4.3000E-02 3.5000E-02
 .6500 2.0000E-02 2.1000E-02
 .7500 -6.0000E-03 7.0000E-04
 10.00 .0000 -100.0
V TAKEOFF = 23.55
MAX CURRENT DRAW(amps) = 39.25
MAX MOTOR POWER(hp) = .1798
MAX MOTOR POWER(watts) = 134.1
STATIC THRUST (lb)=  1.186
STATIC CURRENT DRAW (amps)=  16.73
STATIC PROP RPS=  99.71
TATIC  PROP  RPS=   99.71ps)=   16.73)  =  .3840
```

```
V AT TO (FT/SEC) = 23.76
DISTANCE(FT) = 45.06
BATTERY DRAIN(mahs) = 16.03
ADVANCE RATIO AT TO = .2892
THRUST(LB) AT TO = .9306
LIFT(LB) AT TO(BEFORE ROTATION) = 1.080
DRAG(LB) AT TO(BEFORE ROTATION) = .1440
FRICTION(LB) AT TO(BEFORE ROTATION) = .3840
CURRENT DRAW AT TO (AMPS) = 18.03
```

```
GROUPD
3.0                ! WEIGHT IN LBS
5.46               ! WING REF AREA IN FT2
.002378            ! AIR DENSITY SLUG/FT3
.3                 ! CL AT TAKEOFF ATTITUDE
.04                ! CD AT TAKEOFF ATTITUDE
1.2                ! CLMAX -
300.               ! LIMIT ON TAKEOFF DIST FT
.2                 ! FRICTION COEFFICIENT
.83333             ! PROP DIAMETER IN FT
8.4                ! BATTERY VOLTAGE
.55                ! KT IN in-oz/amp
.0005              ! KV IN volts/rpm
.06                ! armature resistance
.047               ! battery resistance
20.                ! FUSE AMPS - MAX DRAW
2.21               ! gear ratio
.05                ! INTEGRATION TIME INCREMENT
60.                ! limit on take-off time (SEC)
10                 ! number of prop data points
0.      .104     .07
.24     .092     .05
.29     .085     .079
.34     .079     .047
.39     .072     .045
.49     .054     .039
.55     .043     .035
.65     .02      .021
.75     -.006    .0007
10.     0.       -100.
```

ITEM 10

```
LFORD UNIVERSITY FTN77 VER. 228S     <USER2>S310768966>STUDENT>STRUC1.F77          20:11
MPILER OPTIONS:  LISTING INTL NOMAP CHECK NOBIG LOGL DYNM NOOFFSET LGO NOANSI NODEB
                 FPN NOLUNFREC NOSILENT NO_OPTIMISE NOIMPURE

0001       C*************************************
0002       C*    AE446 - AEROSPACE STRUCTURES    *
0003       C*   Computer program to determine    *
0004       C*   the internal load distribution   *
0005       C*   on an aircraft wing.             *
0006       C*    Written by Michael H. Park      *
0007       C*************************************
0008             PROGRAM STRUC1
0009             REAL  X(50),CL(50),CD(50),CM(50),W(50),PY(50),PZ(50),DMX(50),
0010            +      VY(50),VZ(50),MX(50),MY(50),MZ(50),C(50)
0011
0012             OPEN(UNIT=99,FILE='WING1.DATA',STATUS='OLD')
0013             READ(99,*)RO,ALPHA,V,CR,CT,N
0014             READ(99,*)(X(I),CL(I),CD(I),CM(I),W(I),I=1,N)
0015             CLOSE(UNIT=99)
0016
0017             Q=0.5*RO*V**2
0018             PI=4.0*ATAN(1.0)
0019             A=ALPHA*PI/180.0
0020
0021             WRITE(1,*)'ENTER IWR: '
0022             READ(1,*)IWR
0023
0024             DO 5 I=1,N
0025.01             C(I)=CR-((CR-CT)/X(N))*X(I)
0026.01    5        CONTINUE
0027.01
0028             DO 10, I=1,N
0029.01             PY(I)=Q*C(I)*(CL(I)*COS(A)+CD(I)*SIN(A))-W(I)*COS(A)
0030.01             PZ(I)=Q*C(I)*(CL(I)*SIN(A)-CD(I)*COS(A))-W(I)*SIN(A)
0031.01             DMX(I)=Q*C(I)**2*(-1.0*CM(I)-CL(I)*COS(A)/4.0-CD(I)*SIN(A)/4.0)
0032.01   10        CONTINUE
0033.01
0034             VY(N)=0.0
0035             VZ(N)=0.0
0036             MX(N)=0.0
0037             MY(N)=0.0
0038             MZ(N)=0.0
0039             DO 20 I=N-1,1,-1
0040.01             VY(I)=VY(I+1)+(PY(I+1)+PY(I))*(X(I+1)-X(I))/2.0
0041.01             VZ(I)=VZ(I+1)+(PZ(I+1)+PZ(I))*(X(I+1)-X(I))/2.0
0042.01             MX(I)=MX(I+1)+(DMX(I+1)+DMX(I))*(X(I+1)-X(I))/2.0
0043.01   20        CONTINUE
0044.01
0045             DO 30, I=N-1,1,-1
0046.01             MZ(I)=MZ(I+1)+(VY(I+1)+VY(I))*(X(I+1)-X(I))/2.0
0047.01             MY(I)=MY(I+1)+(VZ(I+1)+VZ(I))*(X(I+1)-X(I))/2.0
0048.01   30        CONTINUE
0049.01
0050             WRITE(IWR,*)' X          Vy(lbs)    Vz          Mx(ft-lbs) My          Mz'
0051             WRITE(IWR,*)'-----------------------------------------------------------
0052            +---'
0053             DO 90 I=1,N
0054.01             WRITE(IWR,1)X(I),VY(I),VZ(I),MX(I),MY(I),MZ(I)
0055.01   90        CONTINUE
0056         1   FORMAT(1X,F5.2,1X,F9.5,1X,F9.5,1X,F9.5,1X,F9.5,1X,F9.5)
0057
0058             STOP
0059             END


) OF COMPILATION CLOCKED      .572 SECONDS
```

X	Vy(lbs)	Vz	Mx(ft-lbs)	My	Mz
0.00	16.23668	1.29189	-20.69218	2.41726	30.24091
0.31	14.83717	1.18189	-18.81430	2.02908	25.36481
0.63	13.44794	1.07263	-16.95127	1.67751	20.95403
0.93	12.07876	0.96484	-15.11737	1.36366	17.02190
1.24	10.74015	0.85929	-13.32781	1.08796	13.57305
1.53	9.44182	0.75669	-11.59669	0.84989	10.59984
1.82	8.19319	0.65776	-9.93779	0.64816	8.08474
2.09	7.00408	0.56321	-8.36553	0.48087	6.00241
2.35	5.88393	0.47376	-6.89396	0.34546	4.31949
2.60	4.84188	0.39013	-5.53662	0.23893	2.99679
2.83	3.88608	0.31299	-4.30560	0.15784	1.99028
3.04	3.02453	0.24303	-3.21270	0.09857	1.25361
3.24	2.26480	0.18096	-2.26930	0.05735	0.73938
3.41	1.61361	0.12748	-1.48536	0.03044	0.40103
3.56	1.07557	0.08321	-0.86707	0.01427	0.19466
3.70	0.65281	0.04858	-0.41562	0.00561	0.08104
3.80	0.34374	0.02372	-0.12537	0.00168	0.02686
3.89	0.14259	0.00831	0.01781	0.00031	0.00614
3.95	0.03600	0.00119	0.04280	0.00002	0.00066
3.99	0.00000	0.00000	0.00000	0.00000	0.00000

0.00237,7.6,23.0,8.2,8.2,20

```
(    1) 0.00237,7.6,23.0,8.2,8.2,20
(    2) 0.00000,0.94210,0.04717,-0.093,0.375
(    3) 0.31384,0.94164,0.04712,-0.093,0.375
(    4) 0.62572,0.94020,0.04699,-0.093,0.375
(    5) 0.93380,0.93769,0.04677,-0.093,0.375
(    6) 1.23608,0.93406,0.04644,-0.093,0.375
(    7) 1.53072,0.92920,0.04602,-0.093,0.375
(    8) 1.81596,0.92279,0.04547,-0.093,0.375
(    9) 2.09000,0.91434,0.04476,-0.093,0.375
(   10) 2.35116,0.90336,0.04386,-0.093,0.375
(   11) 2.59780,0.88944,0.04278,-0.093,0.375
(   12) 2.82844,0.87191,0.04148,-0.093,0.375
(   13) 3.04164,0.84938,0.03992,-0.093,0.375
(   14) 3.23608,0.81984,0.03803,-0.093,0.375
(   15) 3.41056,0.78121,0.03582,-0.093,0.375
(   16) 3.56404,0.73152,0.03332,-0.093,0.375
(   17) 3.69552,0.66802,0.03057,-0.093,0.375
(   18) 3.80424,0.58601,0.02754,-0.093,0.375
(   19) 3.88948,0.47931,0.02417,-0.093,0.375
(   20) 3.95076,0.34342,0.02049,-0.093,0.375
(   21) 3.98768,0.18015,0.01727,-0.093,0.375
```

```
LFORD UNIVERSITY FTN77 VER. 2285     <USER2>S310768966>STUDENT>STRUC3.F77        20:1
MPILER OPTIONS:  LISTING INTL DCLVAR NOMAP CHECK NOBIG LOGL DYNM NOOFFSET LGO NOAN
                 NOFRN FPN NOLUNFREC NOSILENT NO_OPTIMISE NOIMPURE

0001      C*****************************************
0002      C*     AE446 - AEROSPACE STRUCTURES      *
0003      C*    Computer program to determine      *
0004      C*    the centroid location and sec-     *
0005      C*    tion properties relative to the    *
0006      C*    centroid for a nouniform airfoil   *
0007      C*    and the direct stress due to       *
0008      C*    axial, bending and thermal loads   *
0009      C*     Written by Michael H. Park        *
0010      C*****************************************
0011            PROGRAM STRUC4
0012            REAL E(50),A(50),Y(50),Z(50),PT(50),MZT(50),MYT(50),IYY,IZZ,IYZ
0013           +,SIG(50),ALPH(50),MY,MZ
0014            OPEN(99,FILE='PROPS5.DATA',STATUS='OLD')
0015            READ(99,*)N
0016            READ(99,*)(A(I),Z(I),Y(I),E(I),ALPH(I),I=1,N)
0017            CLOSE(UNIT=99)
0018
0019            WRITE(1,*)'ENTER IWR:  '
0020            READ(1,*)IWR
0021      1     WRITE(1,*)'ENTER P, My, Mz, DT:'
0022            READ(1,*)P,MY,MZ,DT
0023
0024            ATOT=0.0
0025            YA=0.0
0026            ZA=0.0
0027            IYY=0.0
0028            IZZ=0.0
0029            IYZ=0.0
0030
0031            I=1
0032            EREF=E(I)
0033            DO 5 I=1,N-1
0034.01            IF(E(I).LT.E(I+1))EREF=E(I)
0035.01   5       CONTINUE
0036.01
0037            DO 10, I=1,N
0038.01            ATOT=ATOT+(E(I)/EREF)*A(I)
0039.01            YA=YA+(E(I)/EREF)*Y(I)*A(I)
0040.01            ZA=ZA+(E(I)/EREF)*Z(I)*A(I)
0041.01   10       CONTINUE
0042.01
0043            YBAR=YA/ATOT
0044            ZBAR=ZA/ATOT
0045
0046            DO 20, I=1,N
0047.01            IYY=IYY+(E(I)/EREF)*A(I)*(Z(I)-ZBAR)**2
0048.01            IZZ=IZZ+(E(I)/EREF)*A(I)*(Y(I)-YBAR)**2
0049.01            IYZ=IYZ+(E(I)/EREF)*A(I)*(Z(I)-ZBAR)*(Y(I)-YBAR)
0050.01
0051.01            PT(I)=E(I)*ALPH(I)*DT
0052.01            MYT(I)=E(I)*A(I)*Z(I)*DT
0053.01            MZT(I)=E(I)*A(I)*Y(I)*DT
0054.01   20       CONTINUE
0055.01
0056            DO 30, I=1,N
0057.01            B=E(I)*(P+PT(I))/(EREF*ATOT)
0058.01            C=(E(I)/EREF)*((MZ-MZT(I))*IYY+(MY+MYT(I))*IYZ)*Y(I)
0059.01            D=(E(I)/EREF)*((MY+MYT(I))*IZZ+(MZ-MZT(I))*IYZ)*Z(I)
0060.01            SIG(I)=B+(D-C)/(IYY*IZZ-IYZ**2)-E(I)*ALPH(I)*DT
0061.01   30       CONTINUE
0062.01
0063            WRITE(IWR,*)'YBAR = ',YBAR,'in. '
0064            WRITE(IWR,*)'ZBAR = ',ZBAR,'in. '
0065            WRITE(IWR,*)'Iyy = ',IYY,'in^4'
0066            WRITE(IWR,*)'Izz = ',IZZ,'in^4'
0067            WRITE(IWR,*)'Iyz = ',IYZ,'in^4'
0068            WRITE(IWR,*)'P = ',P,'lbs'
0069            WRITE(IWR,*)'My = ',MY,'in-lbs'
0070            WRITE(IWR,*)'Mz = ',MZ,'in-lbs'
0071            WRITE(IWR,*)'DT = ',DT,'degrees F'
0072
0073            WRITE(IWR,*)' '
0074            WRITE(IWR,98)
0075            WRITE(IWR,*)'----------------------'
```

ITEM 12

```
SALFORD UNIVERSITY FTN77 VER. 228S     <USER2>S3437282171STUDENT>CG2.F77          20:0
COMPILER OPTIONS:   LISTING INTL DCLVAR NOMAP CHECK NOBIG LOGL DYNM NOOFFSET LGO NO
                    NOFRN FPN NOLUNFREC NOSILENT NO_OPTIMISE NOIMPURE

0001      C
0002      C
0003      C
0004      C
0005      CC
0006      C
0007      C
0008            REAL IY, X(30),Z(30),W(30)
0009      C
0010            WRITE(1,*) 'ENTER OUTPUT CODE: [1] FOR SCREEN, [6] FOR PRINTER'
0011            READ(1,*) IWR
0012          1 CONTINUE
0013            XC=0.
0014            ZC=0.
0015            WT=0.
0016            IY=0.
0017
0018            X(1)=1.125
0019            Z(1)=2.625
0020            W(1)=7.5
0021            X(2)=4.0
0022            Z(2)=2.625
0023            W(2)=3.23
0024            X(3)=6.0
0025            Z(3)=0.625
0026            W(3)=0.95
0027            X(4)=6.0
0028            Z(4)=2.28
0029            W(4)=2.0
0030            X(5)=18.94
0031            Z(5)=2.44
0032            W(5)=1.2
0033            X(6)=9.0
0034            Z(6)=3.0
0035            W(6)=2.0
0036            X(7)=14.834
0037            Z(7)=2.25
0038            W(7)=5.22
0039            X(8)=12.62
0040            Z(8)=0.75
0041            W(8)=10.36
0042            X(9)=33.67
0043            Z(9)=4.25
0044            W(9)=0.4574
0045            X(10)=35.58
0046            Z(10)=4.0
0047            W(10)=0.7226
0048            X(11)=9.0
0049            Z(11)=-3.0
0050            W(11)=2.4
0051            W(12)=5.46
0052            WRITE(1,*)'ENTER X- AND Z-POSITIONS OF BATTERY PACK'
0053            READ(1,*)X(12),Z(12)
0054            N=12
0055            DO 20 J=1,N
0056.01             XC=XC+X(J)*W(J)
0057.01             ZC=ZC+Z(J)*W(J)
0058.01             WT=WT+W(J)
0059.01       20 CONTINUE
0060            XCG=XC/WT
0061            ZCG=ZC/WT
0062
0063            DO 30 K=1,N
0064.01             IY=IY+((X(K)-XCG)**2+(Z(K)-ZCG)**2)*W(K)
0065.01       30 CONTINUE
0066                IY=IY/(144.*16.*32.2)
0067            WRITE(IWR,90)
0068
0069            DO 40 L=1,N
0070.01             WRITE(IWR,91) L,X(L),Z(L),W(L)
0071.01       40 CONTINUE
0072.01
0073            WRITE(IWR,*) ' '
0074            WRITE(IWR,92) XCG
0075            WRITE(IWR,93) ZCG
```

```
0076            WRITE(IWR,95)WT
0077            WRITE(IWR,94) IY
0078            WRITE(1,*) 'CONTINUE ? [1] FOR YES'
0079            READ(1,*) NN
0080            IF(NN.EQ.1) GOTO 1
0081         90 FORMAT(2X,'COMPONENT',3X,'X-POS',4X,'Z-POS',2X,'WEIGHT [oz]')
0082         91 FORMAT(5X,I2,6X,F7.4,2X,F7.4,2X,F8.4)
0083         92 FORMAT(2X,'X-POSITION OF THE C.G.    = ',F7.4,1X,'INCHES')
0084         93 FORMAT(2X,'Z-POSITION OF THE C.G.    = ',F7.4,1X,'INCHES')
0085         94 FORMAT(2X,'MOMENT ABOUT Y-AXIS (Iy) = ',F7.4,1X,'SLUG*FT**2')
0086         95 FORMAT(2X,'TOTAL WEIGHT              = ',F7.4,1X,'OZ')
0087
0088            STOP
0089            END
```

END OF COMPILATION CLOCKED .500 SECONDS

COMPONENT	X-POS	Z-POS	WEIGHT [oz]
1	1.1250	2.6250	7.5000
2	4.0000	2.6250	3.2300
3	6.0000	0.6250	0.9500
4	6.0000	2.2800	2.0000
5	18.9400	2.4400	1.2000
6	9.0000	3.0000	2.0000
7	14.8340	2.2500	5.2200
8	12.6200	0.7500	10.3600
9	33.6700	4.2500	0.4574
10	35.5800	4.0000	0.7226
11	9.0000	-3.0000	2.4000
12	9.5000	1.5000	5.4600

X-POSITION OF THE C.G. = 9.6998 INCHES
Z-POSITION OF THE C.G. = 1.6286 INCHES
TOTAL WEIGHT = 41.5000 OZ
MOMENT ABOUT Y-AXIS (Iy) = 0.0251 SLUG*FT**2

NOMENCLATURE

AETC	Aerospace Engineers for the Twenty-First Century
AR	Aspect Ratio
α	Angle of Attack
b	Wing Span
β	Propeller Blade Angle Yaw Angle
c	Wing Mean Chord
C_D	Drag Coefficient
C_{Do}	Parasite Drag Coefficient
CG	Center of Gravity
C_L	Lift Coefficient
C_l	Roll Moment Coefficient
CL_{at}	Change in Lift Coefficient with Angle of Attack for the Tail
CL_{av}	Change in Lift Coefficient with Angle of Attack for the Vertical Tail
CL_o	Lift Coefficient at Zero Angle of Attack
CL_α	Change in Lift Coefficient with Angle of Attack
$C_{l\beta}$	Roll Moment due to Yaw
CL_w	Wing Lift Coefficient
C_m	Pitch Moment Coefficient
Cm_{acw}	Moment Coefficient About the Aerodynamic Center of the Wing
Cm_α	Change in Moment Coefficient with Angle of Attack
$Cm_{\alpha f}$	Change in Moment Coefficient for the Fuselage
$Cm_{\alpha t}$	Change in Moment Coefficient for the Tail
$Cm_{\alpha w}$	Change in Moment Coefficient for the Wing
Cm_o	Total Zero Lift Moment Coefficient
Cm_{of}	Zero Lift Moment Coefficient for the Fuselage
Cm_{ot}	Zero Lift Moment Coefficient for the Tail
Cm_{ow}	Zero Lift Moment Coefficient for the Wing
$Cm_{\delta e}$	Change in Moment Coefficient with Rudder Deflection
C_n	Yaw Moment Coefficient
$Cn\beta$	Yaw Moment Coefficient due to Yaw Angle b
$Cn_{\delta r}$	Rudder Control Power
C_p	Propeller Power Coefficient

C_t	Propeller Thrust Coefficient
e	efficiency factor
ε_o	Downwash Angle at Zero Angle of Attack
Γ	Dihedral
i_t	Tail Incidence Angle
i_w	Wing Incidence Angle
J	Advance Ratio
J4D	SCREEM-J4D aircraft
l_h	Horizontal Tail Moment Arm
l_v	Vertical Tail Moment Arm
mahr	Milliamp-hours
n	Load Factor
η	Efficiency Factor
PA	Power Available
PR	Power Required
Re	Reynolds Number
SFSM	Stick Fixed Static Margin
S_H	Horizontal Tail Surface Area
S_v	Vertical Tail Surface Area
S_W	Wing Surface Area
τ	Flap Effectiveness
V_H	Volume Ratio of Horizontal Tail
V_V	Volume Ratio of Vertical Tail
W	Weight
X_{ac}	Distance From Leading Edge to Aerodynamic Center of Wing
X_{cg}	Distance From Wing Aerodynamic Center to Center of Gravity
X_{NP}	Stick Fixed Neutral Point